Comparative Analysis of Phenotypic and Functional Attributes of Antigen-specific Naïve and Memory T cell Subsets Potentially Affecting The Efficacy of Adoptive T cell Therapy

A Dissertation

Presented to the Faculty of the Weill Cornell Graduate School of Medical Sciences

In Partial Fulfillment of the Requirements for the Degree of Doctor of Philosophy

by

Tzu-yun Kuo

June 2017

Comparative Analysis of Phenotypic and Functional Attributes of Antigen-specific Naïve and Memory T cell Subsets Potentially Affecting The Efficacy of Adoptive T cell Therapy

Tzu-yun Kuo, Ph.D.

Cornell University 2017

ABSTRACT

The quality of the T cells that are selected for expansion and adoptive transfer has been identified as a critical factor that determines the persistence, and therefore, efficacy, of transferred cells. The memory T-cell compartment is heterogeneous and encompasses multiple T cell subsets with divergent properties. Latent human cytomegalovirus (CMV) infection is controlled by a limited repertoire of immunodominant T cells specific for viral peptides. The antigen-specific T cell subsets responsible for maintaining memory T cells and repopulating them in response to periodic viral reactivations are not well characterized. In the first chapter of my thesis work, I developed a human xenograft model in NOG mice to conduct comparisons of CMV-specific T_{CM} and T_{EM} derived cells *in vivo*, when administered together with the cytokine IL-2 or IL-15. These studies specifically compared CMVpp65 specific T_{CM} and T_{EM} derived cells as to their capacity to selectively target, accumulate in and induce inhibition of human colon carcinoma xenograft transduced to express CMVpp65. The experiments also evaluated the kinetics and level of T-cell accumulation in these

targets and their persistence both in the xenografts and other tissues, particularly the marrow. In the second chapter of my thesis work, I focused on identifying the most effective T-cell memory population that would provide higher in vivo proliferation, survival, and overall functional activity. The studies comparatively evaluated CMVpp65 epitope-specific tetramer^{+} T-cell populations within the memory T-cell compartment as to their origins, phenotype, functional attributes, T-cell clonal diversity, proliferation and survival. In the third chapter of my thesis work, I evaluated the differential functional activity of low and high affinity chimeric antigen receptor constructs encoding T-cell receptor mimics specific for an immunogenic peptide of an oncognic protein, WT-1, presented by HLA A0201.

Overall, the thesis work has implications for the design of T cell-based immunotherapies. First, the studies indicate that while T_{CM} and T_{EM} derived T-cells exhibit differences in phenotype and in the kinetics and degree of their respective accumulations in CMVpp65^{+} CoCa xenografts, their antigen-specific activities and their persistence *in vivo* were fairly equivalent. The differences lies in the cytokine treatment: in IL-15/IL-15Rα treated mice there was a more prolonged persistence of both T_{CM} and T_{EM} derived T-cells compared to IL-2 treated mice. Second, the studies suggested Tet^{+} T_{SCM} rather than Tet^{+} T_{N} are the principal reservoir for rapid repopulation of immunodominant T_{EM} cells in the circulation. T_{SCM} could potentially provide better disease control by facilitating early recovery of more short-lived immunodominant virus-specific T_{EM} cells that

normally control latent infection and thereby provide sustained long-term protection from disease. Finally, the studies validate the superior specific binding and HLA-restricted WT-1 peptide specific cytoxicity of T-cell expressing the high affinity CAR against HLA A0201^{+}WT-1^{+} human tumor cells compared to low affinity CAR against the same antigen.

BIOGRAPHICAL SKETCH

Tzu-yun Kuo was born and raised in the lovely country of Taiwan, which is situated in the western region of the Pacific Ocean. She received her bachelor degree in 2002 from the National Taiwan University majoring in biochemistry and technology. Driven by strong curiosity about science, she spent time after graduation exploring the biotechnology field at Academia Sinica, a government-owned research institute in Taiwan, while learning about the basic techniques and applications in Molecular Biology.

Tzu-yun got really excited in the field of human immunology when she trained as an immunologist while she accomplished her Master's degree at National Taiwan University. During her Masters study, she started her research in tumor immunology under the guidance of Dr. Hong-Nerng Ho. Her Master's thesis work was published as a paper addressing the role of $FOXP3^{+}$Tumor-infiltrating lymphocytes in human cervical cancer. For this, she was awarded the American Society for Reproductive Immunology's Graduate Student Award in 2006. She then received a national award from Taiwan's Ministry of Education Scholar in 2007.

In 2008, Tzu-yun started pursuing her academic journey at Weill Cornell Medical College of Cornell University. She joined Dr. Richard O'Reilly's lab in 2009 at the Memorial Sloan-Kettering Cancer Center as a Ph.D. graduate student. She spent her time learning the basic science of adoptive T cell therapy as well as the clinical research that could be used to enhance the resistance of bone marrow transplant recipients to not only serious infections but also their underlying cancers.

During the time in Dr. O'Reilly's lab, Tzu-yun summited a paper as first author addressing

the contribution of different memory subsets to the maintenance of the overall memory compartment of antigen-specific T cells. The method she developed to generate antigen-specific T cells in a less differentiated subset was also filed for provisional patent as an inventor in 2016. She was also involved in another project which was focused on chimeric antigen receptor (CAR) T cell therapy. There she generated the first TCR-like CAR-T cell design to treat WT-1 expressing leukemia and solid cancers and licensed to Novartis.

This dissertation is dedicated to my beloved parents Chao-Wen Kuo and Chun-Chen Liu. My achievements would not be possible without your unconditional love and support over the years.

ACKNOWLEDGEMENTS

I would like to thank my thesis advisor, Dr. Richard O'Reilly, for his mentorship. He is like a family member to me when my family is in Taiwan. I've learned a lot from his passion about science, his curiosity about knowledge, and his attitude for being such a great leader in clinical research and practice. It is such an honor to work in his lab with his guidance along the way.

I would also like to thank Dr. Aisha Hasan to direct me with all the experimental designs, data analysis and the written skills in paper and thesis writing. I would not be able to achieve my thesis without her direction. I would also like to thank my thesis committee members Drs. Eric Pamer, Michel Sadelain, and Jayanta Chaudhuri for their helpful feedback and advice.

To my family: my mother, father and my little brother, I am grateful for your love and support. Your faith in me has helped me maintain my motivation to come this far. To my friends, thank you for standing beside me all the time. To my boyfriend, Alex, thank you for your help in the past six months to motivate and support me to finish the last part of my journey.

TABLE OF CONTENTS

LISTS OF FIGURES

Chapter One: Comparative analysis of the contribution of the cytokines IL-2 and IL-15/IL15Rα complex to the engraftment, antigen-targeted accumulation, effector function and persistence of human central memory and effector memory derived CMV specific T-cells in immunodeficient mice

Chapter Two: Stem cell-like memory T cells (T_{SCM}) rapidly repopulate circulating virus-specific effector T cells

LIST OF ABBREVIATIONS

AAPC artificial antigen presenting cell

ACT adoptive cell transfer

AICD activation-induced cell death

ALL acute lymphoblastic leukemia

APC antigen presenting cell

BMT bone marrow transplantation

CAR chimeric antigen receptor

CD cluster of differentiation

CD95 FAS receptor

CLL chronic lymphocytic leukemia

CML chronic myelogenous leukemia

CMV cytomegalovirus

CR complete remission

CTL cytotoxic T lymphocyte

DLI donor lymphocyte infusion

DCS donor calf serum

DMEM Dulbecco's Modified Eagle Medium

DMSO dimethyl sulfoxide

EBV Epstein–Barr virus

FBS fetal bovine serum

GVHD graft-versus-host disease

GVL graft-versus-leukemia

GzmB granzyme B

HCT Hematopoietic cell transplantation

HLA human leukocyte antigen

HSCT hematopoietic stem cell transplantation

Ig immunoglobulin

IL interleukin

i.p. intraperitoneal

i.v. intravenous

KLRG-1 killer cell lectin-like receptor subfamily G member 1

MDSC myeloid-derived suppressor cell

MHC major histocompatibility complex

NOD non-obese diabetic

NOG mice NOD-scid IL2 receptor-γ knock out mice

NLV CMV pp65 peptide NLVPMVATV

PBMC peripheral blood mononuclear cell

PBS phosphate-buffered saline

PD-1 programmed death 1

PD-L1 programmed death-ligand 1

PE phycoerythrin

Pfn perforin

PHA phytohemagglutinin

PR partial remission

RPMI Roswell Park Memorial Institute

s.c. subcutaneous

scFv signal chain variable fragment

SCID severe combined immunodeficiency

STAT signal transducer and activator of transcription

TAA tumor-associated antigen

T_{CM} central memory T cell

TCR T cell receptor

Teff effector T cell

T_{EM} effector memory T cell

TGF-β tumor growth factor beta

Th T helper cell

TIL tumor infiltrating lymphocyte

TLR toll-like receptor

T_{reg} regulatory T cell

T_N naïve T cell

T_{RM} tissue resident memory T cell

T_{SCM} stem cell memory T cell

WT1 Wilms' tumor gene 1

THESIS INTRODUCTION

Adoptive T-cell therapy using naturally occurring antigen-specific T cells or antigen targeted genetically engineered T-cells has demonstrated clinical efficacy in the treatment of infections and cancer. Infusions of ex vivo expanded, naturally occurring tumor infiltrating lymphocytes (TILs) responding to self-tumor antigens, have successfully mediated durable, complete tumor regressions in a proportion of patients with melanoma (*1*). Such TILs potentially target somatic mutations exclusive to each cancer, which are responsible for their clinical activity. More recently, the ability to genetically engineer lymphocytes to express conventional T cell receptors or chimeric antigen receptors has further extended the spectrum for successful application of adoptive cell therapy for cancer treatment (*2*).

Adoptive immunotherapy is an approach that focuses on the therapeutic transfer of antigen-specific T cells targeted to a specific viral or tumor antigen. The maximal efficacy of this approach can be realized when the infused T-cells can effectively engraft in the recipient host, or, at least, continue to replicate and regenerate functional effector and memory T cell populations for extended periods of time after initial cell transfer, and thereby provide ongoing immunity against disease. This can be achieved if autologous virus-specific or tumor-reactive T-cells can be generated in vitro, and when such T-cells are selectively expanded from a marrow transplant donor and infused into the patient after transplant (*3*). However, a deeper understanding of the types and growth requirements of the T-cells that are effective is still needed if adoptive therapies

are to be consistently able to induce lasting responses. Similarly, since autologous T-cells cannot be consistently generated and are often inactive, alternative approaches such as the use of banked third party T-cells of demonstrated activity will be required for broad application of this approach.

In 1986, Rosenberg et al. showed that lymphocytes infiltrating the tumor stroma were a concentrated source of lymphocytes capable of recognizing tumor in vitro. These observations were validated in murine tumor models, in which the adoptive transfer of these tumor-infiltrating lymphocytes, expanded in IL-2 prior to infusion, could mediate regression of established tumors (*4*). In 1988, Rosenberg et al. first reported objective regression of cancer upon infusion of ex-vivo expanded autologous TILs in patients with metastatic melanoma (*1*). To further improve their efficacy, this approach was modified to include a lymphodepleting chemotherapy regimen prior to TIL transfer. It was postulated that the lymphodepletion would decrease the burden of regulatory T-cells as well as other myeloid suppressor cells, thereby rendering a more supportive immune environment for the activity of transferred cytotoxic lymphocytes (*5*).

Since then, the application of this treatment approach has further evolved to include the use of genetically modified T-cells transduced to express TCRs or chimeric antigen receptors targeted to tumor antigens. Morgan et al. first demonstrated that the administration of normal circulating lymphocytes transduced with a retrovirus encoding a TCR that recognized the MART-1 melanoma antigen could mediate tumor regressions (*6*). Lymphocytes

transduced to express a chimeric antigen receptor (CAR) against CD19 were shown in 2010 to mediate regression of an advanced B cell lymphoma (*7*). In sum, naturally occurring or genetically engineered T cells set the stage for the extended development of adoptive cell therapy.

In recipients of allogeneic hematopoietic stem cell transplant (HSCT), T cell responses against pathogens can also be reconstituted by adoptive transfer of pathogen specific T cells derived from the quiescent memory T-cell pool of the donor. In 1991, Riddell et al, first demonstrated that adoptive transfer of cloned transplant donor derived T cells sensitized in vitro could prevent CMV infections in HSCT recipients without causing GVHD (*8*). In 1994, Papadopoulos et al. (*9*) at MSKCC demonstrated that adoptive transfer of unselected lymphocytes containing as few as 600 EBV-specific CTL population from an HCT donor could induce durable complete remission of EBV lymphomas complicating allogeneic T-cell depleted transplants. Subsequent studies confirmed that adoptively transferred virus-specific T cell clones or polyclonal T cells specific for CMV or EBV, that were isolated and expanded from seropositive stem cell donors, could effectively clear CMV infections and EBV lymphomas in HSCT recipients (*10, 11*).

In studies using both tumor antigen selective and virus specific T-cell transfers, the infused T-cells have varied significantly in their persistence after transfer. Limitations to the persistence of the T-cells have been potentially ascribed to T-cell senescence or exhaustion. These limitations have major clinical significance

since the persistence of transferred antigen-specific T cells in the blood, measured by clonotypic analysis of T cell receptor gene sequences or by MHC tetramer staining, has been correlated with antitumor activity (*12*). Tumor-reactive T cells infiltrating the tumor microenviroment in cancer patients acquire a terminally differentiated effector phenotype, which may limit their ability to proliferate and survive after adoptive transfer. However, Dudley and colleagues (*5*) showed that administering lymphodepleting chemotherapy prior to T-cell infusion can enhance the initial expansion of the transferred T-cell in vivo, and thereby potentially contribute to an enhanced persistence of infused T-cells. That lyophodepletion prior to adoptive transfer radically increases the initial proliferation and population size of the transferred T-cells has been repeatedly confirmed, and variously ascribed to homeostatic expansion within lympho-depleted mice, responses to increased levels of cytokines such as IL-15 and IL-7 generated in response to lyphodepletion and/or elimination of regulatory T-cell populations. However, the in vivo persistence of infused T cells still remains unpredictable in individual patients. An alternative approach that has been proposed to enhance the persistence of transferred T-cells is to isolate T cells that preserve a less differentiated phenotype based on the hypothesis that such T-cells would provide superior proliferation, survival, and sustained effector function in vivo. Studies in a non-human primate model in which autologous gene marked-CMV-specific T cell clones derived from sorted central or effector memory T-cell subsets (T_{CM} or T_{EM}) were adoptively transferred, demonstrated that T_{CM} derived clones could persist for months after adoptive transfer and could

also re-establish diverse memory subsets. These data illustrated that, even after in vitro activation and culture, therapeutic T cells derived from T_{CM} have a superior capacity to persist in vivo (*13*).

Under physiological conditions, antigen-specific T cells originate from a small number of naïve precursor cells that expand vigorously upon initial priming, and acquire effector functions. Following this effector phase, most T-cells undergo senescence, with only a small fraction that survive beyond the contraction phase and persist as memory T cells that then serve to provide the secondary response. Long-lived memory T cells are subdivided phenotypically as well as functionally into different subsets. This phenotypic and functional diversity within epitope-specific T cell populations generated during infection, is increasingly recognized to be critical for the quality of antigen-specific immunity. Memory T cells can be phenotypically sub classified based on distinct expression patterns of the lymph node–homing molecules CD62L and CCR7, into central memory T cells (T_{CM}) and effector memory T cells (T_{EM}). The expression patterns of these molecules translate into migratory differences; wherein, T_{CM} cells continuously re-circulate via the blood stream to lymphoid organs whereas T_{EM} cells preferentially migrate to targeted tissues and not to lymphoid tissues (*14*). The recent identification of tissue resident memory T cells (T_{RM}), which might be further subdivided depending on the respective organ they reside in, further adds to the complexity and diversity of the memory T cell compartment (*15*). More recently, the expression of CD95, also known as FAS, in naïve phenotype T cells now

defines a new memory T cell subset in humans and mice, designated stem cell memory T cells (T_{SCM}). T_{SCM} cells have a high proliferative capacity and are both self-renewing and multipotent, in that they can further differentiate into other T cell subsets, including T_{CM} and T_{EM} cells(*16*). Recent evidence also supports a role for $CD4^+$ helper T cells in sustaining the proliferative potential and persistence of $CD8^+$ effector memory T cells. For certain antigens, such as adenovirus, $CD4^+$ T cells may also respond directly as effector cells and mediate the clearance of virus-infected host cells (*17*).

To develop an approach for enhancing persistence and overall efficacy of adoptive immunotherapy, the studies conducted during the course of this thesis project focused on identifying the most effective T-cell memory population that would provide higher in vivo proliferation, survival, and overall functional activity. The studies comparatively evaluated antigen-specific T-cell populations within the memory T-cell compartment as to their origins, phenotype, functional attributes, proliferation and survival, as well as their in vivo homing and persistence in humans. Later, through TCR sequencing analysis of sorted T-cell populations, a lineage relationship within epitope specific T cells was elucidated.

A series of studies also evaluated the differential functional activity of low and high affinity chimeric antigen receptor constructs encoding T-cell receptor mimics specific for an immunogenic peptide of an oncognic protein, WT-1, presented by HLA A0201.

CHAPTER ONE

Comparative analysis of the contribution of the cytokines IL-2 and IL-15/IL15Rα complex to the engraftment, antigen-targeted accumulation, effector function and persistence of human central memory and effector memory derived CMV specific T-cells in immunodeficient mice

1. Introduction

The adoptive transfer of antigen-specific T cells that have been expanded ex vivo is being actively pursued to treat infections and malignancy in humans. Ex vivo expanded antigen-specific T cell clones have provided a means for treating patients with specific types of cancer such as melanoma by providing a patient with an antigen-specific tumoricidal immune response. While the results of early clinical trials support the use of adoptively transferred T cells as a strategy for the treatment of melanoma, they have also elucidated potential obstacles to these therapies (*12, 18*). In particular, a major limitation to the efficacy of adoptive immunotherapy in humans is the failure of cultured T cells, particularly cloned T cells, to persist in vivo. The basis for the poor survival of the transferred cells is still poorly understood.

The persistence of transferred tumor-reactive T cells, either generated from the blood or expanded directly from tumor infiltrating lymphocytes, has not been consistent, even when the host has received lymphodepleting chemotherapy before T cell transfer and is also treated with IL-2 (*19*). In adoptively transferred virus-specific T cells, the effector T cells are derived from virus-specific memory T cells isolated from immune donors. However, studies in which virus specific T-cell clones or gene marked polyclonal T-cell lines have been adoptively transferred have shown that not all T effector cells derived from memory precursors are capable of durable engraftment (*13, 20*).

The pool of lymphocytes from which CD8 T cells for adoptive immunotherapy can

be derived includes naïve T cells and antigen-experienced memory T cells, which can be divided into central memory (T_{CM}) and effector memory (T_{EM}) subsets that differ in phenotype, homing, and function. T_{CM}, which express CD62L and CCR7, reside predominantly in lymph nodes where they are capable of extensive proliferation and differentiation upon antigen re-encounter. On the other hand, T_{EM}, which lack the expression of CD62L and CCR7, are prevalent in the blood and peripheral tissues, and capable of rapid accumulation in and lysis of virus-infected or malignant cells expressing the targeted antigen. In a nonhuman primate model system, virus-specific effector CTL derived from T_{CM}, but not T_{EM}, established persistent, functional T cell immunity following adoptive transfer to lymphoreplete healthy macaques (*13*). Furthermore, adoptive transfer of human antigen-specific CD8 T cells derived from T_{CM} have exhibited superior engraftment in human NOG mice supplemented with low dose IL-15 when compared with such T-cells derived from T_{EM} (*21*).

IL-15 can sustain T cell proliferation without the robust pro-differentiating activity that characterizes IL-2. Although IL-2 promotes T cell differentiation into T effector cells, priming of T cells in the presence of IL-15 results in the generation of T cells with the phenotypic, functional, metabolic and gene expression attributes found in naturally arising T_{CM} cells (*22, 23*). As a result, tumor-reactive T cells have exhibited greater antitumor responses when generated in the presence of IL-15 than when grown in the presence of IL-2 (*22*). To better understand differences in the engraftment of T_{CM} and T_{EM} derived T cells in the

presence of IL-2 or IL-15, we created a humanized mouse model in which human CMVpp65 specific T-cells of defined epitope specific and HLA restriction are adoptively transferred into immunodeficient NOG mice bearing human tumor xenografts that do or do not express CMVpp65, the immunodominent protein of human CMV. In order to be able to better examine conditions and attributes of CMV-specific T cells that contribute to their activity against infected human cells, we employed a human colon carcinoma, which, like human colon epithelial cells can be lytically infected by CMV, and transduced this carcinoma to express the antigen CMVpp65. We then compared T_{CM} and T_{EM} derived CMVpp65 specific T-cells for their capacity to achieve sustained engraftment accumulate specifically in targeted CMVpp65^{+} tumors and induce regression of these tumors. Our data demonstrate that human CMV-specific T cells derived from T_{CM} and T_{EM} achieve similar levels of engraftment, and that mice co-treated with IL-15/IL-15Rα but not IL-2 have superior engraftment and provide superior CMVpp65-specific, HLA-restricted antitumor activity. The engrafted T_{CM} and T_{EM} derived HLAA0201 restricted CMVpp65-specific T-cells preferentially accumulate in the colon carcinoma xenografts coexpressing CMVpp65 and HLAA0201 as well as in the bone marrow in the mice treated with IL-15/IL-15α. Furthermore, the T-cells in the marrow are functional, exhibiting antigen-specific IFN-r production and T cell proliferation when harvested and expanded to CMVpp65 ex vivo.

2. Materials and Methods

Donors

Blood samples were obtained from healthy volunteer HLA-A0201$^+$ CMV-seropositive donors. High resolution HLA typing was performed by analysis of HLA allele-specific nucleotide sequences using standard high-resolution typing techniques. CMV serostatus was determined by standard serologic techniques in the clinical microbiology laboratory at Memorial Sloan-Kettering Cancer Center.

Generation of CMV-specific T cell clones

PBMC were isolated from whole blood by Ficoll-Hypaque density gradient separation (Accurate Chemical & Scientific Corporation, Westbury, NY USA). T cells were subsequently enriched from PBMC by depletion of CD19$^+$, CD14$^+$, and CD56$^+$ cells, using mAb-coated immunomagnetic beads (Pan T-Cell Isolation Kit II, Miltenyi Biotec Inc, Auburn, CA USA). Enriched T cells were labeled with fluorescent Abs: anti-CD8 PerCP, anti-CD45RO PE, and anti-CD62L FITC (all purchased from BD Biosciences, CA, USA). T cell populations representing T_{CM} and T_{EM} were gated and sorted on a BD FACS Aria-II SORT (BD Biosciences, CA, USA) based on the following markers: T_{CM} as CD8$^+$CD45RO$^+$CD62L$^+$ and T_{EM} populations as CD8$^+$CD45RO$^+$CD62L$^-$. Single cell sorted T cells were replated at 1 cells/well in 96-well round-bottom plates with 2 × 10^4 γ-irradiated HLA A0201$^+$, CMVpp65$^+$ AAPCs, 5 × 10^5 γ-irradiated autologous peptide-pulsed PBMCs and 2 × 10^5 γ-irradiated BLCLs as feeders in T cell media with 50 U/ml IL-2 and 25ng/ml IL-15. T cell were cultured in Yssel's medium with 15% heat inactivated human

serum (Gemini, CA, USA) in humidified incubators at 37°C and 5% CO_2.

Flow cytometry phenotypic analysis

T cell clones were analyzed by flow cytometry after staining with fluorochrome-conjugated mAbs to CD3, CD8, CD62L, and CD45RA. Commercially available CMVpp65 MHC-peptide tetramers for HLA-A 0201-bearing peptide sequences NLVPMVATV (Beckman Coulter) were used. Functional activity of T cells was evaluated after short secondary stimulation by several parameters including T cell generation of intracellular cytokines (IFN-γ, TNF-α and IL-2) as quantified by intracellular fluorescence staining. Briefly, irradiated autologous BLCLs loaded with NLVPMVATV peptide were co-incubated with T cells at an effector to target ratio of 1:5 for 6 hours in the presence of 1 μg/ml brefeldin A (Sigma-Aldrich, MO, USA). Co-cultured T cells were then labelled with anti-CD3 APC and anti CD8 PE for 15 mins at room temp, washed and then permeabilized with Perm solution (BD Biosciences). There were then co-incubated with anti-IFN-γ PE (BD Biosciences) and anti-TNF-α APC (Miltenyi Biotec), or anti-IL-2 FITC (BD Biosciences). Samples were analyzed on a FACSCalibur using CellQuest Software (BD).

Characterization of CMV-specific T cell clones by quantitative analysis of TCRV β repertoire

CMV peptide-HLA tetramer$^+$ T cells were analyzed for their TCRV β repertoire

via flow cytometry using a commercially available kit containing antibodies to 24 subfamilies of the Vβ region of the human TCR (IO Test β Mark; Beckman Coulter) according to procedures provided by the manufacturer (*24*).

Cytotoxicity of CMV-specific CTLs by in vitro cytotoxicity assays

T cells clones were assessed for their capacity to lyse CMVpp65-loaded targets using a standard ^{51}Cr release assay as previously described (*25*). Targets were autologous EBV-BLCL alone, and EBV-BLCL pulsed with CMVpp65 peptide nonamer NLVPMVATV at a T cell: BLCL ratio, 1:1 or 10:1.

Bioluminescent labeled CMV-specific T cell lines

Sort-purified CD8$^+$CD45RO$^+$CD62L$^+$ T_{CM} and CD8$^+$CD45RO$^+$CD62L$^-$ T_{EM} cells were cocultured with 1 × 10^5 γ-irradiated HLA A0201$^+$, CMVpp65$^+$ AAPCs and 1 × 10^5 γ-irradiated autologous peptide-pulsed PBMCs per 10^6 of T cells. On day 4, cells were transduced with retrovirus supernatant carrying the extRLuc construct as previously described (*26*). This vector introduces genes directing the expression of two reporters, a membrane-anchored form of the Gaussia luciferase enzyme (extGLuc) and green fluorescent protein. T cells were cultured with the extGLuc retrovirus supernatant together with 1 × 10^5 γ-irradiated mouse pro-B cell Baf-3 cells transduced to express the IL-15Rα and IL-15 genes (BAF3 IL15/15Rα) (*27*) on retronectin coated plates. Retrovirus transductions were repeated on day 5 and day 6. T cell cultures were supplemented with IL-2 (20 U/ml) and 10 ng/mL rhIL-15 starting on day 12 and then three times per week. Thereafter, cells were re-stimulated every 10-days with AAPCs and irradiated autologous PBMC feeders.

The extGLuc$^+$ T cells were sorted by GFP on a BD FACS Aria-II SORT (BD Biosciences, CA, USA) on day 38 and 78. After enrichment by antigen stimulation, the CMV pp65-specific extGLuc$^+$ T cells were expanded using a rapid expansion method by which 10^6 T cells were stimulated with 30 ng/mL anti-CD3ϵ (OKT3; Ortho Biotech), 5 × 10^7 γ-irradiated autologous PBMCs, and 10^7 γ-irradiated autologous BLCLs in 50-mL culture media (*21*). Cultures were then supplemented with 50 U/mL IL-2 and 10 ng/mL rhIL-15 every 48 hours. OKT3 expansions of T cells were performed on day 53, 71 and 78 to reach enough cell numbers for *in vivo* studies.

Xenograft models

In vivo studies utilized six- to 10-week old NOD/Scid IL-2RγC null (NOG) mice. Two tumors models were generated by subcutaneous injection of 3 × 10^5 cells from an colon HLA A0201$^+$ carcinoma cell line transduced to express CMVpp65 (Coca pp65) and an ovarian carcinoma cell line also expressing HLA A0201$^+$ (SKOV-A2). The two tumor cells lines were both transduced to express firefly luciferase five days before T cell transfer. The growth of these tumors could then be imaged by bioluminescence following I.P. injection of luciferin. In the adoptive transfer experiment, we injected 1 × 10^7 T_{CM} or T_{EM} derived extGluc$^+$GFP$^+$ CMV-specific T cells on day 0 by retro-orbital injection into tumor-bearing NOG mice. Irradiated BAF3 IL15/15Rα cells as previously described (*27*) (1 × 10^6) were administered intraperitoneally once a week starting on day 0 to provide a systemic supply of human IL15/15Rα complex in IL-15 treated groups in vivo. In IL-2 treated groups, IL-2 was given twice a week (2000U/mice). The mice were

then monitored in weight and general health. Tumors were imagined by bioluminescence at 0, 7, 14, 21, and 30 days post T-cell infusion. At 40 days, the mice were euthanized and autopsied. Tumors, spleen, and liver were examined for T-cells by immunohistochemistry.

Bioluminescence imaging

Bioluminescence was detected using a Xenogen IVIS Imaging System (Xenogen) as previously described (*28*). We performed imaging of the T cells either immediatedly following retro-orbital injection with coelenterazine (250 µg) (Nanolight Technology) or tumors 10 mins after intraperitoneal injection of D–luciferin (150 mg kg) (Xenogen). We imaged mice individually whenever coelenterazine substrate was used whereas 5 mice were simultaneously imaged in luciferin-based acquisitions. Time of image acquisition was in the range of 0.5 to 3 min. Field of view of 15, 20, or 25 cm with low, medium, or high binning in an open filter was utilized to maximize signal intensity and sensitivity. We obtained acquisition of image data sets and measurement of signal intensity through region of interest (ROI) analysis using Living Image software (Xenogen), and normalized images displayed on each data set according to color intensity.

Immunohistochemistry

For in situ expression analysis of T cells, immunohistochemistry analysis was performed. Formalin-fixed paraffin-embedded samples of tissue biopsies were performed of the Department of Pathology at MSKCC. IHC was performed as described previously (*29*). Briefly, slides were subjected to a heat-based antigen

retrieval procedure (30 minutes, 98°C) followed by the application of the first primary antibody (CD8 and CD45, DAKO) overnight at 4°C. A biotinylated horse-anti-mouse secondary antibody (1:200; Vector Laboratories) was used to detect the primary antibody, followed by an avidin-biotin-complex system with peroxidase as a reporter enzyme (elite ABC kit; Vector Laboratories); 3,3-diaminobenzidine tetrahydrochloride (liquid DAB; Biogenex) served as chromogen for the visualization of CD45 and CD8 expression. Appropriate negative controls omitting the primary reagent were included for each case.

Statistical analysis

We performed statistical analyses using Prism (GraphPad Software). We used a nonparametric Mann-Whitney test to compare two groups between different tumor growth. Two-sided p values were used; where indicated in figures signifies **p = 0.01

3. Results

3.1. Characterization of CMV-specific CD8$^+$ T cell clones derived from T_{CM} and T_{EM} cell population for adoptive T cell transfer

Clonally derived CD8$^+$ T cells isolated from central memory T cells are functionally distinct from those derived from effector memory T cells in nonhuman primates (*13*). To examine whether this is also the case for antigen-specific human T cells, CD8$^+$ CMV-specific T cell clones were isolated from CMV seropositive HLA-A 0201$^+$ donors by single cell sorting CD62L$^+$CD45RO$^+$CD8$^+$ T_{CM} cells and CD62L$^-$CD45RO$^+$CD8$^+$ T_{EM} cells and then sensitizing the sorted T cells with artificial antigen presenting cells (AAPCs) exclusively expressing HLA-A 0201, CMVpp65 and T cell costimulatory molecules as previously described (*30*), using irradiated autologous PBMCs and BLCLs as feeder cells. (figure 1) CD8$^+$ CMV-specific T cell clones derived from T_{CM} and T_{EM} were then isolated 21 days after in vitro sensitization. CMV antigen specific T cells can be identified by NLV-Tetramers, which contain the CMVpp65 epitope NLVPMVATV (NLV) enfolded by HLA A0201. That the T-cells were clonal was confirmed by evaluating the Vβ usage of Tetramer$^+$ T_{CM} and T_{EM} derived clones. (figure 2) In one representative clone, analysis of TCR Vβ chain in the T cell clone derived from the T_{EM} cell population revealed a single Vβ13.1 peak. Another T cell clone derived from the T_{CM} cell population of the same individual exhibited a single Vβ14 peak. Thus, our TCR Vβ repertoire analysis of NLV-Tet$^+$ populations provided evidence that CMV-specific T cell clones derived from both T_{CM} and T_{EM} population could be generated using our AAPC platform.

We then evaluated the phenotype of T cell clones derived from the T_{CM} and T_{EM} populations isolated from each donor's PBMC. After the 21 day expansion, the Tetramer^{+} T cell clones generated from both the T_{CM} and T_{EM} populations exhibited a CD62L^{-}CD45RA^{-} T_{EM} phenotype. This is shown in two representative clones from both populations in figure 3A (left two: T_{CM} derived clones; right two: T_{EM} derived clones).

We then evaluated the T_{CM} and T_{EM} derived clones at a functional level. We first evaluated the capacity of T_{CM} and T_{EM} derived Tet^{+} clones to secret cytokines after antigen stimulation. Accordingly, T_{CM} and T_{EM} derived clones were secondarily stimulated for 6 hours with autologous BLCLs loaded with the NLV-peptide to test for antigen-specific response or with BLCLs loaded with an unrelated peptide, RPH as a control. As shown in figure 3B, T cell clones derived from either T_{CM} or T_{EM} cell populations had the ability to secrete high levels of the cytokines TNF-α and IFN-γ, but not IL-2. T cell clones pulsed with control peptide RPH did not secrete cytokines. Thus, the T cell clones we generated from T_{CM} and T_{EM} populations secreted cytokines in an antigen-specific manner. We further evaluated the cytotoxic activity of T_{CM} and T_{EM} derived clones by ^{51}Cr release assay. The cytotoxic activity of the CMV-specific clones was examined at an E/T ratio of 10:1 and 1:1 using autologous BLCLs pulsed with NLV peptide as target cells. Specific lysis of these target cells was quantitated in comparison to lysis of un-pulsed autologous BLCLs as controls. All of the T_{CM} and T_{EM} derived

clones could specifically lyse the target cells (figure 3C). Of the 4 clones derived from T_{CM} population, 3 exhibited 20-40% specific lysis, and one clone exhibited 80% specific lysis (left panel). Of four representative T_{EM} derived clones, all 4 exhibited a similar level of specific lysis, ranging from 40-60% (right panel). No Significant differences were observed in the cytotoxicity exhibited by the T_{CM} or T_{EM} clones at E/T ratios of 10:1 and 1:1. Thus, based on our functional analysis of T_{CM} and T_{EM} derived clones, both T_{CM} and T_{EM} derived clones have a similar level of functional ability to secrete cytokine and induce cytotoxcicity in response to CMV antigen. Therefore, our data are consistent with those of Berger et al. (*13*) in that CMVpp65 specific T-cell clones derived from T_{CM} and T_{EM} populations in the blood after extended in vitro expansion exhibit a T_{EM} phenotype and are indistinguishable in their effector function.

3.2. Evaluation of the persistence, homing capacity and functional properties of CMV-specific $CD8^+$ T cell derived from T_{CM} and T_{EM} cell populations following adoptive transfer in vivo

We next wished to examine the acticity of CMV-specific cells derived from T_{CM} and T_{EM} populations in vivo. Unfortunately, despite several attempts, we were unable to expand T cell clones derived from T_{CM} and T_{EM} to numbers adequate to perform the in vivo studies planned. Accordingly, we decided to analyze the activity of the full spectrum of CMVpp65-specific memory T cells generated from T_{CM} and T_{EM} populations in our in vivo model. To visualize the T-cells in vivo we used a modification of a bioluminescence system to image T-cells expressing a

membrane-anchored form of the Gaussia luciferase (GLuc) enzyme, termed extGLuc, previously described by Santos et al. (*26*). Accordingly, as outlined in figure 4, we first sorted $CD62L^+CD45RO^+CD8^+$ T_{CM} and $CD62L^-CD45RO^+CD8^+$ T_{EM} cell populations from the PBMC of seropositive HLA $A0201^+$ donors and sensitized them with the artificial antigen presenting cells (AAPCs) expressing HLA-A 0201 and CMVpp65. Four days post stimulation, the T-cells were transfected with a retroviral vector encoding extGLuc in the presence of irradiated BAF3 cells constitutively expressing IL15/15Rα complex (BAF3-IL15/15Rα) at a ratio of 10 T-cells : 1 BAF3-IL15/15Rα cells were added to increase the proliferation of the sensitized T cells in order to enhance transduction efficiency with the extGLuc vector. To maximize the number and concentration of CMV-specific T cells derived from T_{CM} and T_{EM} population labeled with extGLuc, we FACS sorted GFP^+ cells after 4 rounds of antigen-stimulation, and further expanded with 2 rounds of sensitization with the $CMVpp65^+$ AAPC in the presence of OKT3 (figure 5), this protocol yielded sufficient numbers of CMVpp65 Tet^+ cells of high purity for the in vivo experiments. The phenotypic and functional characteristics of the CMV-specific T cells were validated before T cell infusion. The T_{CM} and T_{EM} derived cells contained 86% and 89% NLV-$Tetramer^+$ T-cells (figure 6A). As previously shown for T_{CM} and T_{EM} derived T cell clones, both T_{CM} and T_{EM} derived GFP^+ cells exhibited a T_{EM} phenotype before infusion. The level of GFP expressing cells was also confirmed in both populations (figure 6A). We also examined the capacity of the Tet^+ GFP^+ T-cells to specifically secrete cytokines in response to

antigen stimulation after 78 days of expansion. In vitro expanded GFP^+ T_{CM} and T_{EM} derived cells were secondarily stimulated for 6 hours with autologous NLV peptide loaded BLCLs, and compared to the unpulsed control. Both GFP^+ T_{CM} and GFP^+ T_{EM} derived cells specifically secreted high levels of TNF-α and IFN-γ in response to the CMVpp65 peptide (figure 6B).

For our studies of the T-cells *in vivo,* we established a human xenograft model in NSG mice (IL-2R-γc-KO on NOD/SCID mice), mice which have been described as the most permissive hosts for engraftment of human cells and tissues (*31*). In this model, two human tumor xenografts are grown in each mouse, one an HLA A0201+ colon carcinoma transduced to express CMVpp65 (Coca pp65), and the other an ovarian cancer control tumor expressing HLA-A 0201 (SKOV-A2) but not CMVpp65. The expression of HLA-A 0201, CMVpp65, and the co-stimulatory molecules ICAM-1, B7.1 and LFA-3 in Coca pp65 and SKOV-A2 are illustrated in figure 7A. Compared with an HLA-A 0201 BLCL cell line that expresses high levels of HLA-A 0201, ICAM-1, B7.1 and LFA-3, the Coca pp65 and SKOV-A2 cells express similarly high levels of HLA-A 0201 and ICAM-1, but low levels of B7.1. Coca pp65 express high levels of LFA-3 (78%), while SKOV-A2 cells express low levels of LFA-3 (21%). The expression of CMVpp65 in the Coca pp65 cell line was confirmed by IHC staining using a florescence labeled CMVpp65 antibody (figure 7B).

To assess the *in vivo* function of T_{CM} and T_{EM} derived CMV-specific T cell populations, we subcutaneously injected 0.3 million Coca pp65 cell line in the

right thigh and SKOV-A2 tumor cell line in the left flank of each mouse. At day 5, we intravenously infused HLA A0201-restricted extGLuc$^+$ CMV-specific T_{CM} or T_{EM} derived cells into each mouse. We also injected one group of mice with HLA B0702 restricted CMV-specific T cells as a control. To compare the differences between IL-2 and IL-15 treatment, groups of mice were treated with recombinant IL-2 protein (2000U per mouse two times a week) or irradiated BAF3-IL15/15Rα cell line alone. The model and the treatment groups are summarized in figure 11. The level of IL-15 concentration maintained in mouse serum ranged between 100-400 pg/ml in each mouse. Bioluminescent imaging was performed by infusing coelenterazine as the substrate of extGLuc to detect T cell signal, and luciferin as the substrate of luciferase to detect tumor cell growth.

We first compared the accumulation of T cells from T_{CM} and T_{EM} derived cells in IL-2 treated mice. We observed that after infusion, CMV-specific T_{CM} and T_{EM} derived cells were initially detected in the lungs (Day 0 figure 9A). T cells in both populations started to be detected in the spleen from day 3. At no time were they detected in the SKOV-A2 tumor. However, by day 7, T cells from both populations selectively accumulated in the Coca pp65 xenograft expressing CMVpp65. This accumulation in the targeted tumor was transient. Indeed, we failed to detect T cells at the CMVpp65$^+$ tumor site by day 21 (figure 9A). In contrast, we detected a different kinetics and distribution of T cells in mice co-treated with the irradiated BAF3-IL15/15Rα cell line. While the accumulation of both T_{CM} and T_{EM} were again detected only in the Coca pp65 xenograft, T_{CM}

derived T cells accumulated later: by day 14 in one mouse and day 21 in the other 3 representative mice. In contrast, T_{EM} derived T cells accumulated at tumor expressing CMVpp65 earlier, by day 7 in one mouse and day 14 in the other 3 in 4 representative mice (figure 9B). Furthermore, in contrast to the mice treated with IL-2, by day 31, T cells also began to accumulate to the bone marrow (figure 9B).

To compare the T cell accumulation at antigen-bearing tumor sites, we performed quantitative analysis of the bioluminescence signal at the indicated time points, comparing CMV-specific T_{CM} and T_{EM} derived cells in both IL-2 and IL-15 treated mice. In vivo T cell bioluminescent signals were quantified by photons/sec to evaluate the total flux on the different days post transfer. Results are presented in Figure 9C. In mice treated with IL-2, both T_{CM} and T_{EM} derived cells peaked in their accumulation at the Coca pp65 tumor site on day 7 and were detected only in T_{EM} treated mice by day 14. Accumulation of T_{CM} and T_{EM} derived cells, did not differ significantly in IL-2 treated mice (figure 9C: upper panel). In mice treated with irradiated BAF3-IL15/15Rα cell line, T_{CM} derived cells achieved a greater accumulation of T cells at the Coca pp65 tumor site compared to T_{EM} derived cells (figure 9C: lower panel). Mice treated with irradiated BAF3-IL15/15Rα cell also sustained the accumulation of T_{CM} cells in these tumors through 21 days and T_{EM} through 14 days thus providing evidence that L15/15Rα treatment also enhanced CMV-specific T cell persistence at the targeted tumor site when compared to IL-2. (figure 9C) Our experiments thus

showed that both T_{CM} and, to a lesser degree T_{EM} CMV-specific CD8 T cells persisted longer at the targeted tumor sites in IL-15 treated mice.

To evaluate the in vivo function of CMV-specific T_{CM} and T_{EM} derived cells, we next quantified the tumor growth by total flux and converted to the percentage of tumor growth post transfer to evaluate the antitumor activity of the T-cells and cytokines in different treatment groups. In IL-2 treated mice, we failed to show any differences in the growth of Coca pp65 tumors with or without when treated T_{CM} or T_{EM} derived cells or with CMVpp65 specific HLA B0702 restricted, the negative control (figure 10A). On the other hand, in growth of the Cocapp65 tumors in mice treated with irradiated BAF3-IL15/15Rα cells together with either T_{CM} or T_{EM} derived cells was significantly inhibited compared to mice treated with the BAF3-IL15/15-Rα cells alone (figure 10C; **p= 0.01). There were no differences observed on the growth of the SKOV-A2 tumors with or without T cell transfer in either the IL-2 or the IL-15 treated mice (figure 10B and D).

We next evaluated the persistence of detectable CMV-specific human T cells in the spleen, the tumors and the bone marrow of mice bearing the human tumor xenografts by FACS analysis of single cell suspension obtained at autopsy 45 days post treatment. Consistent with our bioluminescent imaging results at day 31, we failed to detect human $CD8^+CD45^+$ T-cells in the spleen from mice treated with either T_{CM} or T_{EM} derived cells irrespective of whether they were treated with IL-2 or IL-15 (figure 11 A and B). For each treatment group one representative graph is presented in the upper panel. The human CD8 T cell frequencies in all

of the mice in each group are presented in the lower panel (n=6).

We attempted to make single cell suspensions for the tumors. However, homogenization of the tumor xenografts, unlike the spleen, yielded mucinous debasing preventing separation of cell suspensions appropriate for FACS. However, each of the tumors was submitted to immune histology evaluation. While human T-cells were detected selectively in the Caco pp65 xenografts, as shown in Figure 12E, they were rare. These findings are consistent with the results of the bioluminescence imaging since, by day 31, accumulation of neither T_{CM} nor T_{EM} could be detected in the Coca pp65 tumors. In contrast to the spleen and Coca pp65 tumors, but consistent with our bioluminescent imaging, we did identify $CD8^+CD45^+$ human CD8 T cells from both T_{CM} and T_{EM} derived cells in the bone marrow of mice co-treated with IL-15/IL-15Rα (figure 12 A and B). In contrast, we failed to detect either T_{CM} or T_{EM} derived T cells in the marrow of mice co-treated with IL-2. In addition, we did not find human T-cells in mice treated with the control CMVpp65-specific, HLA B0702 restricted T-cells. These results not only provide evidence that IL-15/IL-15Rα compared to IL-2, can prolong T cell persistence, but also indicate that the human T_{CM} and T_{EM} T cells preferentially accumulate and can persist in the bone marrow after population of T-cells accumulated in the targeted tumors have dissipated.

We also examined whether the T_{CM} and T_{EM} derived cells persisting in the marrow exhibited phenotypic and/or functional differences from these infused at the time of adoptive transfer into NSG mice. Accordingly, we extracted T cells

from the bone marrow of mice sacrificed 45 days post transfer that had been treated with irradiated BAF3-IL15/15Rα cells. Phenotypic analysis was performed gated on $CD8^+CD45^+$ human CD8 T cell populations. As shown in figure 12C, both T_{CM} and T_{EM} derived cells have the same $CD62L^-CD45RA^-CCR7^-CD127^-$ effector cell phenotype and are not different from those initially infused. We also evaluated whether the T-cells in the marrow of the NSG mice extracted from bone marrow after engraftment for 45 days are functional. Accordingly, we re-challenged these T-cells with autologous BLCL pulsed with NLV-peptide. IFN- γ secretion and BrdU assays were performed to evaluate T cell proliferation and effector function in the presence or absence of CMVpp65 peptide stimulation. As shown in figure 12I, from one representative mouse, 46% of $CD8^+CD45^+$ human T_E cells secreted IFN-γ in response to CMVpp65 peptide loaded BLCL compared to 0.4% of the T-cells stimulated with BLCLs alone. Similarly, after secondary challenge with NLV-peptide pulsed BLCLs 14.3% of the T-cells were $BrdU^+$ compared to 9.3% of T-cells pulsed with BLCLs alone (figure 12J). These results indicate that T cells persisting in the bone marrow are functional and exhibit antigen-specific IFN-γ production and T cell proliferation. To further evaluate the effects of IL-15/IL-15Rα, we also evaluated the relative expression of IL-15Rα in these T_{CM} and T_{EM} derived T_E cells. Cells in the $CD8^+CD45^+$ gated population exhibited a higher level of IL-15Rα expressing cells in T_{CM} compared to T_{EM} derived cells (T_{CM}: 4.5%; T_{EM}: 0.8% figure 12H). This result is consistent with previous findings in a nonhuman primate model that the T_{CM} but not T_{EM} derived clones expressed higher levels of IL-15Rα (*13*). That study suggested that the

superior persistence of T_{CM} derived cells was due to their higher expression of IL-15Rα (*13*). Our data suggest that the higher expression level of IL-15Rα in T_{CM} derived cells might also explain the greater accumulation of T_{CM} derived cells at the targeted Coca pp65 tumor site compared to T_{EM} derived cells.

4. Discussion

The characteristics of antigen-specific memory T-cells have been postulated to be major determinants of the persistence of transferred cells and correlates of therapeutic efficacy. Previous studies by Berger et al. (*13*) of autologous CMV-specific T-cells in macaques have demonstrated that $CD8^+$ effector T cells derived from macaque $CD62L^+CD95^+$ T_{CM} precursors, retain the capacity to engraft and reconstitute functional memory upon adoptive transfer, whereas effectors derived from $CD62L^-$ T_{EM} precursors do not. In a subsequent study from the same group, Wang et al. (*21*) adoptively transferred human CMV pp65-specific T-cells generated from the $CD8^+CD45RO^+CD62L^+$ T_{CM} or $CD8^+CD45RO^+CD62L^-$ T_{EM} fractions of PBMCs derived from seropositive donors into NSG mice, and observed that while both fractions were able to achieve engraftment, the T_{CM} derived cells engrafted to a markedly greater extent, and that the T_E derived from these cells exhibited greater diversity, secreted higher levels of IL-2 and were able to prevent outgrowths of intravenously administered autologous EBV transformed BLCL transduced to express CMVpp65. While both T_{CM} and T_{EM} derived T_E cells proliferated *in vivo*, a significantly higher proportion of T_{EM} derived T-cells underwent apoptosis. Furthermore, in their model, growth of both T_{CM} and T_{EM} derived T-cells were sustained only in NSG mice that also received twice weekly intraperitoneal injections of irradiated murine NSO myeloma cells transduced to express human IL-15 such that the mice were able to maintain IL-15 levels of 6-8 pg/ml. From these experiments, they concluded

that while both T_{CM} and T_{EM} derived T-cells were dependent on IL-15, T_{CM} derived T-cells had a markedly greater potential of sustained survival and were therefore more likely to provide sustained, antigen-specific function.

In our study, we wished to further define conditions and attributes of CMV-specific T-cells that contributed to their activity against human cells that are actually targets of CMV infection, and to compare T_{CM} and T_{EM} cells under these conditions for their capacity to achieve sustained engraftment, selectively accumulate in sites of antigen expression, and inhibit or eradiate cells expressing the targeted CMV antigen. Accordingly, we developed a human xenograft model in NSG mice in which the mice bear two human carcinomas with similar growth characteristics, both selectively expressing class I HLA A0201, and one, a colon carcinoma line, also transduced to express CMVpp65. The colon carcinoma was chosen because it, like normal colonic epithelium, but unlike human B cells, is naturally susceptible to productive infection by CMV. Indeed, CMV colitis is a significant cause of morbidity and mortality in transplant recipients and other immunocompromised patients. In addition, transduction of the tumor cells to express firefly luciferase permitted sequential evaluations of the growth of the CMVpp65^{+} and CMVpp65^{-} xenografts *in vivo*. In order to contemporaneously delineate the homing characteristics of the transferred T-cells and distinguish their effects on targeted CMVpp65^{+} tumor xenografts, we transduced the T_{CM} and T_{EM} derived CMVpp65-specific T-cells to express both GFP and a Gaussia luciferase which employs a different substrate, coelenterazine, and emits a

different light spectrum in bioluminescence imaging.

An initial important finding of our study was that human CMV-specific $CD8^+$ T cells derived from T_{CM} and T_{EM} exhibit superior engraftment in IL15/15Rα treated mice compared to IL-2 treated mice. This result extends the findings of Wang et al. (*21*), who found that the IL-15 provided by irradiated IL-15 providing NSO cells was required for sustained *in vivo* engraftment and survival of transferred human antigen-specific T cells. However, in contrast to their findings that antigen-specific $CD8^+$ T-cell clones derived from T_{CM}, but not T_{EM}, were capable of engrafting long-term, we failed to show a significant difference in the long-term engraftment of T cells derived from T_{CM} and T_{EM}. We did observe, however, that T_{CM} derived $CMVpp65^+$ specific T-cells selectively accumulated in the CoCa $CMVpp65^+$ tumors to a much greater degree and for a longer interval than T_{EM} derived $CMVpp65^+$ specific T-cells. However, despite the differences in accumulation in the $CoCapp65^+$ tumors, the T_{CM} and T_{EM} derived T-cells induced an almost identical degree of suppression of the growth of these tumors. Furthermore, the absence of any accumulation of T-cells in or inhibition of the growth of the SKOV-A2 tumors suggests that neither the T_{CM} nor the T_{EM} derived CMVpp65-specific T-cells exert an antigen-nonspecific effect.

A striking characteristic of both T_{CM} and T_{EM} derived CMVpp65 specific T-cells in this model was their long term persistence in the bone marrow of NSG mice that received injections of the irradiated BAF-3 cells secreting IL-15 and IL-15/IL-15Rα complex. Similar to the findings of Wang el al. (*21*) in mice that did not

receive IL-15 secreting cell supplementation, neither T_{CM} derived nor T_{EM} derived T-cells were detected in the marrow of mice treated with IL-2. Unlike the findings of Wang et al. (*21*) in mice treated with NSO cells secreting IL-15 alone, the levels of T_{CM} and T_{EM} derived T-cells that persisted in the marrow of our mice were not significantly different. However, in agreement with their findings, we found that the T-cells in the marrow consisted exclusively of T_{EM} and T_E T-cells. We did not detect any T-cells exhibiting a $CD45RO^+CD62L^+CCR7^+$ T_{CM} phenotype as has been described in primates infused with autologous CMV-specific T_{EM} and T_E cells generated from T_{CM} precursors in the blood. We did, however, observe that the T_{CM}-derived T_E cells persisting in the marrow differed from T_{EM}-derived T_E cells in that a proportion of these T_E cells expressed IL-15Rα, a finding also reported by Berger et al. (*13*) for T_{CM} derived T-cells that persist long-term in non-human primates. The T_{CM}-derived T_E cells in the marrow were also able to proliferate and to generate IFN-γ in response to CMVpp65 peptide indicating their functional competence.

Taken together, our studies indicate that while T_{CM} and T_{EM} derived T-cells exhibited differences in phenotype and in the kinetics and degree of their respective accumulations in $CMVpp65^+$ CoCa xenografts, their antigen-specific activities and their persistence *in vivo* were equivalent. The differences between our findings and those of Wang et al. (*21*) principally hinge on the limited levels of engraftment and persistence of T_{EM} derived T-cells in the marrow that they observed, attributes that they ascribed to the markedly increased level of

apoptosis detected in the T_{EM} derived T-cell populations even early after antigen-stimulation. While multiple factors may contribute to this disparity in results, one clear possibility is that in our model, the NSG mice received regular injections of irradiated BAF-3 cells generating both human IL-15 and IL-15Rα while the NSG mice in the studies of Wang et al. (*21*) received injections of irradiated NSO cells secreting human IL-15 alone. The levels of IL-15 thereby sustained in the blood of the mice were markedly different, ranging from 100 to 400 pg/ml blood in the mice receiving the BAF3 cells secreting IL-15 and IL-15Rα compared to 4-6 pg/ml in the mice treated with the NSO cells secreting IL-15. Furthermore, since IL-15/IL-15Rα are also secreted and can act in trans (*32*), they may provide an adequate stimulus to the T_{EM} derived T-cells to enhance and sustain their survival and function. This mechanism may also, in part, explain why, in both models, the bone marrow is the only site where significant populations of CMVpp65-specific T_{EM} derived T-cells are detected, since antigen-specific memory $CD8^+$ T-cells have been shown to receive proliferative signals from IL-15 secreting cells in the marrow (*33*), and in human bone marrow, cells expressing IL-15Rα can trans-present IL-15 on their surface (*32*).

A unique finding in our study is the disparity between the transient accumulations of the CMVpp65-specific T_{CM} and T_{EM} in the Cocapp65 xenografts in the mice co-treated with IL-15/IL-15Rα and their persistence in the marrow of the same mice for more than 14 days after accumulation of T-cell in the tumors had decreased to levels no longer imaginable. The fact that the T_{CM} and T_{EM} derived T-cells

isolated from the marrow retained their capacity to generate cytokines and lyse targets co-expressing the NLV peptide and its presenting HLA A0201 allele indicates that the T-cells persisting in the marrow are not tolerized. Rather, it suggests either that these T-cells never migrated to the tumor xenograft, or, if they did, subsequently emigrated to the marrow seeking either a less inhibiting or more supportive microenvironment than that provided by the former xenograft.

In summary, our comparisons of CMV-specific T_{CM} and T_{EM} derived cells, both as T-cell clones studied *in vitro* and as polyclonal CMVpp65-specific T-cell *in vivo* have shown that T_{CM} and T_{EM} derived cells exhibit a similar effector memory phenotype as determined by CD62L and CD45RA expression level. *In vitro*, both T_{CM} and T_{EM} clonal populations exhibit comparable HLA-restricted cytotoxic activity against CMVpp65^{+} target cells and secretion of high levels of IFN-γ and TNF-α, but not IL-2. In NSG mice bearing CMVpp65^{+} and CMVpp65^{-} HLA A0201^{+} human tumor grafts that are also treated with irradiated IL-15 and IL-15Rα secreting cells (but not in mice treated with IL-2), both T_{CM} and T_{EM} derived T cells selectively but transiently accumulate in the tumors coexpressing CMVpp65 and HLA A0201, induce an equivalent degree of inhibition of the growth of these tumors and thereafter, either die off or leave the tumor site by 31 days persist at similar levels in the marrow for at least 45 days post infusion. The differences we found lie in the greater and more prolonged accumulation of T_{CM} derived cells at CMVpp65^{+} tumor sites compared to T_{EM} derived cells in the IL-15/IL-15Rα treated mice. Whether and to what degree these findings reflect the

higher level of IL-15Rα expression observed in T_{CM} derived cells or other signaling molecules promoting their more sustained accumulation in targeted tumors remain to be determined.

Figure 1.

Experimental design for isolation and expansion of human CMV-specific CD8 T cell clones from T_{CM} and T_{EM} population

T cell populations representing T_{CM} and T_{EM} were gated and sorted based on the following markers: T_{CM} as $CD8^+CD45RO^+CD62L^+$ and T_{EM} populations as $CD8^+CD45RO^+CD62L^-$. Single cell sorted T cells were replated at 1 cells/well in 96-well round-bottom plates with 2×10^4 γ-irradiated HLA $A0201^+$, $CMVpp65^+$ AAPCs, 5×10^5 γ-irradiated autologous peptide-pulsed PBMCs and 2×10^5 γ-irradiated BLCLs in T cell media with 50 U/ml IL-2 and 25ng/ml recombinant IL-15.

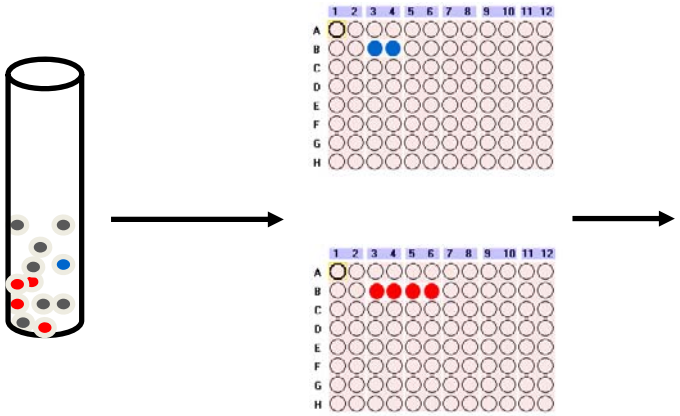

Stimulated with feeder cell mixture
A2pp65 AAPC-3T3 based artificial antigen presenting cells express HLA A0201, CMVpp65 and costimulatory molecules (ICAM-1, B7.1, LFA-3 and β2m)
autologous PBMC
autologous BLCLs

Blue: T_{CM}-CMV specific T cells
Red: T_{EM}-CMV specific T cells

T cells from CMV- seropositive donor bearing HLA-A0201 sorted by
T_{CM}: $CD8^+CD62L^+CD45RO^+$
T_{FM}: $CD8^+CD62L^-CD45RO^+$

Figure 2.

T_{CM} and T_{EM} derived clonal population were confirmed by TCR Vβ repertoire analysis

TCR Vβ repertoire analyses were shown from one of the representative clones from both T_{CM} and T_{EM} derived cells. Each bar graph represents the TCR Vβ usage from T_{EM} and T_{CM} derived cells. T_{EM} derived clone 58 revealed a single Vβ13.1 peak (upper graph), whereas T_{CM} derived clone 25 from the same individual exhibited a single Vβ14 peak (lower graph).

T_{EM}: Clone 58

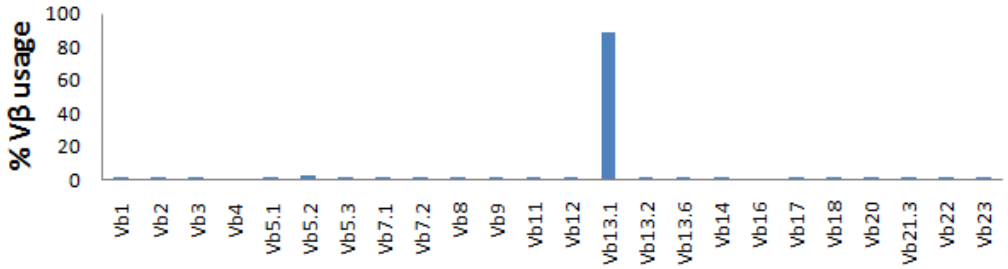

T_{CM}: Clone 25

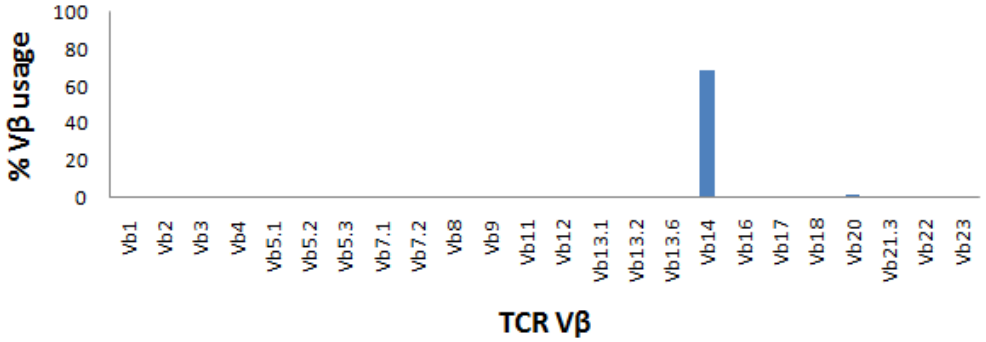

Figure 3.

Phenotypic and functional characterization of T_{CM} and T_{EM} derived CMV-specific CD8 T cell clones

(A) T cell clones derived from the T_{CM} (clone 12 and clone 15; Left 2 lanes) and T_{EM} (clone 46 and clone 66; Right 2 lanes) populations isolated from the same donor. HLA-A2-NLV tetramer binding gated on CD8 T cells was confirmed in each T_{CM} and T_{EM} derived clones (upper graph). Expression of CD62L and CD45RA on individual T_{CM}- and T_{EM}-derived clones was evaluated (lower graph). The data were from two representative clones in each population. (B) Expanded T cell clones derived from T_{CM} (left lane) and T_{EM} (middle lane) were stimulated for 6 hours with NLVPMVATC (NLV) peptide loaded autologous BLCLs at a ratio of 5:1 from one representative clone. T-cells co-cultures with autologous BLCLs with unrelated peptide RPH loaded autologous BLCLs served as controls (right lane). Cytokine secretion of T_{CM} and T_{EM} derived clones were evaluated by intracellular staining within T cell clones using anti-IFN-γ, anti-TNF-α, and anti-IL-2 antibody. (C) Cytotoxic activity of T_{CM}-derived (left panel) and T_{EM}-derived clones (right panel) were examined at an effector-to-target ratio (E/T ratio) of 1:1 and 10:1 using autologous BLCLs loaded with or without NLV-peptide as target cells.

(A)

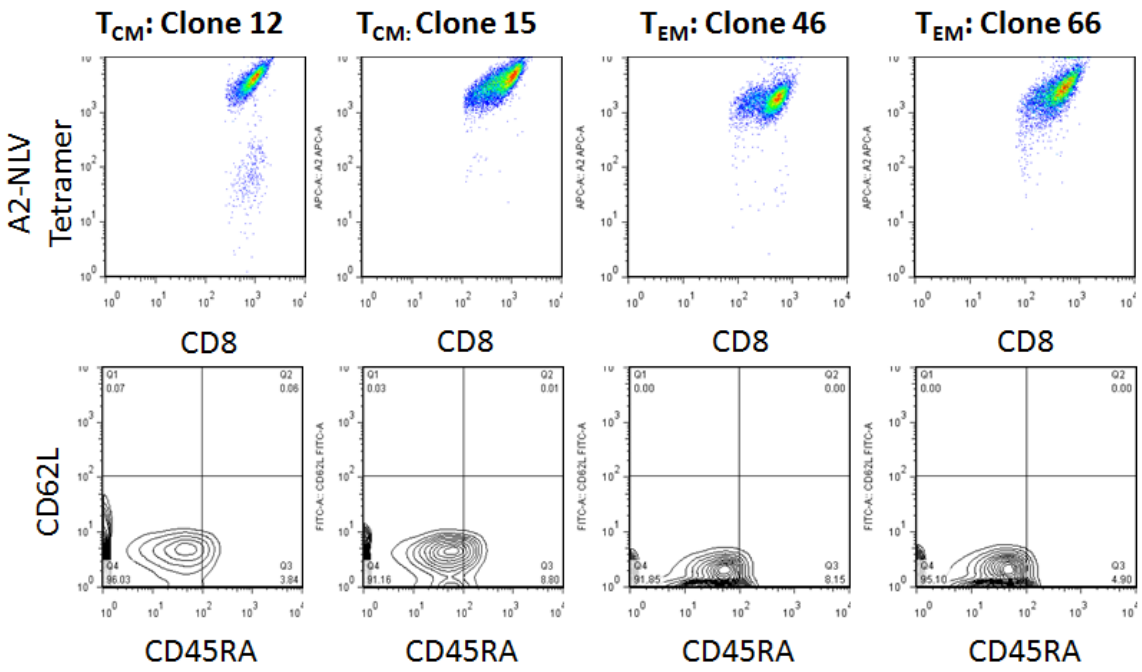
T_CM: Clone 12
T_CM: Clone 15
T_EM: Clone 46
T_EM: Clone 66
A2-NLV Tetramer
CD8
CD62L
CD45RA
Q1 0.07
Q2 0.06
Q4 96.03
Q3 3.84
Q1 0.03
Q2 0.01
Q4 91.16
Q3 8.80
Q1 0.00
Q2 0.00
Q4 91.85
Q3 8.15
Q1 0.00
Q2 0.00
Q4 95.10
Q3 4.90

(B)

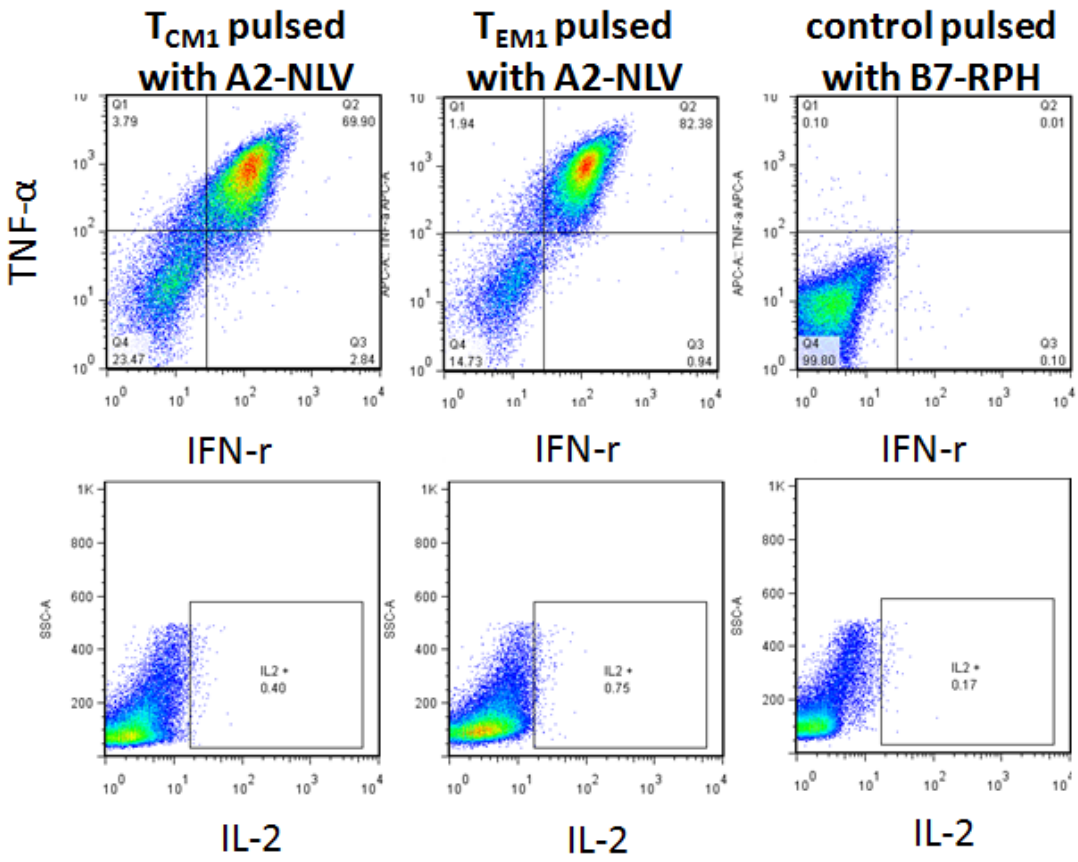
T_CM1 pulsed with A2-NLV
T_EM1 pulsed with A2-NLV
control pulsed with B7-RPH
TNF-α
IFN-r
IL-2
Q1 3.79
Q2 69.90
Q4 23.47
Q3 2.84
Q1 1.94
Q2 82.38
Q4 14.73
Q3 0.94
Q1 0.10
Q2 0.01
Q4 99.80
Q3 0.10
IL2 + 0.40
IL2 + 0.75
IL2 + 0.17

Figure 3 (Continued)
(C)

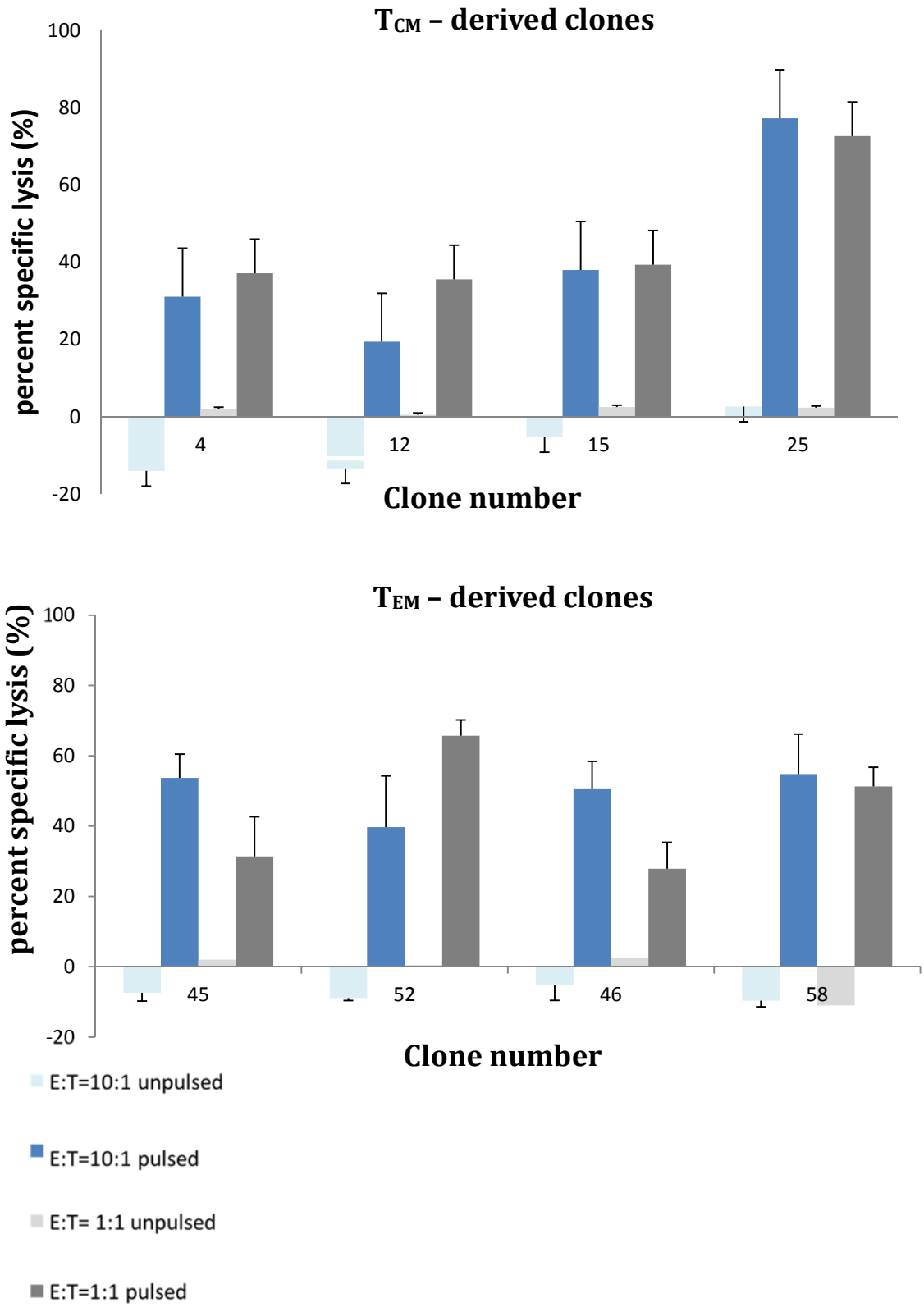

Figure 4.

Experimental design for generation of genetically modified CMV-specific T cells expressing reporters for bioluminescent imaging *in vivo*

Retroviral gene transduction

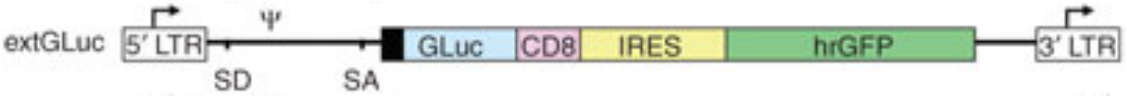

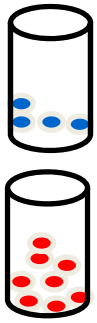

feeder cell mixture:
A2pp65 AAPC x
autologous PBMC x
BAF3 IL15/15Rα x

retrovirus infection

sorting GFP^{+}

OKT3 expansion to 10×10^{6} per mice

Blue : T_{CM}
Red : T_{EM}

Figure 5.

Schematic of the methods for generating CMVpp65 specific T cells transduced to express extGLuc

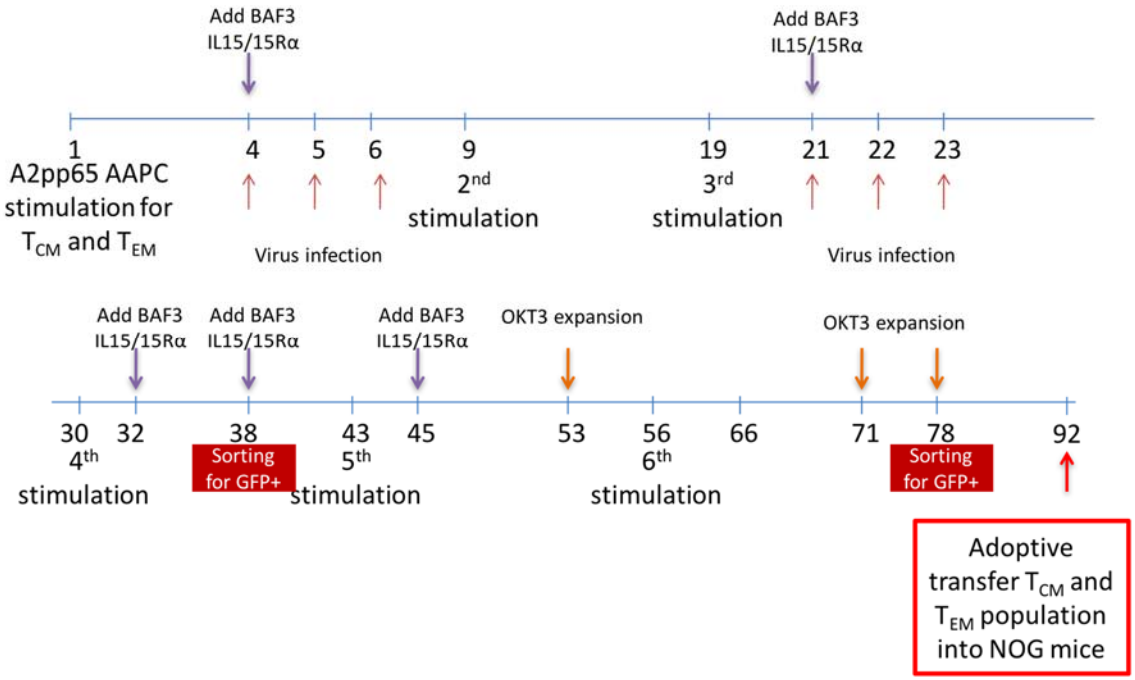
Add BAF3
IL15/15Rα
Add BAF3
IL15/15Rα
1
A2pp65 AAPC
stimulation for
T_{CM} and T_{EM}
4
5
6
9
2nd
stimulation
19
3rd
stimulation
21
22
23
Virus infection
Virus infection
Add BAF3
IL15/15Rα
Add BAF3
IL15/15Rα
Add BAF3
IL15/15Rα
OKT3 expansion
OKT3 expansion
30
4th
stimulation
32
38
Sorting
for GFP+
43
5th
stimulation
45
53
56
6th
stimulation
66
71
78
Sorting
for GFP+
92
Adoptive
transfer T_{CM} and
T_{EM} population
into NOG mice

Figure 6.

Phenotypic and functional characterization of bioluminescent-labeled T_{CM} and T_{EM} derived CMV-specific CD8 T cell lines

(A) Phenotypic analysis of extGLuc$^+$ T cell lines derived from the T_{CM} and T_{EM} populations expanded for 92 days. HLA-A2-NLV tetramer binding gated on CD8 T cells was confirmed in T_{CM} and T_{EM} derived cells. Retrovirus transduced to express extGLuc was confirmed by GFP expression. Expression of CD62L and CD45RA on individual T_{CM}- and T_{EM}-derived clones was evaluated (lower graph). (B) Cytokine secretion of T cell population derived from T_{CM} and T_{EM} expanded for 78 days. T cells derived from T_{CM} (middle lane) and T_{EM} (middle lane) were stimulated for 6 hours with NLVPMVATC (NLV) peptide loaded autologous BLCLs at a ratio of 5:1. T-cells co-cultures with unpulsed autologous BLCLs served as controls (left lane). CD8$^+$ T-cells secreting IFN-γ and TNF-α were evaluated by intracellular staining.

(A)

Day92 before transferred

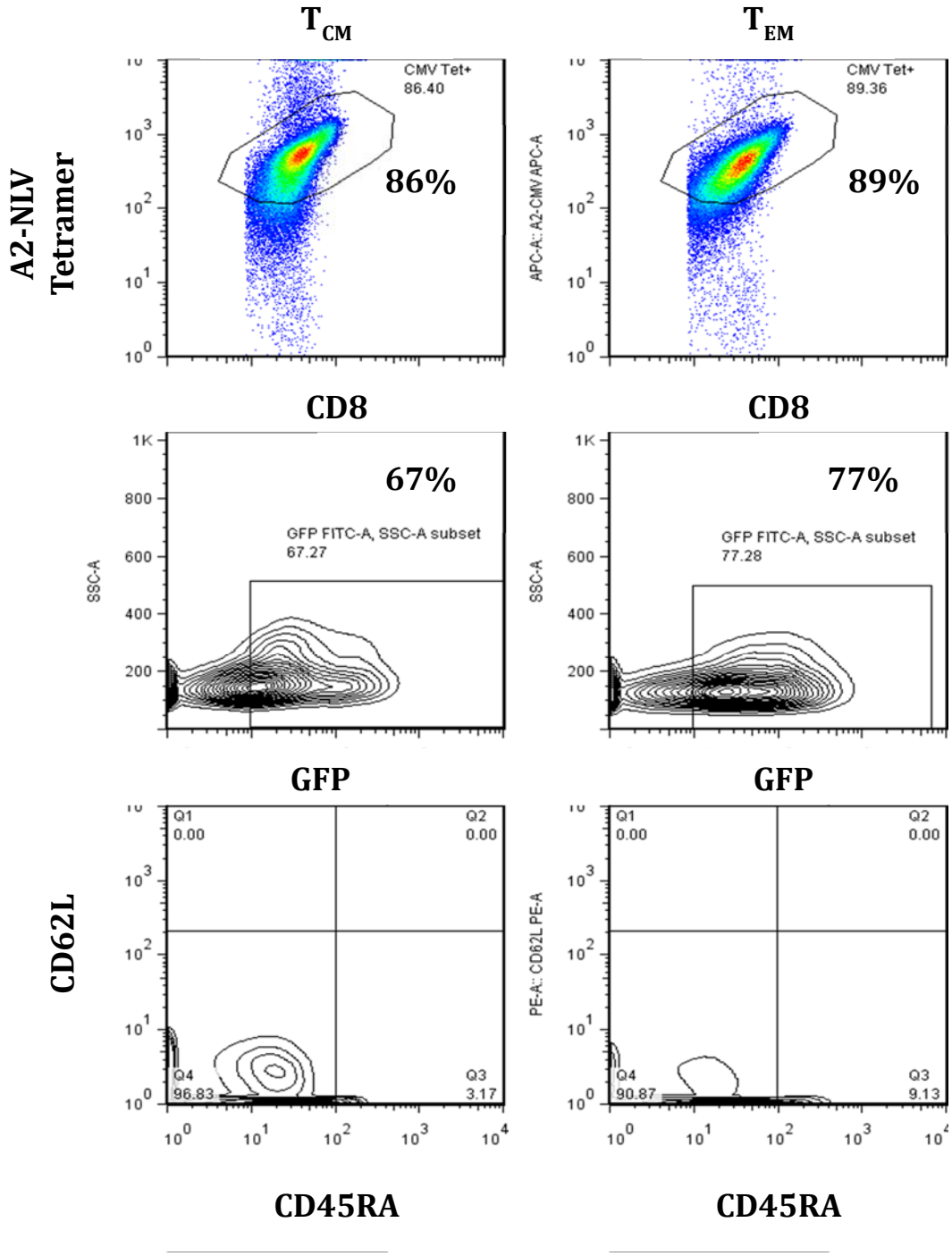

Figure 6 (Continued)

(B) **Gated on $CD8^+$ T cells**

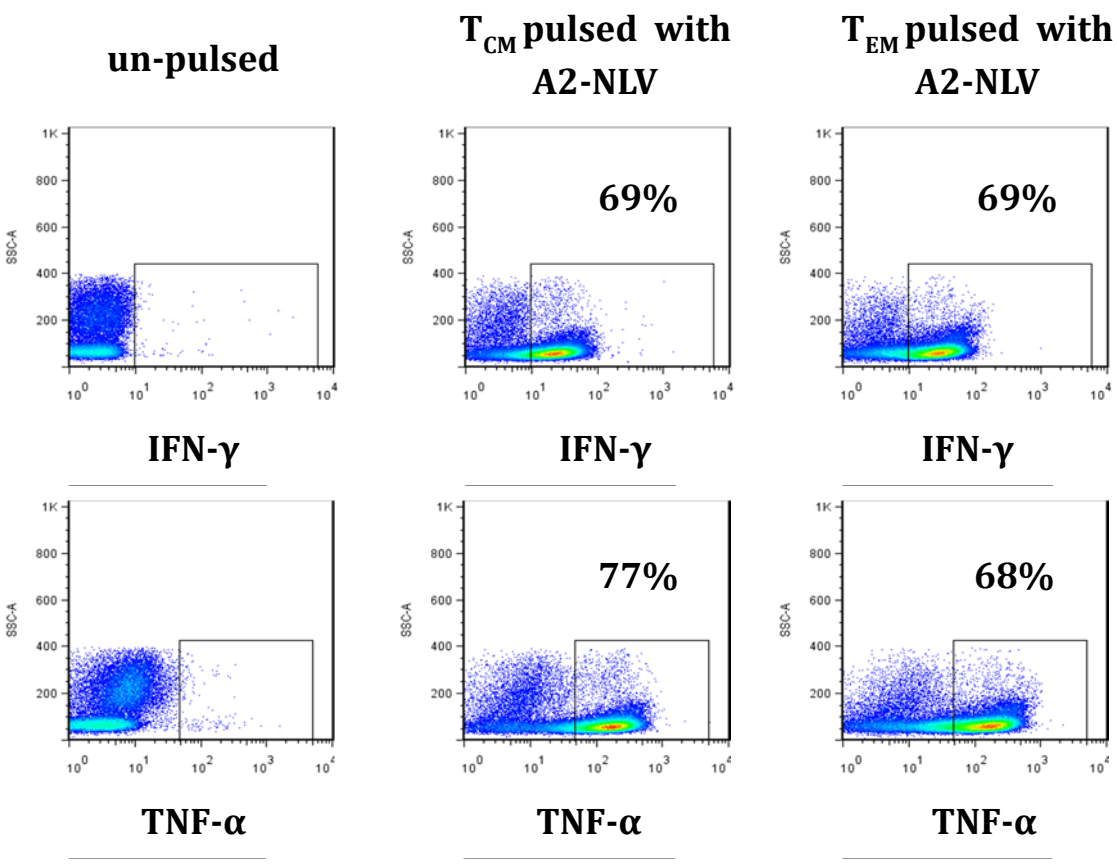

Figure 7.

Expression level of costimulatory molecules in different cell lines

(A) Level of costimulatory molecules expression, including HLA-A2, ICAM-1, B7.1 and LFA-3 on tumor lines (SKOV-A2: middle lane; Coca pp65: right lane) compared to BLCLs (left lane) were evaluated by flow cytometry. (B) Coca tumor cell line transduced to express CMV antigen pp65 was confirmed by IHC staining.

(A)

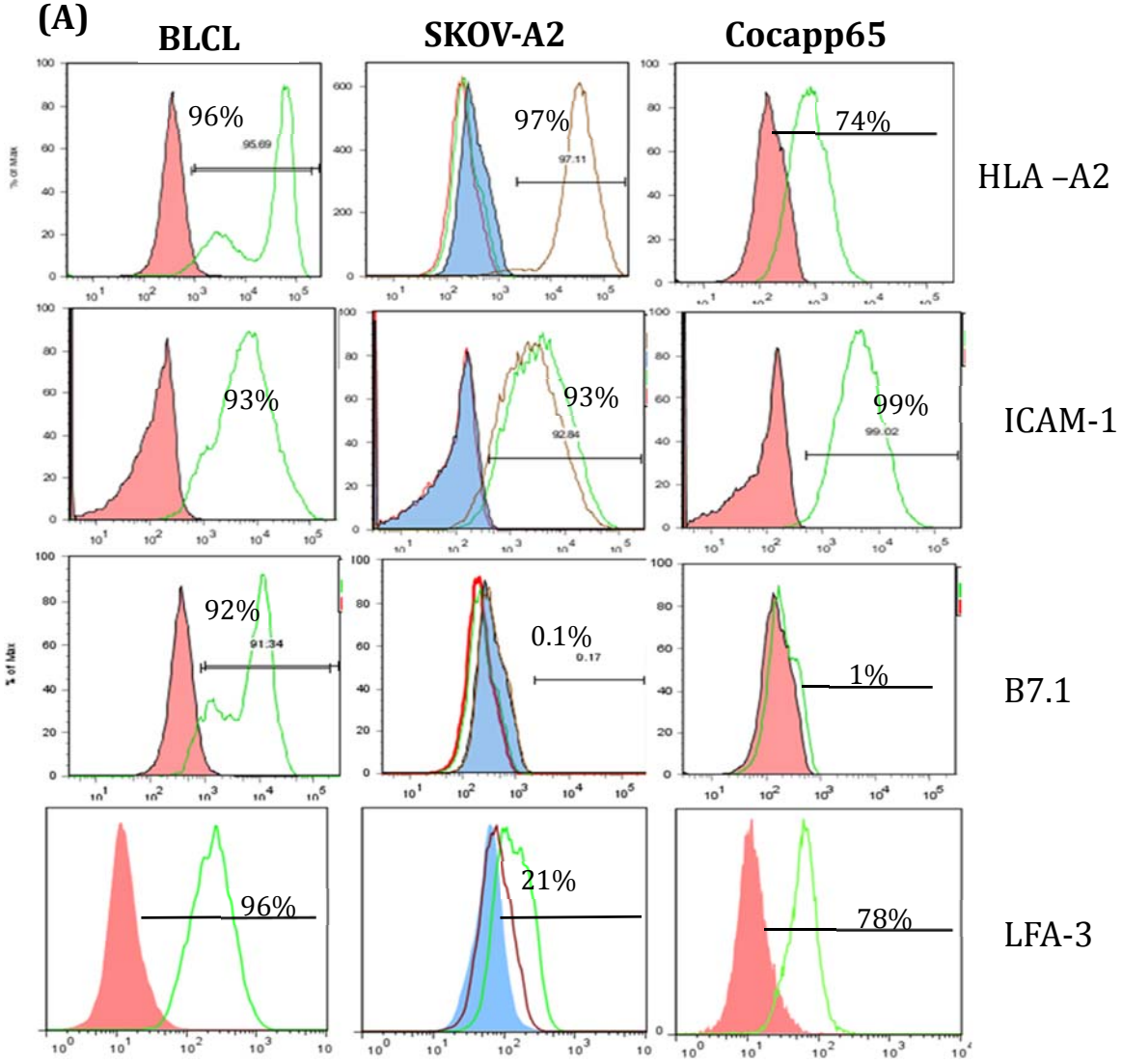

(B)

Cocapp65

expression of CMV pp65

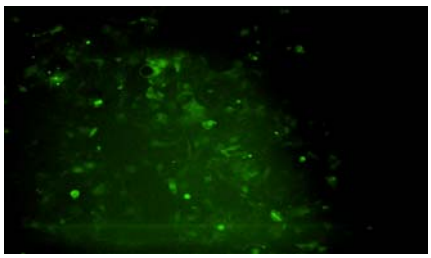

Figure 8 –

Experimental design of bioluminescent imaging for tumor and T cell engraftment in different combination treatment of CMV-specific T cells and cytokines *in vivo*

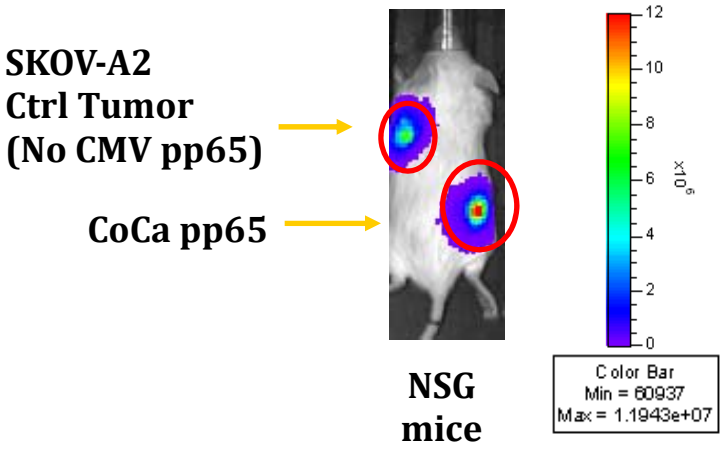

Group number	Cell transfer	Cytokine
Gp1	no	IL2
Gp2	no	BAF3 IL15/15Rα
Gp3	T_{CM}	IL2
Gp4	T_{EM}	IL2
Gp5	T_{CM}	BAF3 IL15/15Rα
Gp6	T_{EM}	BAF3 IL15/15Rα
Gp7	B7- CMV T cell	IL2

Figure 9.

In vivo comparison of T_{CM} and T_{EM} derived CMV-specific T cell bioluminescent signaling in a xenograft tumor model

NOG mice injected with T cells expressing extGLuc imaged by bioluminescent imaging on day 0, 3, 7, 14, 21 and 31 after intravenous injection of coelenterazine. (A) T_{CM} (left panel) and T_{EM} (right panel) derived CMV-specific T cell engraftment in IL-2 treated mice. Strong T cell signal detected at Coca pp65 tumor on day 7 (red circle) (n=6) (B) T_{CM} (left panel) and T_{EM} (right panel) derived CMV-specific T cell engraftment in mice treated with irradiated BAF3 IL15/15Rα cells. T cell accumulated at tumor sites in different mice (red circle). T cell accumulated in bone marrow in different mice (yellow arrow) (n=6). 4 out of 5 mice imaging have shown in (A) and (B). (C) Quantitative analysis of signal at the indicated time points. T cell accumulated at Cocapp65 tumor in T_{CM} (black) and T_{EM} (red) derived CMV specific T cells in comparison to IL-2 treated (upper graph) or IL15/15Rα treated mice (lower graph) (n=6).

(A)

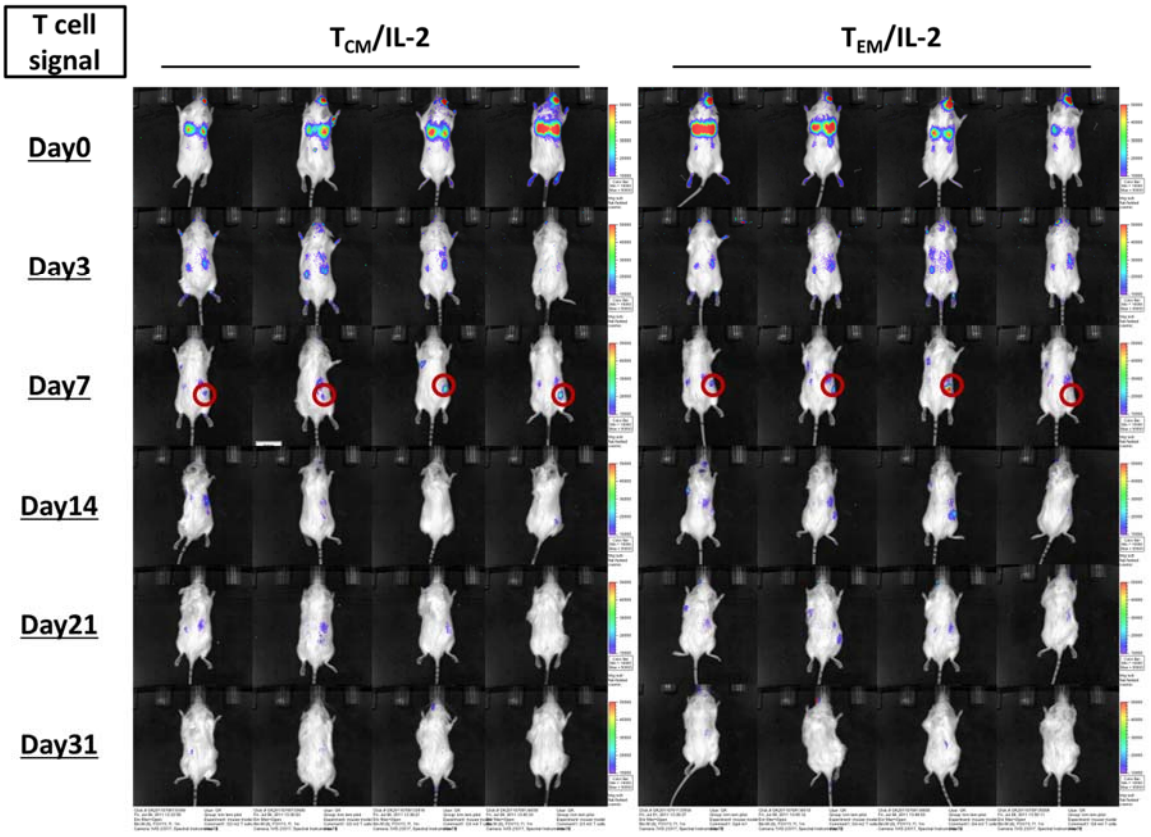
T cell signal
T_{CM}/IL-2
T_{EM}/IL-2
Day0
Day3
Day7
Day14
Day21
Day31

Figure 9 (Continued)
(B)

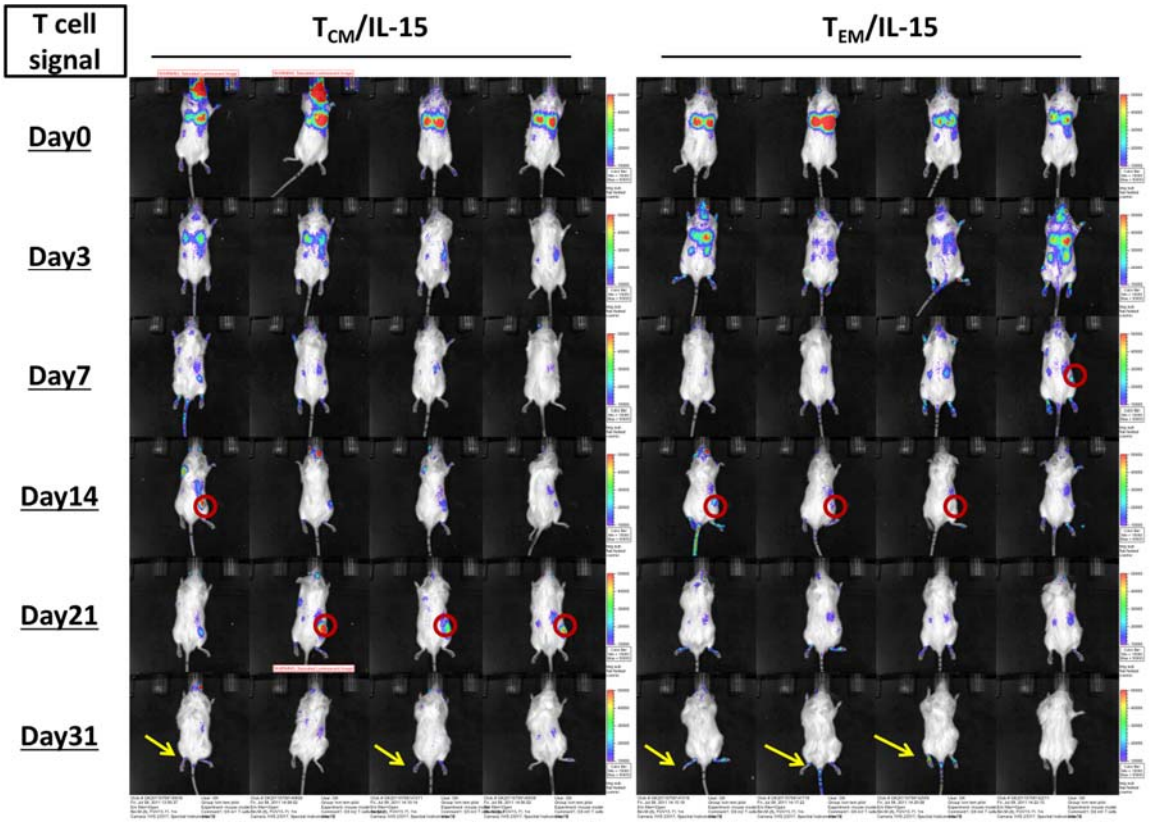

Figure 9 (Continued)
(C)

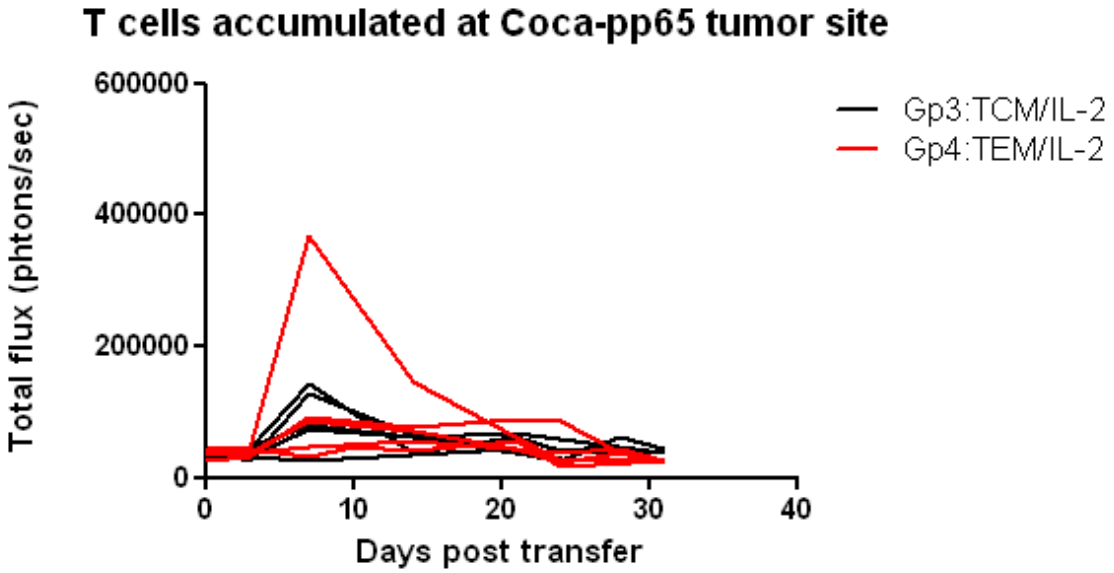

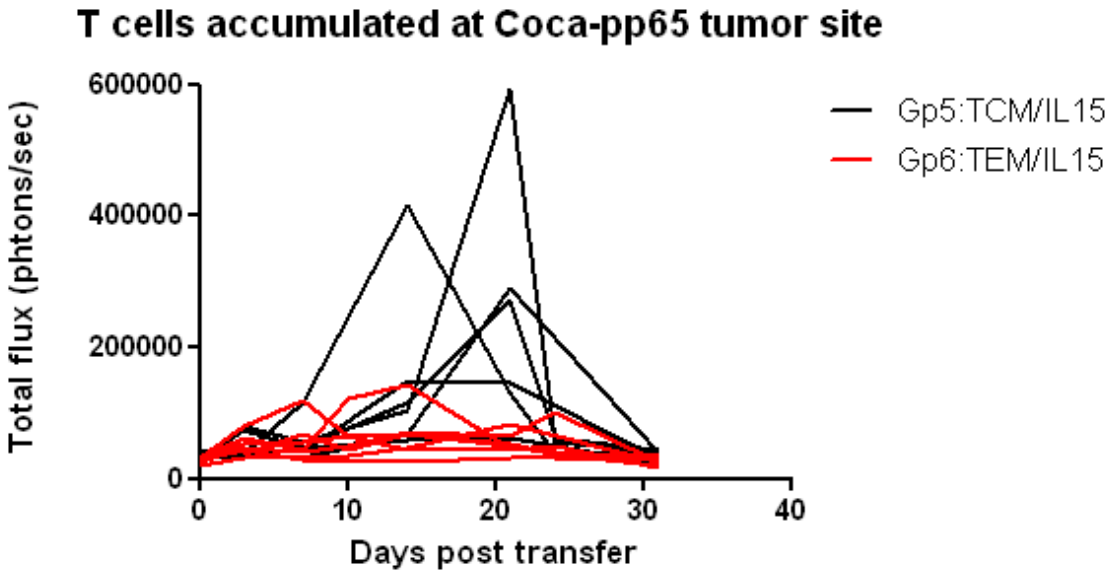

Figure 10.

Adoptively transferred CMV-specific CD8 T cells exhibit superior protection from tumor growth in IL-15 treated mice

To assess the in vivo function of CMV-specific T cells derived from T_{CM} and T_{EM} populations, quantitative analysis of tumor growth signals at different dates post transfer were evaluated in Coca pp65 (A and C) and SKOV-A2 (B and D) tumors. (n=6 in each group) NOG mice adoptively transfered with T cells in comparison of mice treated with IL-2 or irradiated BAF3 IL15/15Rα cells. Unrelated HLA 0702 CMV-specific T cells served as control (Gp7) (n=6). Engraftment of Luciferase expressing Coca pp65 and SKOV-A2 tumors were determined by Xenogen imaging. Total flux levels of luciferase activity were depicted for each group. (**p=0.01 by Mann-Whitney test)

(A) **IL-2**

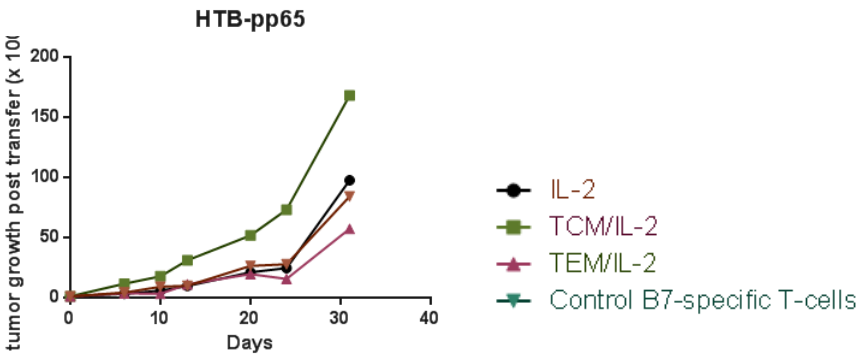

(B) **IL-2**

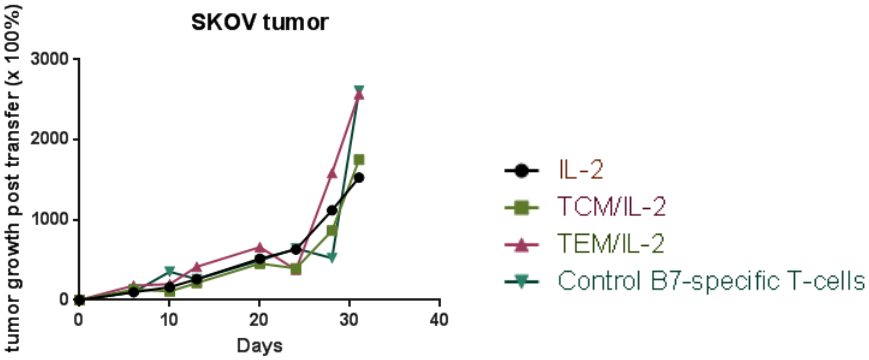

(C) **IL-15/15Rα complex**

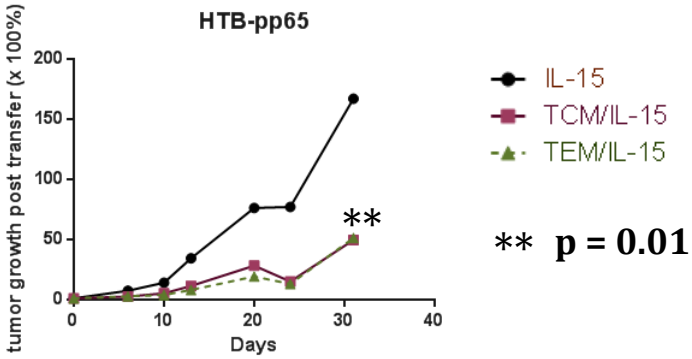

** **p = 0.01**

(D) **IL-15/15Rα complex**

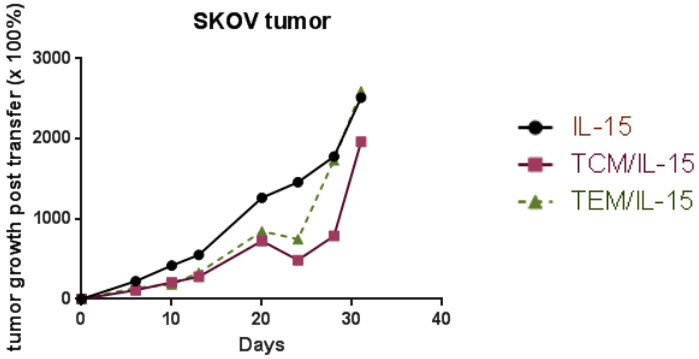

Figure 11.

T_{CM} and T_{EM} derived CMV-specific T cell engraft in the spleen were not detected

T_{CM} and T_{EM} derived CMV-specific T cell engrafted in the spleen were determined by flow cytometry. (n=6 in each group) (A) Flow cytometry analysis was shown from one representative mouse in each group. Human CD8 T cells in the spleen ($CD8^+CD45^+$) were evaluated in mice treated with IL-2 (left two graphs) or irradiated BAF3 IL15/15Rα cells (right two graphs). Percentage of human CD8 T cell frequencies summarized in (B)

(A)

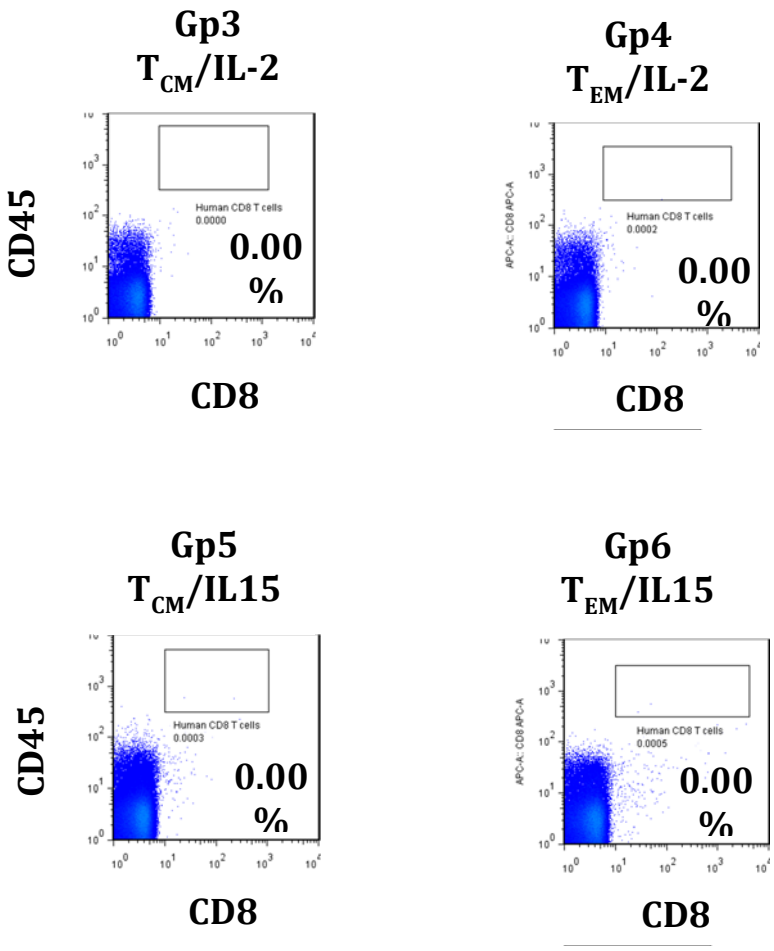
Gp3
T_{CM}/IL-2
Gp4
T_{EM}/IL-2
Gp5
T_{CM}/IL15
Gp6
T_{EM}/IL15
CD45
CD8
Human CD8 T cells
0.00
%

(B)

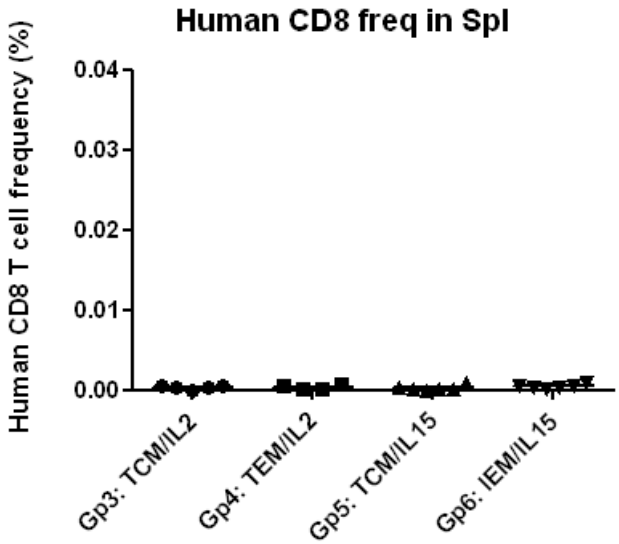
Human CD8 freq in Spl
Human CD8 T cell frequency (%)
0.04
0.03
0.02
0.01
0.00
Gp3: TCM/IL2
Gp4: TEM/IL2
Gp5: TCM/IL15
Gp6: IEM/IL15

Figure 12.

IL-15 dependent engraftment of phenotypic and functional characterization of T_{CM} and T_{EM} derived CMV-specific CD8 T cell lines in the bone marrow

T_{CM} and T_{EM} derived CMV-specific T cell engrafted in the bone marrow 45 days post transfer were determined by flow cytometry. (n=6 in each group) (A) Flow cytometry analysis was shown from one representative mouse in each group. Human CD8 T cells in the bone marrow ($CD8^+CD45^+$) were evaluated in mice treated with IL-2 or irradiated BAF3 IL15/15Rα cells. Percentage of human CD8 T cell frequencies summarized in (B). T_{CM} and T_{EM} derived CMV-specific T cell engrafted in the bone marrow (C), Spleen (D), Coca pp65 tumor(E) and SKOV-A2 (F) were evaluated in mice treated with irradiated BAF3 IL15/15Rα cells by immunohistochemistry staining. CD8 staining positive was detected in bone marrow and Coca pp65 tumor (C and E). No positive signal was detected in Spleen and SKOV-A2 tumor (D and F). (G) and (H) Engrafted T cell phenotype derived from T_{CM} and T_{EM} population in IL-15 treated mice. *Ex vivo* expression of CD62L, CD45RA, CCR7, CD127, IL15Rα and CD132 on T_{CM}- and T_{EM}-derived CMV-specific CD8 T cell gated on human CD8 T cells ($CD8^+CD45^+$) was evaluated. The data was from one representative mouse in each population. (I) and (J) Engrafted T cells are functional in IL-15 treated mice. T cells were stimulated *ex vivo* with NLVPMVATC (NLV) peptide loaded autologous BLCLs at a ratio of 5:1 from one representative mice. T-cells co-cultures without peptide loaded as controls. (I) Cytokine secretion of T cells was evaluated by intracellular staining using anti-IFN-γ. (J) T cell proliferation was evaluated by BrdU assay.

(A)

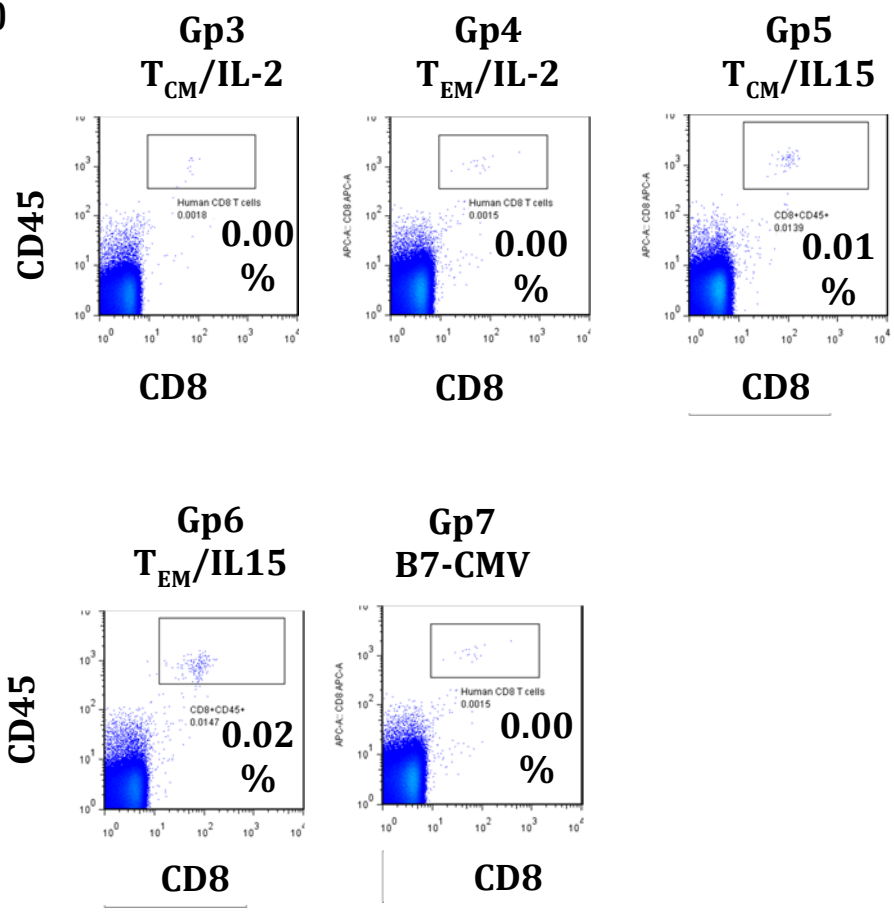
Gp3
T_CM/IL-2
Gp4
T_EM/IL-2
Gp5
T_CM/IL15
CD45
0.00 %
0.00 %
0.01 %
CD8
CD8
CD8
Gp6
T_EM/IL15
Gp7
B7-CMV
CD45
0.02 %
0.00 %
CD8
CD8

(B)

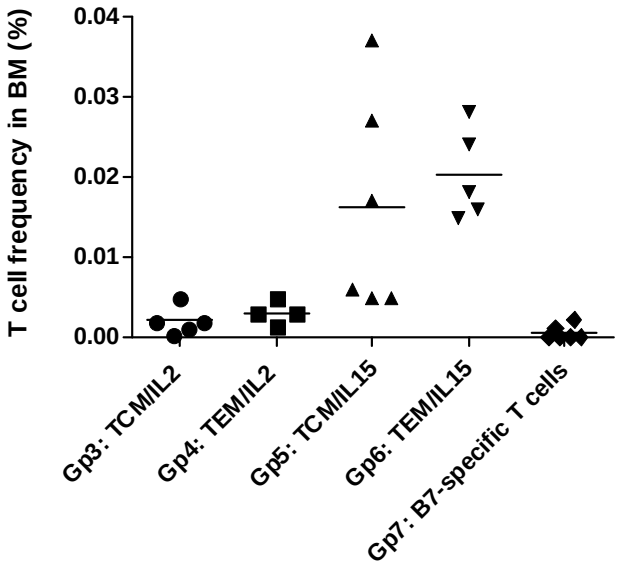
T cell frequency in BM (%)
0.04
0.03
0.02
0.01
0.00
Gp3: TCM/IL2
Gp4: TEM/IL2
Gp5: TCM/IL15
Gp6: TEM/IL15
Gp7: B7-specific T cells

Figure 12 (Continued)

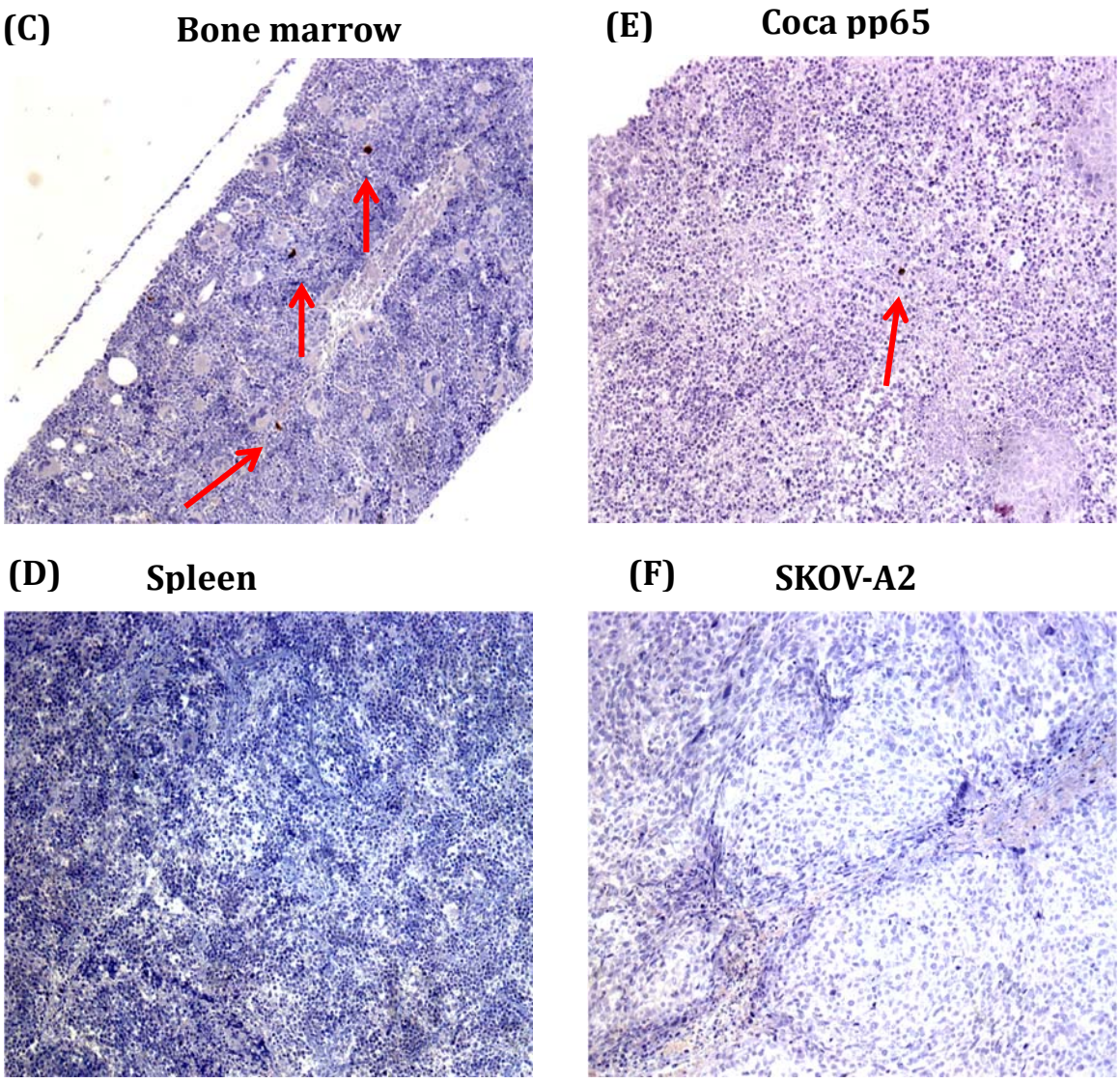

Figure 12 (Continued)

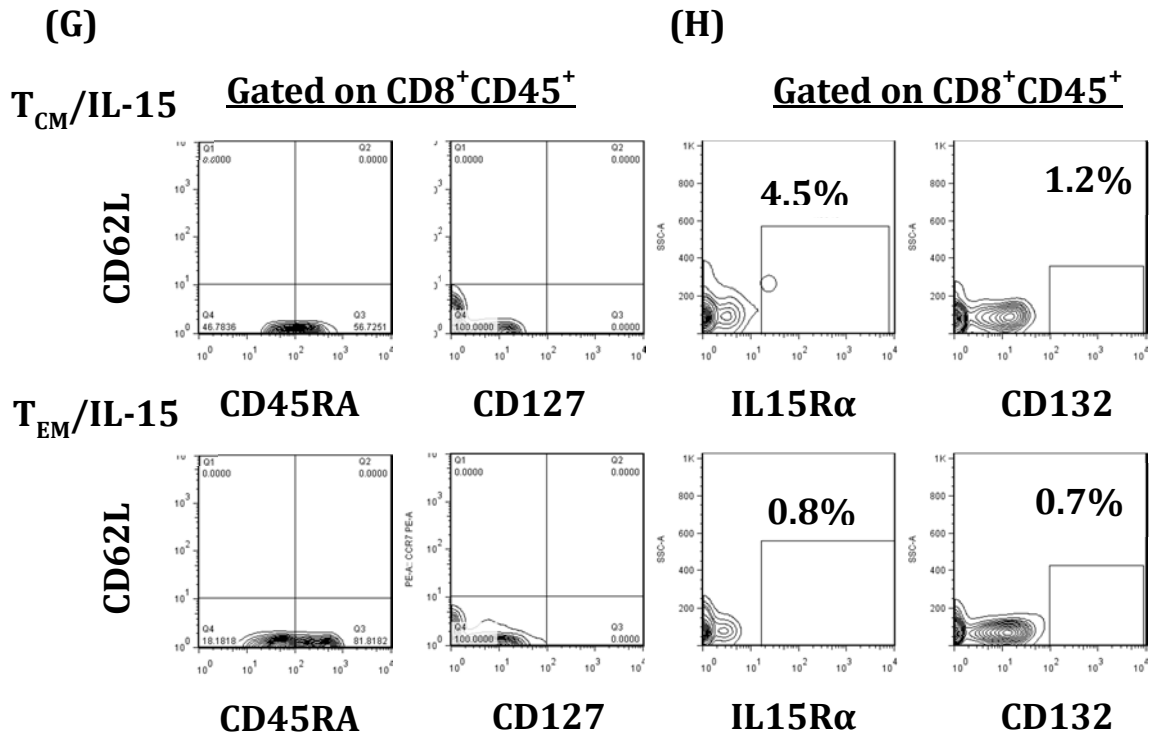

Figure 12 (Continued)

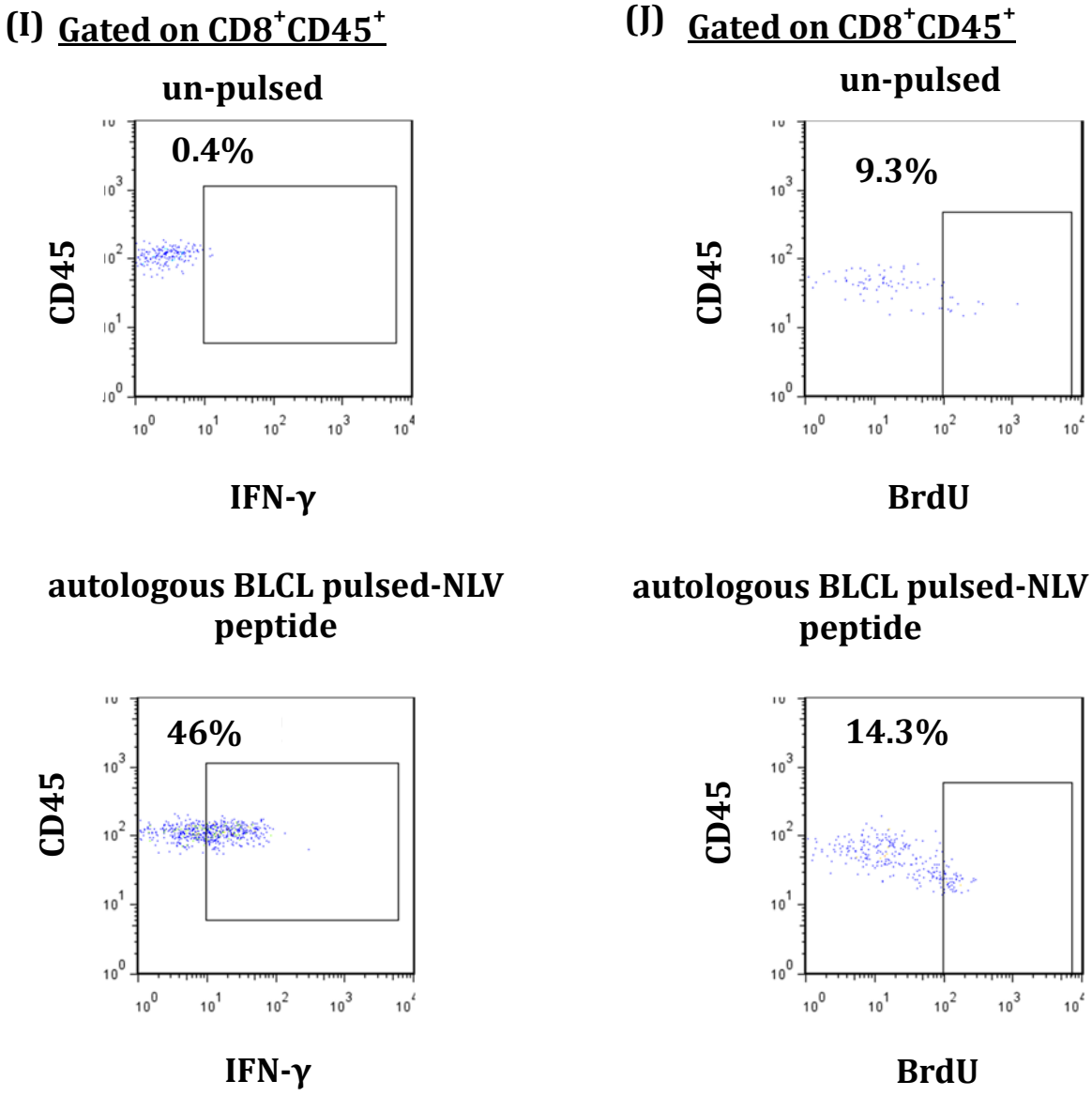

CHAPTER TWO

Stem cell-like memory T cells (T_{SCM}) rapidly repopulate circulating virus-specific effector T cells

1. Introduction

The characteristics of T cells that are selected for expansion and adoptive transfer have been identified as a critical factor that determines the efficacy and persistence of transferred cells. Antigen-specific T cells responding to infections can expand and differentiate into effector T cells, devoted to rapidly clearing the pathogens, as well as memory T cells that can persist long-term and defend against recurrence of disease. The memory T cell compartment is heterogeneous and encompasses multiple subsets with distinctive properties. Current evidence indicates that central memory T cells (T_{CM} cells) that express high levels of CD62L and CCR7 are less differentiated, while $CD62L^{-}CCR7^{-}$ effector memory T-cells (T_{EM} cells) represent committed progenitor cells that undergo terminal differentiation (*13*). Furthermore, studies in mice and nonhuman primates have shown that infusion of T cells derived from T_{CM} populations exhibit greater replicative potential in response to antigen, and prolonged in vivo persistence compared with those derived from the T_{EM} population (*13, 21*). Recently, the spectrum of immunological memory has been extended with the identification of stem cell-like memory T cells (T_{SCM} cells) that express CD45RA, CCR7 and CD62L like naive T cells, but also express CD95. Human T_{SCM} cells have been expanded in vitro (*16, 34*). When compared with other memory T cell populations, human T_{SCM} cells have exhibited increased proliferative capacity. T_{SCM} transduced to express a mesothelin-specific chimeric antigen receptor have also exhibited greater proliferation and superior antitumor responses following adoptive transfer in a humanized mouse model. (*16*) While

T_{SCM} can differentiate into T_{CM}, T_{EM} and effector T cells, they also have a marked potential for self-renewal as shown by serial transplantation experiments. (*34*) Because of these attributes, T_{SCM} have attracted considerable interest as a critical source of antigen-specific T cells for reconstituting immunity following human allogeneic hematopoietic cell transplants (allo HCT). (*34-37*) Indeed, analysis of T cell receptor CDR3 sequences have shown that T_{SCM} undergo marked proliferation and clonal diversification early after allo HCT. (*37, 38*) Furthermore, T_{SCM} clones, distinguished by sites of retroviral vector insertion, may persist in humans for up to 12 years post infusion. (*36*) While these studies have underscored the potential of T_{SCM} as a class of memory T cells, both for transplantation and adoptive cell therapy, the low frequency of antigen-specific T_{SCM} cells has limited their detailed characterization in humans. (*39*) Furthermore, the contribution of different memory subsets to the maintenance of the overall memory compartment of antigen-specific T cells has not been fully elucidated.

In the previous chapter, we have evaluated the differences in their function or persistence between T_{CM} and T_{EM} derived T cells in vitro but failed to show a significant difference when adoptively transduced into NSG mice bearing human tumor xenografts expressing their targeted antigen in vivo. In this chapter, we sought to examine the newly characterized T_{SCM} cells and conducted a full spectrum, side-by-side comparison of T_{SCM} with other memory subsets. Accordingly, we have evaluated human CMVpp65-specific T_{SCM} cells from normal CMV seropositive donors comparing their in vitro responses to antigen to

those of CMV-specific T_{CM} and T_{EM} as well as to antigen-specific naïve T cells (T_N). These studies have identified phenotypic and functional features induced by antigen stimulation that are common to all memory subsets, as well as characteristics of T_{SCM} that distinguish this subset of memory T cells as a reservoir for rapid replenishment of immunodominant T_{EM} and T_{CM} in the circulation.

2. Materials and Methods

Donors

Blood samples were obtained from 12 healthy volunteer HLA-A0201^{+} CMV-seropositive donors. High resolution HLA typing was performed by analysis of HLA allele-specific nucleotide sequences using standard high-resolution typing techniques CMV serostatus was determined by standard serologic techniques in the clinical microbiology laboratory at Memorial Sloan-Kettering Cancer Center.

Generation of CMV-specific T cells

PBMC were isolated from whole blood by Ficoll-Hypaque density gradient separation (Accurate Chemical & Scientific Corporation, Westbury, NY USA), from which T cells were enriched by depletion of CD19^{+}, CD14^{+}, and CD56^{+} cells, using mAb-coated immunomagnetic beads (Pan T-Cell Isolation Kit II, Miltenyi Biotec Inc, Auburn, CA USA). Enriched T cells were labeled with fluorescent Abs: anti-CD3 PerCP, anti-CD45RO PE, anti-CD95 APC, anti-CD62L FITC (all purchased from BD Biosciences, CA, USA), and anti-CD45RA (eBiosciences, CA, USA). T cell populations representing T_N, T_{SCM}, T_{CM} and T_{EM} were gated and sorted on a BD FACS Aria-II SORT (BD Biosciences, CA, USA) based on the following markers: T_{SCM} as CD3^{+}CD45RO^{-}CD62L^{+}CD95^{+}, T_N as D3^{+}CD45RO^{-}CD62L^{+}CD95^{-}, and the T_{CM} and T_{EM} populations as CD3^{+}CD45RO^{+}CD62L^{+} and CD3^{+}CD45RO^{+}CD62L^{-} respectively. Sorted T cell subsets ($1x10^6$) were then sensitized with irradiated HLA A0201+ and CMVpp65^{+} AAPCs ($0.1x10^6$) as previously described (*30*) and were additionally cultured in the

presence of irradiated autologous PBMCs ($2x10^6$) as feeder cells in culture medium X-VIVO™ 15 with gentamicin (Lonza, Allendale NJ, USA) and 15% heat inactivated human serum (Gemini, CA, USA) in humidified incubators at 37°C and 5% CO_2. T cells were supplemented with IL-7 (5 ng/ml), and IL-15 (5 ng/ml) on day 4 and day 7 after culture initiation and were re- stimulated every 10-days with AAPCs and autologous PBMC feeders. After day 12, IL-7 (5 ng/ml), IL-15 (5 ng/ml), and IL-2 (20U/ml) were supplemented to T cell cultures every other day.

Quantitation of antigen-specific $CD8^+$ T cells by tetramer analysis

CMVpp65 specific T cells responsive to the NLV peptide within the cultured T cells were enumerated by Tetramer analysis as previously described (*30*). Commercially available CMVpp65 MHC-peptide tetramers for HLA-A 0201 and A 2402-bearing peptide sequences NLVPMVATV and QYDPVAALF (Beckman Coulter) were used. Briefly, T cells were incubated with CD3 FITC, CD8 PE, CD4 PerCP (BD Biosciences) and an APC-conjugated tetrameric complex for 20 min on ice, washed and analyzed by FACS using a FACSCalibur flow cytometer with dual laser for four-color capability. Data were analyzed using FlowJo software (Tree Star). T cells were gated on CD3- and CD8-positive cells to determine the percentage of tetramer-positive CD8 T lymphocytes.

Phenotypic Analysis of T cell Subsets

T cell subsets were further characterized by flow cytometry using specific T cell memory and co-stimulatory markers. T cells were labelled with fluorescent antibodies against CCR7 PE (BD Biosciences), CD27 FITC (Miltenyi Biotec),

CD57 FITC (Miltenyi Biotec), CD127 PE (Miltenyi Biotec), CD28 PECy7 (BD Biosciences), KLRG1 PE (Miltenyi Biotec) and PD1 PECy7 (eBioscience), and analyzed by FACS. Doublet exclusion for lymphocytes was achieved by gating on forward scatter (FSC) vs side scatter followed by FSC (height) versus FSC (area).

Functional characterization of Ag-specific T cells

Functional activity of T cells was evaluated after short secondary stimulation using several parameters including T cells generating intracellular cytokines (IFN-γ and TNF-α), activation marker expression (CD137), and cytotoxicity (CD107a) by intracellular fluorescence staining. All Abs were purchased from BD bioscience. Irradiated autologous BLCLs loaded with NLVPMVATV peptide co-incubated with T cells in an effector to target ratio of 1:5 for 16 hours in the presence of 1 µg/ml brefeldin A (Sigma-Aldrich, MO, USA). Co-cultured T cells were then labelled with anti-CD3 APC and anti CD8 PE for 15 mins at room temp, washed and then permeabilized with Perm solution (BD Biosciences) and then co-incubated with anti-IFN-γ PECy7 (BD Biosciences) and anti-TNF-α APC (Miltenyi Biotec), or anti-CD137 PE (BD Biosciences), or anti-CD107a FITC (BD Biosciences).

Analysis of T cell proliferation and apoptosis

EdU labeling (ThermoFisher, MA, USA) was used to evaluate T cell proliferation. 10 µM EdU was added to the culture media for 1h at 37 °C. Labeled cells were washed with PBS and resuspended in T cell culture media. T cells were then

analyzed by flow cytometry, and the proportion of proliferating T cells was determined by the percentage EdU^+ gated T cells using the FlowJo software (Treestar, CA, USA). Apoptotic T cells were defined by Annexin V staining (BD Biosciences).

TCR next-generation sequencing

T cell receptor Vβ (TCRVβ) chain hypervariable complementarity-determining region 3 (TCRβ CDR3) was amplified and sequenced from DNA extracted from NLV-Tet^+ T cell subsets (T_N, T_{SCM}, T_{CM}, and T_{EM}) isolated by fluorescence-activated cell sorting (FACS) (purity > 95%) from days 0, 15 or 30 post-stimulation using the Immuno SEQ platform at Adaptive Biotechnologies (WA, USA). Rearranged CDR3 sequences were classified as nonproductive if they included insertions or deletions resulting in frameshift or premature stop codons, and were excluded from subsequent analyses, according to the Immuno SEQ validated algorithm. TCR clonality and sample overlap was determined using the Immuno SEQ Analyzer 2.0. wherein, within a range of 0 to 1, a low number indicates higher diversity, while a high number indicates higher clonality within the sample. Sample overlap indicates the percent of similar clones within a pair of sample types.

Statistical analysis

We performed statistical analyses using Prism (GraphPad Software). For most of the comparisons we used a nonparametric Mann-Whitney test to compare two groups between different populations of the T cells. Within the comparison of

Tet^+ and Tet^- of the same population, we used paired T-test, Wilcoxon signed rank test Significance of differences between two groups was calculated using the t test ($\alpha = 0.05$). For all comparisons, two-sided p values were used; where indicated in figures signifies *$p < 0.05$; **$p < 0.01$, and ***$p < 0.001$.

3. Results

3.1. Comparison with different cytokine treatments for generating antigen-specific human T cells in vitro

There have been a series of discussions about developing optimal methods of antigen-specific priming of human T cells in vitro. Our lab has previously developed an in-vitro system for generation of stable 15Rα/15 complexes obtained when both IL-15Rα and IL-15 genes were co-transduced in AAPCs. Our data suggested that 15Rα/15 complex, but not sIL-15, sustained in-vitro expansion of $CD62L^+$ and $CCR7^+$ central memory phenotype cells (*27*). A previous report also showed that requirements for the generation of long-lived memory stem cells, described as $CD62L^+CCR7^+CD45RA^+CD45R0^+IL\text{-}7R\alpha^+CD95^+$ cells, include CD3/CD28 engagement and culture with IL-7 and IL-15 (*34*). It has also been shown that when exposed to IL-21 during primary stimulation, central memory type CTL are enriched, in addition, IL-21 also maintains the proliferative capacity of antigen-specific T cells, with addition of IL-7 and IL-15 for robust and strong expansion (*40*). Accordingly, we performed a comparative study to determine which cytokine cocktail would be most effective in promoting the growth of antigen-specific T cell populations. We cultured the T-cells with 7 different combinations of cytokine treatment as well as a non-cytokine control, and then quantified the number of antigen-specific cells generated, as well as the fold expansion of antigen-specific T-cells observed post culture initiation. T cells were stimulated with AAPCs presenting CMVpp65 antigen and

HLA A0201. The yield of antigen-specific T-cells was calculated and normalized to the number of NLV-Tet^{+} T-cells present in peripheral blood. The seven different sensitizing conditions tested are as follows: 1. AAPC alone. 2. AAPC with IL-2. 3. AAPC transduced to express IL-15Rα and IL-15 genes. 4. AAPC transduced to express IL-15Rα and IL-15 genes with exogenous IL-2. 5. AAPC with recombinant IL-7 and IL-15. 6. AAPC with recombinant IL-7 and IL-15 and IL-2. 7. AAPC with recombinant IL-7, IL-15 and IL-21. 8. AAPC with recombinant IL-7, IL-15, IL-21 and IL-2. We tested the antigen-specific T-cell number after 7, 15 and 22 days post-stimulation. The number of antigen-specific cells in millions is shown in figure 1A; fold expansion normalized to day 0 is shown in figure 1B. The results show that in the presence of IL-7 and IL-15 there is a robust expansion of antigen-specific T cell (1300x). IL-2, along with IL-7 and IL-15, induces a further T cell expansion (3000x). However, IL-21 shockingly halted T cell expansion with (116x) or without IL-2 (105x). In addition, 15Rα/15 complex also promoted T cell expansion to a slightly lower degree than IL-7 and IL-15 with (750x) or without (1100x) IL-2. In conclusion, our data provide evidence that sensitizing and expansion in the presence of IL-7, IL-15 and IL-2, yield the highest number of antigen-specific T cells.

3.2. Detection and isolation of CMVpp65 -specific T_{SCM} cells from healthy seropositive donors

T cells were isolated from peripheral blood mononuclear cells (PBMC) of 12

healthy HLA A0201^{+} CMV seropositive donors. In each of these CMV-seropositive donors, we identified T_{SCM} as CD3^{+}CD45RO^{-}CD62L^{+}CD95^{+}, T_N as CD3^{+}CD45RO^{-}CD62L^{+}CD95^{-}, and T_{CM} and T_{EM} populations as CD3^{+}CD45RO^{+}CD62L^{+} and CD3^{+}CD45RO^{+}CD62L^{-} respectively (fig. 2). The proportion of T_{SCM} cells ranged from 1.2%-10.8% within the T cell populations in the peripheral blood in the absence of any in vitro stimulation. Despite low proportions within the PBMCs, we were consistently able to identify the T_{SCM} cells in all donors tested (n=12). In comparison, the proportion of T_N, T_{CM} and T_{EM} cells were 3.8%-28.9%, 1.7%-32.4% and 15.4%-34.9% respectively (table. 1).

Using CMVpp65 as a model antigen, we then examined the memory phenotype of the antigen-specific T cells. Accordingly, we evaluated the CMVpp65-specific T cell populations in the blood of 11 of 12 donors. In each of the donors tested, we were able to identify a discrete population of antigen specific T cells using HLA peptide tetramers that were responsive to the well known CMVpp65 epitope NLVPMVATV (NLV) presented by HLA A0201. Further analysis of these NLV-specific tetramer positive T cells (NLV-Tet^{+}) demonstrated that the majority of memory T cells in peripheral blood that recognize NLV epitope bear either a T_{CM} or T_{EM} phenotype (0.9%-31% and 15.1%-70.6% respectively), and the remainder were effector T cells. (table. 1) We were also interested to determine if there was a population of T_{SCM} cells circulating in the peripheral blood of healthy donors that were also antigen specific. Of 11 donors tested, 10 had a distinct population of T_{SCM} cells within the CD95^{+} naïve T-cell precursors (CD45RO^{-}CD62L^{+}), that could bind to the A2-NLV tetramer (0.6% - 8.3%) (table. 1).

Recently, other groups have also demonstrated the feasibility of generating CMV specific T cells from the naïve T cell compartment (*41, 42*). We therefore examined the proportion of NLV-Tet$^+$ cells within the CD95 negative naïve T-cells (T_N). However, in only 2 of 11 donors could we detect T_N cells within the NLV-Tet$^+$ population in the peripheral blood. Taken together, our data suggest that a minor proportion of NLV-tetramer binding CD8 T cells exist within the CD45RO$^-$CD62L$^+$ naïve T cell compartment and consist of both the CD95$^+$ T_{SCM} and CD95$^-$ T_N cells.

3.3. In vitro expanded epitope specific T_{SCM} cells maintain a less differentiated memory phenotype during antigen specific stimulation

We next wished to evaluate which of the memory T cell populations detected in these healthy latently infected seropositive donors served as the reservoir of T cell immunity from which antigen-specific T cells were generated upon secondary challenge. Based on the properties of T_{SCM} cells described earlier, we particularly wished to comparatively assess the potential of CMV-specific T_{SCM} cells to expand and act as a durable T cell reservoir. Accordingly we FACS sorted T_N, T_{SCM}, T_{CM} and T_{EM} cell populations from HLA-A 0201 CMV-seropositive donors as described above using the expression markers CD62L, CD45RO and CD95. We then sensitized the sorted T cell subsets with artificial antigen presenting cells (AAPCs) exclusively expressing HLA-A 0201, CMVpp65 and T cell costimulatory molecules as previously described (*30*). Cell cultures were also supplemented with IL-7 and IL-15 every 2 days beginning at day 4 as previously

described (*34*).

Using this method for in vitro sensitization of T_{SCM} derived cells, HLA-A 0201 NLV-tetramer$^+$ CD8$^+$ T cells could be enriched up to 5.5 % by 7 days from 0.6 % at day 0 as shown for one representative donor (figure. 3A). A similar enrichment of HLA-A 0201 NLV-tetramer$^+$ T cells was also observed within the T_{CM} and T_{EM} derived CD8$^+$ T cells (6.1% and 4.1% respectively) (figure. 3A). Over a period of 4 weeks after antigen specific in vitro sensitization, T_{SCM} derived cells gradually acquired T_{CM} and T_{EM} phenotype within both the NLV-Tet$^+$ as well as NLV-Tet$^-$ cell populations (figure. 3B and 3C). Strikingly, within the NLV-Tet$^+$ cells derived from the T_{SCM} subset, we were able to detect a proportion of cells with a CD45RA$^+$ and CD62L$^+$ T_{SCM} phenotype for up to 14 days in culture. By this time, both T_{CM} and T_{EM} derived T cells exclusively expressed a T_{EM} phenotype (figure. 3B). We also detected higher CCR7 expression within both the NLV-Tet$^+$ as well as NLV-Tet$^-$ T cells derived from T_{SCM} derived T cells after 14 days of antigen specific stimulation in comparison to T_{CM} and T_{EM} derived T-cells. CCR7 was expressed in 7.5% of T_{SCM} derived NLV-Tet$^+$ T cells (figure. 3B). These data suggest that the T_{SCM} cells follow a differentiation trajectory progressing to T_{CM}, and then T_{EM} cells during in vitro expansion. These results also suggest that T_{SCM} cells have the ability to maintain a less differentiated phenotype longer than T_{CM} derived T cell subsets.

Using the same approach, we have also been able to generate CMV-specific T cells derived from CD95$^-$ T_N cells. Regardless of whether or not NLV-Tet$^+$ cells

were detected in the sorted T_N cells within the peripheral blood before antigen stimulation, we were able to generate NLV-Tet$^+$ T cells from 6 of 6 different donors by this method of sensitization from sorted T_N cells. Upon stimulation, T_N cells upregulated CD95 expression within 2 days and converted to a T_{SCM} phenotype. T_N cells however, maintained a less differentiated memory phenotype, with expression of CD62L and CCR7 within a proportion of NLV-Tet$^+$ T cells for a longer duration during antigenic stimulation than the T_{CM} and T_{EM} derived cell subsets. In a representative example (figure. 3B), T_N derived T cells demonstrated CCR7 expression in 12% of NLV-Tet$^+$ T cells, and T_{SCM} derived T cells in 7.5% of NLV-Tet$^+$ T cells after 14 days of continuous antigenic stimulation, compared to 0.8% and 0.5% CCR7 expressing NLV-Tet$^+$ T-cells within T_{CM} and T_{EM} derived T-cells respectively. In the group of 6 donors tested, the expression of CCR7 after 14 days of in vitro stimulation in T_N and T_{SCM} derived NLV-Tet$^+$ T cells was significantly higher than that observed in T_{CM} and T_{EM} derived NLV-Tet$^+$ T-cells ($p< 0.05$) (figure. 3D). A similar trend for CCR7 expression was also observed in the NLV-Tet negative T_N and T_{SCM} derived T cells (figure. 3E). These studies thus demonstrate a less differentiated phenotype within antigen experienced T cells derived from T_N and T_{SCM}. However, the enrichment of NLV-Tet$^+$ populations was less pronounced within the T_N derived T cells (0.4%, 0.4% and 3.6% at Day 7, 14 and 30 as shown in figure. 3A, 3B and 3C) than within T cells derived from the memory T cell populations (T_{SCM}, T_{CM} and T_{EM}). This slow enrichment of CMV-specific T cells may reflect the low precursor frequencies in T_N subsets in the peripheral blood.

3.4. Characterization of the co-stimulatory and senescence markers within memory T-cell populations

We next evaluated characteristics within the naïve and different memory T cell subsets, which would identify a particular subset with higher potential for proliferation and persistence. Accordingly, we assessed the expression of a panel of markers including the co-stimulatory markers CD27 and CD28 as well as the IL-7Rα CD127, the activation marker PD-1 and the senescence marker CD57. We compared the expression of each of these markers in cells that recognize the same antigen to rule out differences occurring as a result of differential enrichment of antigen specific T cells within each subset.

CD27 is constitutively expressed as a costimulatory molecule on all T-cells, but is highest on naïve and less differentiated memory T cells. (*16*) Its expression is lost at the fully differentiated effector phase. (*43*) A recent study also demonstrated that CD27 costimulation improves the function of chimeric antigen receptor modified T cells (CARs). (*44*) In our studies, we found a significantly higher proportion of cells expressing CD27 within both the NLV-Tet$^+$ and Tet$^-$ T-cells in T_N derived cells compared to T_{CM} and T_{EM} derived cells, and T_{SCM} derived T-cells compared to T_{EM} derived cells, in 6 donors tested (**$p<0.01$ and *$p<0.05$) (figure. 4A and 4B).

CD57 has been described to be indicative of replicative senescence and antigen-induced apoptosis in HIV-specific CD8$^+$ T cells (*45*). After second antigen specific stimulation, we found a significantly lower proportion of CD57 expressing

cells within T_N-derived NLV-Tet$^+$ T cells, compared to T_{CM} and T_{EM}-derived NLV-Tet$^+$ T cells as shown for 6 donors tested (**p<0.01 and *p<0.05) (figure. 4C and 4D). T_{SCM} derived cells expressed lower levels of CD57 than T_{CM} and T_{EM} derived T cells, though this difference was not statistically significant for the donors tested. Again, expression of CD57 was lower on Tet$^-$ T_N cells, but was similar in its expression when compared to Tet$^+$ T-cells in each of the memory T-cell subsets (figure. 4C and 4D). These data thus demonstrate increasing levels of CD57 expression with increasing T-cell differentiation (T_N < T_{SCM} < T_{CM} <T_{EM}) in both NLV-Tet$^+$ and Tet$^-$ T-cells.

We next examined the expression of the IL-7Rα (CD127), which has been shown to facilitate T cell engraftment and persistence in mouse models (*46*). In our studies, expression of CD127 was lower in both Tet$^+$ and Tet$^-$ T_N, T_{CM} and T_{EM}. A slightly higher level of CD127 expression was observed within T_{SCM} derived NLV-Tet$^+$ and Tet$^-$ T-cells compared to T_N, T_{CM} or T_{EM} derived cells. However, this difference was not statistically significant (figure. 4E and 4F). Taken together, these data suggest that T cells derived from the T_N and T_{SCM} memory subsets demonstrate a less differentiated CCR7^{hi} CD27^{hi} and CD57^{low} phenotype when compared to T_{CM} and T_{EM} derived T cells whether they are antigen specific (Tet$^+$) or not (Tet$^-$).

We also examined the expression of another protein considered a marker of late differentiation, KLRG-1 (*47*). As shown in figure 4G and 4H, KLRG-1 was expressed at low or undetectable levels in Tet$^-$ T_N cells, but at significantly higher

levels in Tet^+ T_N cells. However, like the other differentiation markers previously examined, expression on Tet^+ and Tet^- T-cells was equivalent in T_{SCM}, T_{CM} and T_{EM}.

In contrast to these differentiate markers, two signaling molecules, PD-1 and CD28, were differentially expressed by NLV-Tet^+ T cells at each stage of T cell development. As shown in figure 4I and 4J, PD-1 is highly and equivalently expressed in NLV-Tet^+ T-cells at all stages of development, from T_N to T_{EM}. In contrast, it is expressed at minimal level by NLV-Tet^- T-cells. These differences are highly significant (Tet^+ T_N vs Tet^- T_N ***$p < 0.001$; Tet^+ T_{SCM} vs Tet^- T_{SCM} ***$p < 0.001$; Tet^+ T_{CM} vs Tet^- T_{CM} **$p < 0.01$; Tet^+ T_{EM} vs Tet^- T_{EM} **$p < 0.01$; Wilcoxon signed rank test)

On the other hand, while expression of CD28 was equivalent in Tet^+ and Tet^- T_N and T_{SCM} cells, and was also similar in it's expression in Tet^- T_{CM} and T_{EM} cells, Tet^+ T_{CM} and T_{EM} had a higher level of expression than Tet^- T_{CM} and T_{EM} cells (figure. 4K and 4L). Expression of CD28 in Tet^+ T_{EM} was, in fact, significantly higher than that expressed in Tet^+ T_N derived cells.

3.5. T_{SCM} derived T cells demonstrate higher proliferative capacity and superior expansion of antigen-specific T cells

We next evaluated the in vitro proliferative capacity of different memory T-cell subsets upon antigen specific stimulation with AAPCs expressing CMVpp65, and examined the phenotype of proliferating T cells using EdU labeling (see methods). Within the total T-cell populations stimulated, we observed vigorous T

cell proliferation starting at 3 days after stimulation. Within the NLV-Tet$^+$ T cells 10.2% proliferating cells were observed in a representative donor at day 3, reaching a peak of 52.2% by day 5 post stimulation (figure. 5A). The less differentiated T_{SCM} and T_{CM} cells constituted 32% and 23% respectively, of the proliferating memory NLV-Tet$^+$ T cells at day 3 (figure. 5B). At this time the total NLV-Tet$^+$ cells contained 22% of T_{SCM} cells and 32% T_{CM} cells. By day 5, the T_{SCM} and T_{CM} subsets represented 21% of the proliferating memory NLV-Tet$^+$ T-cells, while they represented 13% of the total NLV-Tet$^+$ memory T cell compartment (figure. 5B). These data suggest that in response to antigen stimulation, there is an early preferential proliferation of NLV-Tet$^+$ T_{SCM} and T_{CM}. By day 7 post stimulation, 98.6% of the NLV-Tet$^+$ T-cells exhibit a T_{EM} phenotype in this donor, and at this time almost all of them proliferating NLV-Tet$^+$ T-cells are also T_{EM}. To compare the proliferative potential of each memory subset we examined the fold expansion of NLV-Tet$^+$ T cells derived from each of these naïve and memory subsets. The yield of antigen-specific T-cells was calculated and normalized to the number of NLV-Tet$^+$ T-cells present in peripheral blood. After two rounds of antigen exposure, we observed a significantly higher fold expansion of antigen-specific T-cells within T_{SCM} derived cells compared to T_{EM} derived cells ($p=0.03$) (figure. 5C). Although the overall fold expansion of T_{CM} derived NLV Tet$^+$ T-cells was lower than T_{SCM} derived cells, this difference was not statistically significant. We were not able to perform the same analysis for some of the T_N donors due to undetectable levels of NLV-Tet$^+$ T-cells in peripheral blood before antigen stimulation. Taken together, these data indicate

that cells derived from the T_{SCM} demonstrate greater proliferation of antigen specific cells and may serve as a significant source of other subsets in the T-cell memory pool.

3.6. In vitro expanded T_N and T_{SCM} derived T-cells demonstrate functional activity against specific epitopes similar to that of T_{CM} and T_{EM}

Given that the epitope specific T_N and T_{SCM} cells maintain a less differentiated phenotype during in vitro expansion, we examined if this would affect their antigen-specific functional activity. Accordingly, we evaluated the ability of cells derived from naïve and memory T-cell subsets to generate cytokines in response to secondary stimulation with antigen. CD137 has been described as a marker of antigen-specific $CD8^+$ T cells that correlates with functional activity including production of cytokines such as TNF-α and IFN-γ, as well as granzyme production and cytotoxicity activity (*48*). Isolated and in vitro expanded naïve and memory derived T cells were secondarily stimulated for 15 hours with autologous NLV peptide loaded BLCLs. Following antigen stimulation, an increased proportion of $CD8^+$ CD137 expressing T cells was observed, as shown for a representative donor in figure 6A (T_N: 3.36%, T_{SCM}: 37%, T_{CM}, 90.4% and T_{EM} 82%). T-cells derived from all subsets, T_N, T_{SCM}, T_{CM} and T_{EM}, were able to produce cytokines. Of note, T_N and T_{SCM} derived T cells were also capable of secreting both TNF-α and IFN-γ, as observed for T_{CM} and T_{EM} derived T cells. Complementing their capacity to secrete cytokines, T_N and T_{SCM} cells also expressed the lysosomal associated membrane protein 1 (LAMP-1) or CD107a

which is a marker of degranulation in T cells, in response to peptide loaded autologous targets. The level of CD107a in T_N and T_{SCM} cells in the $CD8^+$ T cell population was 20% and 22% respectively (figure 6B). Thus, although these epitope specific T_N and T_{SCM} derived T cells, after expansion in vitro, demonstrate a less differentiated memory phenotype than T_{CM} or T_{EM}, they are functional as evidenced by their ability to secrete cytokines and degranulate in response to antigen.

3.7. T_{SCM} derived CMV-specific T cells differentially exhibit a similar oligoclonal repertoire of public TCRs as that of T_{CM} and T_{EM} populations in the blood

We next examined the clonal diversity of NLV-Tet^+ T cells comparing those derived from Tet^+ T_N, T_{SCM}, T_{CM} and T_{EM}. In these studies we wanted to evaluate if there were common TCR sequences within CMV-specific T cells derived from T_N, T_{SCM}, T_{CM} and T_{EM} cells. Accordingly, we expanded T_N, T_{SCM}, T_{CM} and T_{EM} derived T cells in vitro from 2 donors using our artificial antigen presenting cells for 30 days, and sorted the NLV-Tet^+ T cells and NLV-Tet^- T cells. We then performed TCR repertoire analysis by next generation sequencing on the sorted Tet^+ T cells in comparison to the Tet^- T cells. TCR sequencing data were analyzed for similarities in nucleotide sequences by sample overlap. This analysis of Tet^+ T cells from donor CK200D demonstrated a high overlap between TCR sequences for T_{CM} and T_{EM} derived NLV-Tet^+ cells 30 days post stimulation (96% overlap in figure. 7A). T_{SCM} derived cells demonstrated high similarities with T_N and T_{CM} but less similarity with T_{EM} derived cells (T_N: 84%,

T_{CM}, 91% and T_{EM} 57% in figure. 7A). In this donor, T_N derived Tet^+ cells also had a high degree of TCR similarity/overlap with Tet^+ T_{CM} derived cells (87%) but very little overlap with T_{EM} derived cells (14%). In contrast, we did not detect any TCR overlap within NLV-Tet^- T cells derived from either naïve or memory T cells (figure. 7B). Overall, these data indicate that by day 30 Tet^+ T cells recognizing the NLV epitope that are derived from the naïve like T_N subset demonstrate a high degree of overlap with TCR sequences expressed by T_{SCM} and T_{CM}. While the TCR sequences detected in T_{SCM} and T_{CM} memory T-cells were less frequently detected in the T_{EM}, nevertheless, there was a significant representation of specific TCRs common to all memory T cell compartments.

In a second and informative donor CK-42202, we examined if the same trend of TCR overlap would be present prior to antigen stimulation in peripheral blood. We therefore sorted T_N, T_{SCM}, T_{CM} and T_{EM} derived the NLV-Tet^+ T cells from the donor prior to stimulation and evaluated the TCR sequence for clonality and overlap. TCR clonality describes the degree to which one or a few clones dominate the repertoire, with 0 being a flat distribution and 1 being an entirely oligoclonal sample. Prior to antigenic stimulation, T_{EM} derived NLV-Tet^+ T cells demonstrated a high degree of clonality, with a clonality index of 0.66. In comparison, the T_{CM} derived NLV Tet^+ T cells demonstrated a clonality index of 0.06 suggesting higher TCR clonal diversity, while the circulating T_{SCM} and T_N derived NLV Tet^+ T cells were highly diverse with a clonal index of 0.01 (figure.8A). In overlap analysis comparing the Tet^+ T cells in the different subsets, however, T cells detected in the T_{EM} fraction were also differentially

represented in the T_{CM} repertoire. (93.8% in figure 8B) On the other hand, T_{SCM} cells, which had a highly diverse TCR repertoire, demonstrate very little overlap with T_{CM} and T_{EM} TCR sequences (13.2% and 24.6% respectively; figure 8B). Strikingly, we did not identify any TCR overlap between T_N derived NLV-Tet$^+$ T cells and T_{SCM}, T_{CM} or T_{EM} derived NLV-Tet$^+$ T cells in peripheral blood (figure 8B).

After 15 days of antigenic stimulation in vitro, the expanded NLV-Tet$^+$ T cells adopted a restricted clonal diversity, with the clonality index ranging from 0.35 to 0.83 in all subsets (Fig. 8A). In overlap analysis, the T_{CM} and T_{EM} derived NLV-Tet$^+$ T cells demonstrated highly overlapping TCR sequences in 97.1% of the cells (Fig. 8C). Strikingly, T_{SCM} derived NLV-Tet$^+$ T cells developed a restricted TCR repertoire within 15 days post antigenic stimulation, which was highly similar to that of T_{CM} and T_{EM} derived NLV-Tet$^+$ T cells detected at Day 0 (Fig. 8E) as well as Day 15 (T_{SCM}/T_{CM}: 85.8% and T_{SCM}/T_{EM}: 94.8% in figure 8C). Unlike the T_{SCM} early after re-stimulation, T_N-derived NLV-Tet$^+$ T cells demonstrated very different TCR sequences compared to T_{CM} and T_{EM} derived cells with an overlap of 37.5% and 3.8% respectively (figure 8D).

These clonal overlaps are further demonstrated in table. 2 which shows CDR3β sequences most frequently detected in the NLV-Tet$^+$ T_N, T_{SCM}, $T_{CM,}$ and T_{EM} at 0, 15 and 30 days after in vitro expansion. As can be seen in this case, the T_{SCM} preferentially expanded NLV-Tet$^+$ T cells bearing the CASSPQTGASYGYTP sequence that is predominant in the T_{EM} and T_{CM} at day 0. In contrast, the T_N

cells preferentially expanded NLV-Tet$^+$ cells bearing the CASSYVTGTGNYGYTF CDR3 sequences not detected in either the T_{EM} or T_{CM} at any time.

Taken together, these data provide evidence that, upon antigen stimulation, T_{SCM} rather than TN rapidly expand T cell clones expressing NLV-specific TCRs detected in immunodominant NLV-specific T_{CM} and T_{EM} populations in the circulation. On the other hand, T_N-derived cells can maintain a potential for diversity that may not be shared by T_{SCM} which may already be committed to sustaining populations of the immunodominant T cells detected in circulating T_{CM} and $T_{EM.}$

Another feature of the CDR3β sequence, CASSPQTGASYGYTF differentially represented in Tet$^+$ NLV-specific $T_{SCM,}$ T_{CM}, and $T_{EM,}$ and the CASSYVTGTGNYGYTF CDR3β sequence detected in T cells expanded from T_N in donor CK42202 is that they are each identical to CDR3β sequences previously reported in public NLV-specific T-cell receptors analyzed from other seropositive HLA A0201$^+$ donors (*49, 50*). Similarly, three of the CDR3β sequences highly represented in NLV-specific T cells from donor CK200D have the S*$_n$TG*$_n$GY CDR3β motif characteristic of these NLV-specific public receptors that are prevalent among NLV-specific T cells isolated from HLA A0201$^+$ CMV seropositive donors (*51*). These public receptors have been reported to be usually of high affinity, and can persist as dominant clones for one or more years (*52*). The rapid expansion of T cells bearing such receptors from populations of T_{SCM} in which they were initially undetectable raises the possibility that T_{SCM} clones may be differentially signaled to respond to alterations in NLV-specific T_{EM}

and T_{CM} populations bearing such receptors responding to CMV reactivation.

3.8. Immunodominance is not caused by the skewed proliferation of T_{SCM} cells in circulation

We have provided evidence that T_{SCM} derived T cells demonstrate higher proliferative capacity generating superior expansion of Ag-specific T-cells. We next asked whether the phenomenon of epitope specific T-cell immunodominance could be a consequence of either over representation of or preferential proliferation of T_{SCM} cells within T-cells responding to immunodominant compared to subdominant epitopes. To address this question, we compared the in vitro T-cell proliferative capacity within T_{SCM}, T_{CM}, and T_{EM} subsets upon antigen specific stimulation in a CMV seropositive donor co-inheriting HLA-A*0201 and A*2402. The immunodominant anti-CMV T-cell response in donors co-inheriting these alleles has been shown to be directed against the NLV epitope presented by HLA-A*0201 (lidehall et al.). T-cells from the same donor were stimulated with NLV and QYD loaded autologous DC. Within 8 days post stimulation, NLV-Tet$^+$ cells were enriched to 31.7% and QYD-Tet$^+$ cells to 1.6% representing the immunodominant and subdominant response respectively (Fig. 9A). Strikingly, we found a similar memory phenotype for both A2-NLV and A24-QYD T-cells, with no overrepresentation of T cells within the immunodominant A2-NLV cells in culture. To further evaluate the relative proliferative potential between immunodominant and subdominant epitope specific T-cells, we examined T-cells for EdU and Annexin V expression as

proliferation and apoptosis markers. We found similar levels of proliferating cells within A2-NLV and A24-QYD Tet^+ T-cells, with no preferential proliferation within the immunodominant A2-NLV T-cells. However, the A24-QYD T-cells contained a higher percentage of Annexin V^+ cells compared to A2-NLV T-cells (figure 9B). These data suggest that a higher level of T-cell apoptosis within subdominant epitope-specific T-cells might promote the preferential enrichment of immunodominant T-cells.

4. Discussion

In this study, we have characterized HLA A0201 restricted T_N, T_{SCM}, T_{CM} and T_{EM} specific for the immunodominant NLV peptide of CMVpp65 that were isolated by immunoadsorption to tetramers from the blood of healthy seropositive donors and after sequential intervals of in vitro sensitization. We also compared the NLV-Tet$^+$ with Tet$^-$ T cells from the same T cell populations. Our results suggest a major role for T_{SCM} cells as a durable reservoir of T cell memory in the recall immune response.

Analysis of circulating antigen specific T cells within different memory T cell compartments demonstrated that NLV-Tet$^+$ T_{SCM} express a CD45RA$^+$ CCR7$^+$ and CD62L$^+$ phenotype similar to T_N cells, but unlike T_N cells, also express CD95. Both NLV-Tet$^+$ and Tet$^-$ T-cells derived from T_N and T_{SCM} expressed significantly higher levels of the costimulatory marker CD27 than NLV-Tet$^+$ and Tet$^-$ T cells generated from T_{CM} and T_{EM}. Both Tet$^+$ and Tet$^-$ T_{SCM} derived T-cells also demonstrated somewhat higher expression of the IL-7 Rα (CD127). Restifo et. al. have reported high levels of expression of CD127 in T_N, T_{SCM}, T_{CM} and T_{EM} in the blood of healthy donors (*16*). However, Schmueck-Henneresse et. al. (*39*) have reported that expression of CD127 is down regulated in T_{CM} and T_{EM} during growth in vitro when the cells are cultured with IL-7 and IL-15. In contrast, CD127 expression, while initially reduced, rapidly recovered in T_{SCM}. To what degree the differentiated expression of CD127 observed in NLV-Tet$^+$ T_{SCM} in our own and their study contributes to the higher proliferation potential that we observed in

NLV-Tet$^+$ T_{SCM} remains to be determined. Conversely, the Tet$^+$ T_N and T_{SCM} derived cells expressed lower levels of the senescence marker CD57; and Tet$^+$ T_N expressed lower levels of CD28. Thus, even though the T_N and T_{SCM} derived T cells, after 14 days of culture, had largely progressed to a T_{CM} or T_{EM} phenotype, they still expressed markers found on less differentiated T cells and low levels of markers associated with terminal differentiation or senescence.

Strikingly, after in vitro sensitization, all Tet$^+$ subsets generated a similarly high proportion of cells expressing PD-1, which differed significantly from the low proportion of PD-1$^+$ cells in the Tet$^-$ population. PD1 has been thought to be a marker of T cell exhaustion in animal models of chronic infection and within TILs reactive to specific self tumor antigens. However, this protein has been found to be upregulated upon antigen engagement and therefore has also been thought to represent activated antigen specific T-cells (*53*). In addition, the killer-cell lectin like receptor G1 (KLRG1), which is usually considered to be a marker of late differentiation was expressed to a similar degree in the NLV-Tet$^+$ and Tet$^-$ T_{SCM}, T_{CM} and T_{EM} fractions (*47*). In contrast, KLRG-1 was expressed at a minimal level in the Tet$^-$ T_N derived cells but at levels similar to those in T_{SCM}, T_{CM} and T_{EM} after antigen stimulation. Thus, in latently infected healthy seropositive individuals, secondary stimulation with the viral antigen induces expression of PD-1 in T_N and in all stages of T-cell memory and KLRG-1 in antigen responsive T_N-derived cells.

At a functional level, Tet$^+$ T_N, T_{SCM}, T_{CM} and T_{EM} fraction all contained cells capable of secreting TNF-α and IFN-γ, and degranulating in response to antigen stimulation, although the proportion of Tet$^+$ T cells derived from T_{EM} and T_{CM} exhibiting these functions were higher than in Tet$^+$ T cells derived from T_{SCM} or T_N. Thus, in contrast to a previous report in which only a minimal number of CD95$^-$ T cells were found to secrete cytokines after HCMV-specific stimulation (*39*), our studies provide evidence that T_N cells, after antigen stimulation, do exhibit these effector functions and cannot, thereby, be qualitatively distinguished from antigen-responsive T_{SCM} cells. Recent studies by Pulko et al (*54*) have also shown that human memory T cells with a naïve phenotype secrete multiple cytokines in response to secondary stimulation with viral antigens but exhibit longer telomeres and a distinct transcriptome that differentiates them from memory and effector T cells. We also find that NLV-Tet$^+$ CD95$^-$ T_N cells are functionally distinguishable from NLV-Tet$^+$ CD95$^+$ T_{SCM} cells in that they exhibit a markedly lower proliferative response to antigen stimulation. Indeed, the proliferative response of T_{SCM} significantly exceeds not only that of NLV-Tet$^+$ T cells derived from the T_N fraction but also NLV-Tet$^+$ T cells derived from T_{CM} and T_{EM}.

A diverse TCR repertoire has been postulated to mediate optimal control of pathogens by increasing the probability that microbial escape mutations would be recognized by one of the TCR$\alpha\beta$ pairs represented within the repertoire (*55, 56*). Our TCR sequencing analysis has shown that in the peripheral circulation, the T_N

and T_{SCM} cells recognizing the same epitope NLV, are more diverse than T_{CM} and T_{EM} cells. This broad TCR repertoire of T_N and T_{SCM} cells recognizing the same pathogen could be hypothesized to provide better control of virus infection. However, upon antigen stimulation, we observe that T_{SCM} generate T cells that are oligoclonal within 15 days after antigen encounter, and further that these T cells express a repertoire closely related to that of Tet^+ T_{EM} and T_{CM} that are dominant in the circulation. The fact that T_{SCM} derived CMV-specific cells share high overlap of TCR usage with T_{CM} and T_{EM} early post stimulation, provides evidence that T_{SCM} derived cells are particularly effective in reconstituting populations of immunodominant memory T cells in the blood. The fact that the oligoclonal NLV-specific Tet^+ T_{CM} and T_{EM} in the blood, and the responding T_{SCM} of donor CK 42202 differentially express a TCR with the same public CDR3β, and that the most prevalent NLV-Tet^+ T_{CM} and T_{EM} from both donors express T cell receptors bearing such public CDR3βs is also consistent with previous studies indicating the importance of such public T-cell receptors to the control of latent infections and to effective responses to CMV reactivation (*57, 58*). In CMV seropositive healthy donors, NLV peptide specific T cell repertoires exhibit a high prevalence of public TCRs. (*51, 52, 59*). Indeed, seven public CDR3α and six CDR3β motifs have been estimated to account for up to 70% of the total NLV-specific TCR response (*51*). Studies of the crystal structures of the two public TCRs in complex with NLV-HLA A2 have provided evidence that different pairings of TCRα and β chains bearing public CDR3 sequences can engender a multiplicity of high affinity TCRs engaging the same peptide-MHC ligand (*58*),

thereby also providing a diversity of effective T cells specific for the immunodominant NLV epitope. In contrast, the more heterogeneous and distinctive spectrum of clones generated from T_N cells after antigen stimulation, which differs from that of the other memory T- cell compartments, suggests that T_N cells serve as a pool of precursor cells capable of selecting peptide-specific T cells with a broader spectrum of binding characteristics, from which antigen-specific T cells of optimal avidity can be selected for expansion if required to control viral variants.

T cell responses to latent viruses are often focused on a small number of the available antigenic epitopes and use a narrow TCR repertoire, a phenomenon termed “immunodominance”. A number of factors have been reported to influence immunodominance, including antigen presentation, peptide-MHC binding affinity and stability or TCR avidity and the frequency of precursors in the naïve T-cell pool (*60*). In the two donors we tested, we did not find an over-representation or preferential proliferation of T_{SCM} cells within T-cells responding to immunodominant compared to subdominant epitopes. Instead, we detected a higher level of T-cell apoptosis within subdominant epitope-specific T-cells, which might promote the preferential enrichment of immunodominant T-cells. Previous studies have also indicated that the characteristics of TCR binding to pMHC complexes may also regulate clonal apoptosis (*61*). Indeed, TCRs with a subthreshold affinity for pMHCI preferentially undergo apoptosis early in the response via a process that is regulated by the BCL-2 family members BIM, NOXA and MCL1 (*62*). Thus, our data are in accord with that of others and

suggest that apoptosis may also be crucial for shaping adaptive immune responses, thereby enhancing the selection of clones with greater persistence.

In conclusion, our studies demonstrated that both antigen-specific Tet^+ T cells and Tet^- T-cells derived from isolated T_{SCM} exhibit and maintain a less differentiated phenotype than other memory T cell populations. Second, while we could regularly expand Tet^+ NLV-specific T cells from the $CD95^-$ T_N compartment, antigen-specific T cells expanded from T_{SCM} cells differ from Tet^+ T_N as well as T_{CM} and T_{EM} derived T cells in that they proliferate to a much higher degree in response to antigen stimulation. Third, we find that antigen-sensitized Tet^+ T_N and Tet^+ T_{SCM}, unlike Tet^- T_N and T_{SCM}, express PD-1 at levels similar to those expressed by Tet^+ T_{CM} and T_{EM}. They also exhibit effector function, indicated by the capacity to generate TNF-α, IFN-γ and expression of the degranulation marker CD107a. Fourth, we demonstrate that, in response to antigen stimulation, T_{SCM} not only undergo marked proliferation but also rapidly select T cell clones specific for the CMVpp65 NLV epitope presented by HLA-A 0201 that, by TCR sequencing, are public TCRs identical to those expressed by Tet^+ NLV-specific T_{EM} and T_{CM} that are immunodominant in the blood. In contrast, the NLV-Tet^+ T_N cells can generate a distinct and more varied repertoire than that detected in NLV-specific T_{CM} and T_{EM} in the blood, or in T_{SCM} after 15 days of in vitro stimulation. Taken together, these findings provide evidence that T_{SCM} constitute the principal reservoir for rapid repopulation of immunodominant of NLV-specific T_{CM} and T_{EM} that are maintained in the circulation.

Our findings have implications for the design of T cell-based immunotherapies, in that, adoptive transfer of virus-specific T cell lines enriched for T_{SCM} could potentially provide better disease control by facilitating early recovery of those immunodominant virus-specific T cells that normally control latent infection and provide sustained long term protection from disease.

Figure 1.

Comparison with different cytokine treatments for generating antigen-specific human T cells in vitro

T cells sensitized with AAPC transduced to express CMV pp65 with different cytokine treatments. Antigen-specific T cells was evaluated by HLA-A2-NLV tetramer binding gated on CD8 T cells. (A) Numbers of antigen-specific T cells were calculated from the percentage of antigen-specific T cells in culture. (B) Fold expansion of antigen-specific T cells were normalized from T cells before antigen sensitization at day0.

(A)

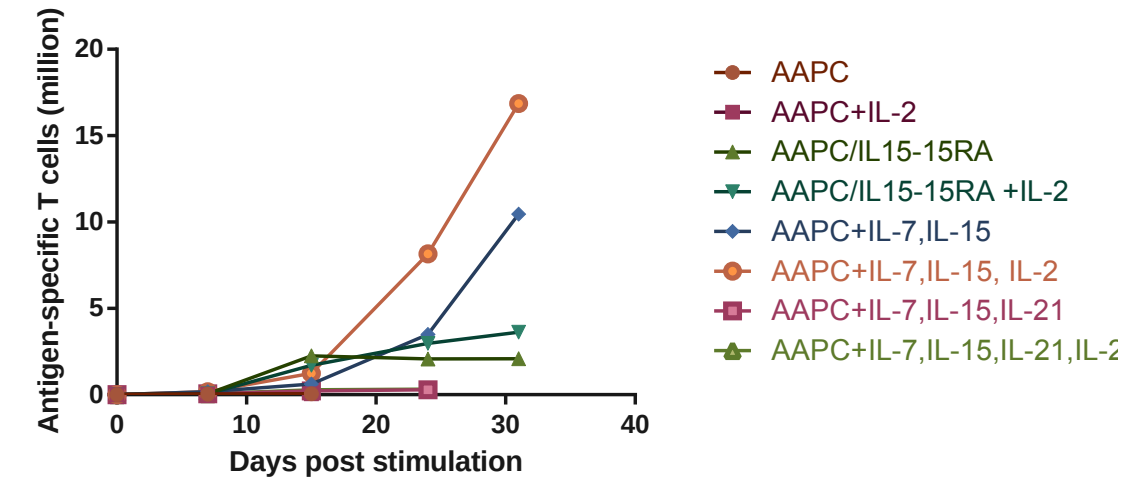
Antigen-specific T cells (million)
20
15
10
5
0
0
10
20
30
40
Days post stimulation
AAPC
AAPC+IL-2
AAPC/IL15-15RA
AAPC/IL15-15RA +IL-2
AAPC+IL-7,IL-15
AAPC+IL-7,IL-15, IL-2
AAPC+IL-7,IL-15,IL-21
AAPC+IL-7,IL-15,IL-21,IL-2

(B)

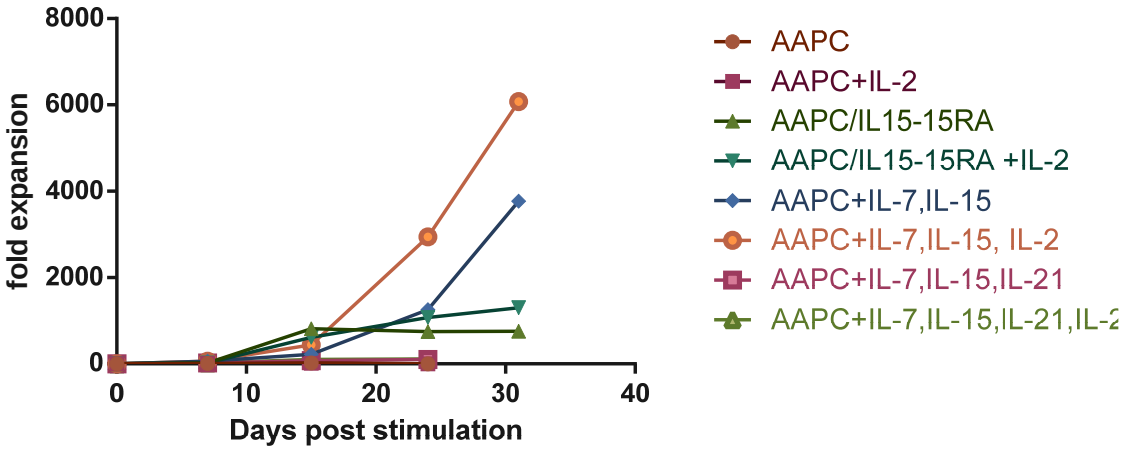
fold expansion
8000
6000
4000
2000
0
0
10
20
30
40
Days post stimulation
AAPC
AAPC+IL-2
AAPC/IL15-15RA
AAPC/IL15-15RA +IL-2
AAPC+IL-7,IL-15
AAPC+IL-7,IL-15, IL-2
AAPC+IL-7,IL-15,IL-21
AAPC+IL-7,IL-15,IL-21,IL-2

Figure 2.

Isolation and characterization of T_N, T_{SCM}, T_{CM} and T_{EM} populations from human peripheral blood

Flow cytometry was used to isolate the T_N, T_{SCM}, T_{CM} and T_{EM} subsets from PBMC. Lymphocytes were first gated within PBMC by forward and side scatter and analyzed for CD45RO, CD95, CD62L and CD3 expression. $CD3^+$ lymphocytes were then gated for $CD45RO^+CD62L^+$ T_{CM} and $CD45RO^+CD62L^-$ T_{EM}, $CD45RO^-CD62L^+CD95^+$ T_{SCM} cells and $CD45RO^-CD62L^+CD95^-$ T_N cells.

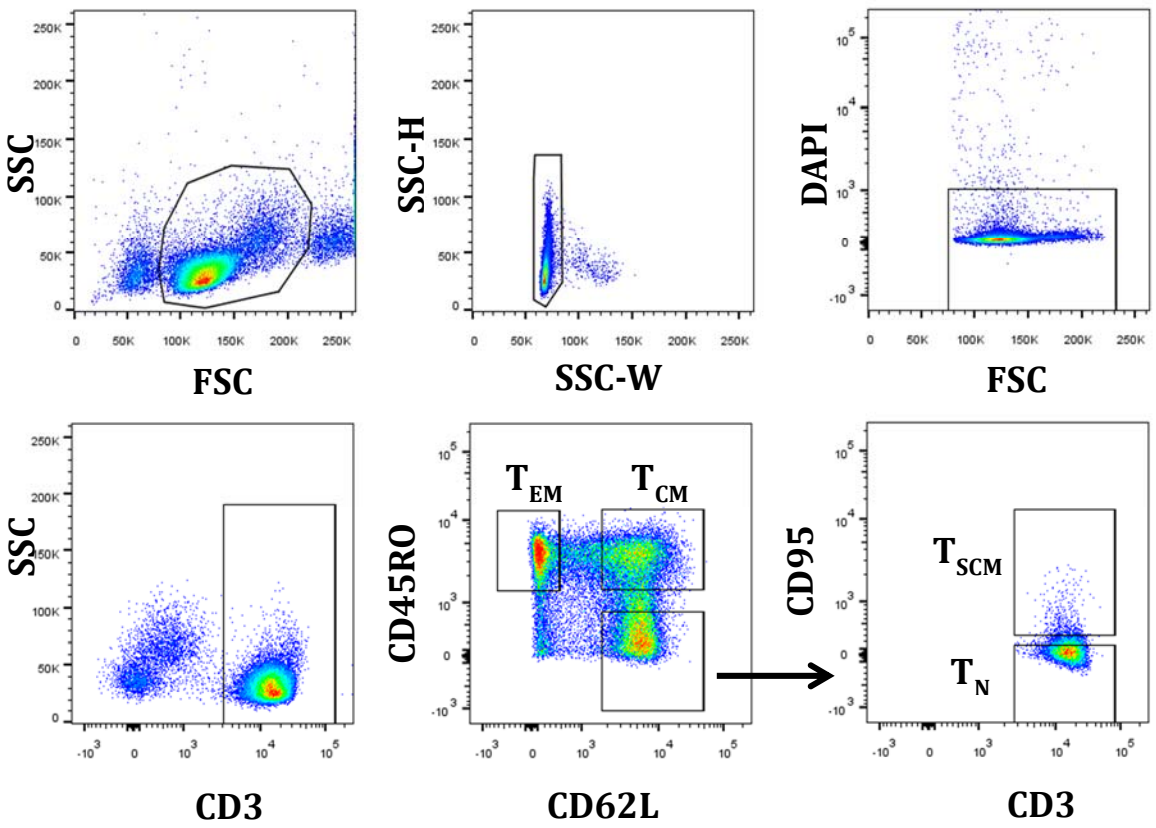
SSC
FSC
SSC-H
SSC-W
DAPI
FSC
SSC
CD3
CD45RO
CD62L
T_{EM}
T_{CM}
CD95
CD3
T_{SCM}
T_N

Table 1.

Composition of naïve and memory TN, TSCM, TCM and TEM) CD8 T cells in healthy CMV seropositive individuals

	Within T cell population					Within NLV-Tet+ population			
Donor	TEM	TCM	TSCM	TN	Tet+	TEM	TCM	TSCM	TN
1	31.9	8.7	4.2	8.7	2.5	35.4	1.1	0.6	ND
2	31.7	7.0	2.5	28.9	4.4	15.1	0.9	2.0	0.2
3	27.4	20.3	5.8	16.0	0.9	47.9	8.3	3.7	ND
4	22.2	13.8	3.8	22.0	0.4	59.7	9.7	2.4	ND
5	34.9	11.0	2.1	5.0	0.5	42.0	1.4	1.4	ND
6	33.0	12.8	3.1	6.0	0.3	79.7	3.4	1.7	ND
7	18.1	32.4	1.2	17.3	2.0	60.2	31.0	6.3	ND
8	21.0	13.0	1.9	28.6	0.1	41.7	2.1	8.3	ND
9	28.4	8.3	10.8	23.5	1.5	70.6	5.9	ND	ND
10	15.4	3.6	2.6	21.8	NA				
11	25.6	1.7	2.0	6.5	1.0	27.8	3.5	3.0	0.1
12	28.9	3.5	2.4	3.8	0.3	35.8	5.3	2.0	ND

(ND= not detectable; NA= not applicable)

Figure 3.

Phenotypic characterization of naïve and memory (T_N, T_{SCM}, T_{CM} and T_{EM}) derived CMV-specific CD8 T cells upon antigen stimulation

Isolated T cells from T_N, T_{SCM}, T_{CM} and T_{EM} cell populations were sensitized with artificial antigen presenting cells (AAPCs) expressing CMVpp65 peptide and HLA-A 0201. T cells were evaluated at 7, 14 and 30 days post stimulation. As shown for a representative donor in panel (A), (B) and (C) $CD8^+$ single, live T cells were gated from $CD3^+$ T lymphocytes. HLA –A 0201-NLV Tet^+ and NLV-Tet^- T-cells were then gated within $CD8^+$ T-cells (left panel), and expression frequencies of CD62L, CCR7 and CD45RA gated on NLV-Tet^+ and NLV-Tet^- population is shown in the middle and right panel (Red: NLV-Tet^+; Blue: NLV-Tet^-). The proportion of CCR7 expressing T-cells post antigenic stimulation are shown for 6 donors tested within (D) NLV-Tet^+ and (E) NLV-Tet^-. (*$P < 0.05$; **$P < 0.01$ by Mann-Whitney test)

(A)

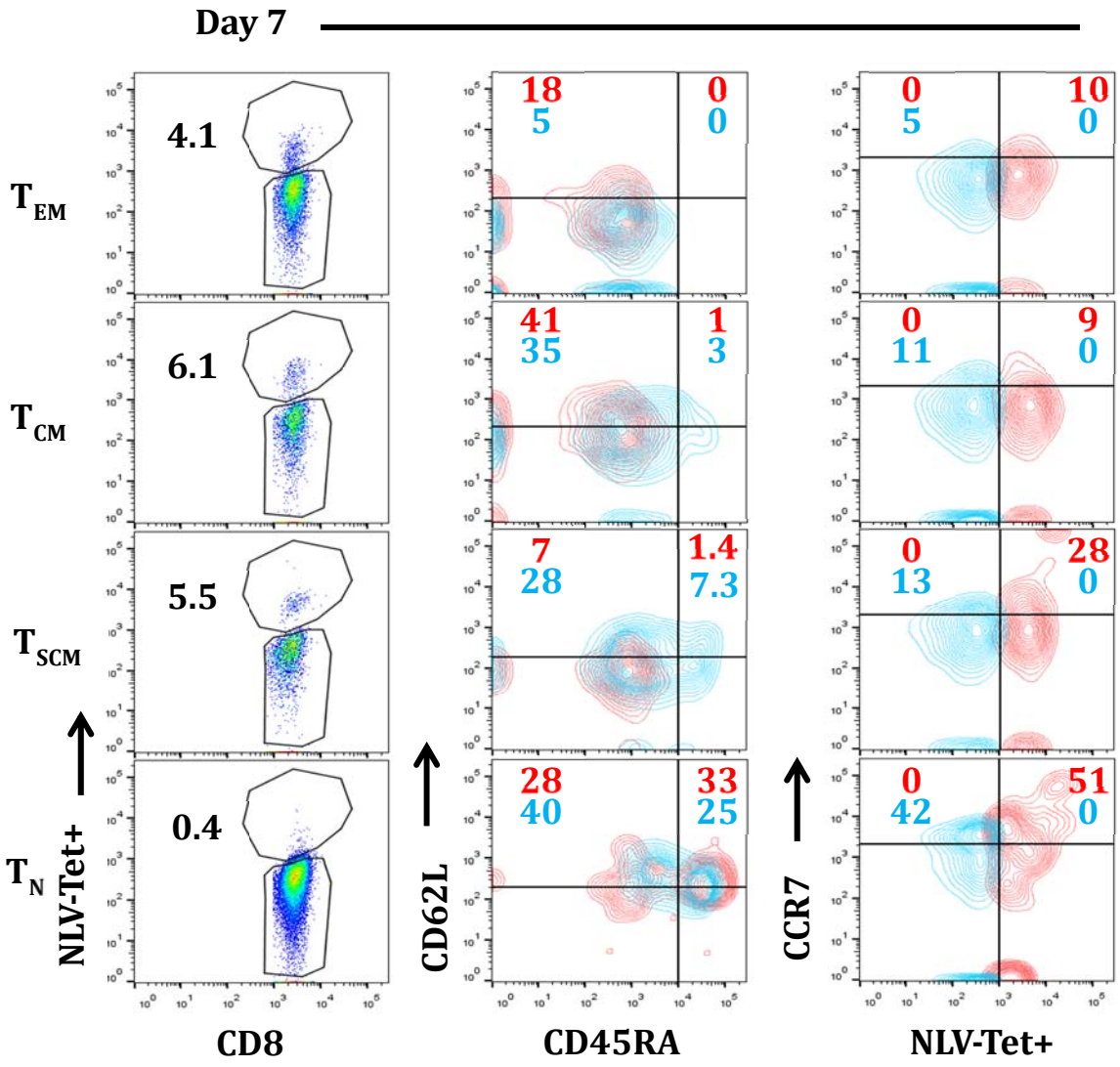

Red: NLV-Tet^{+}

Blue: NLV-Tet^{-}

Figure 3 (Continued)

(B)

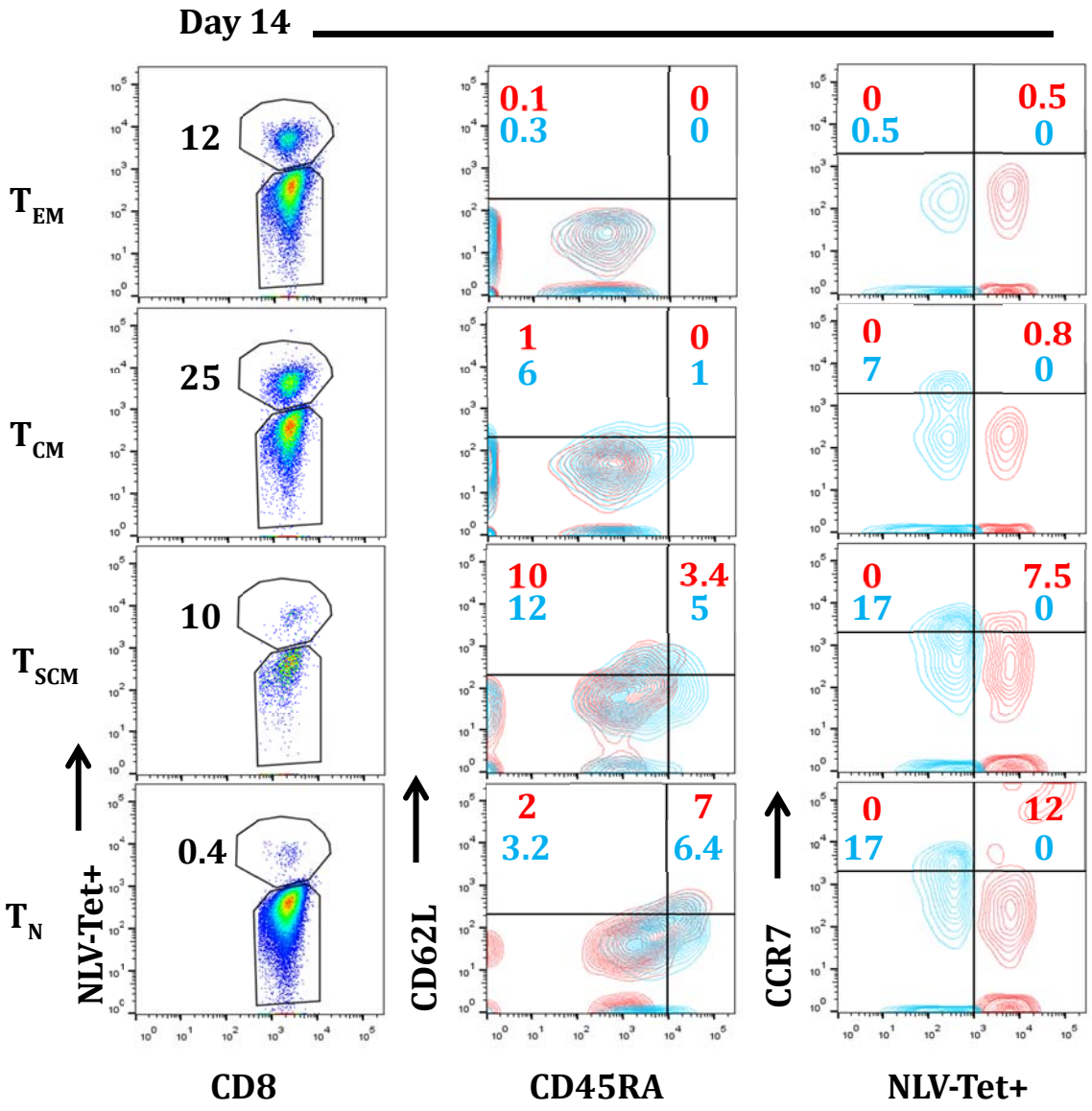

Red: NLV-Tet^{+}

Blue: NLV-Tet^{-}

Figure 3 (Continued)

(C)

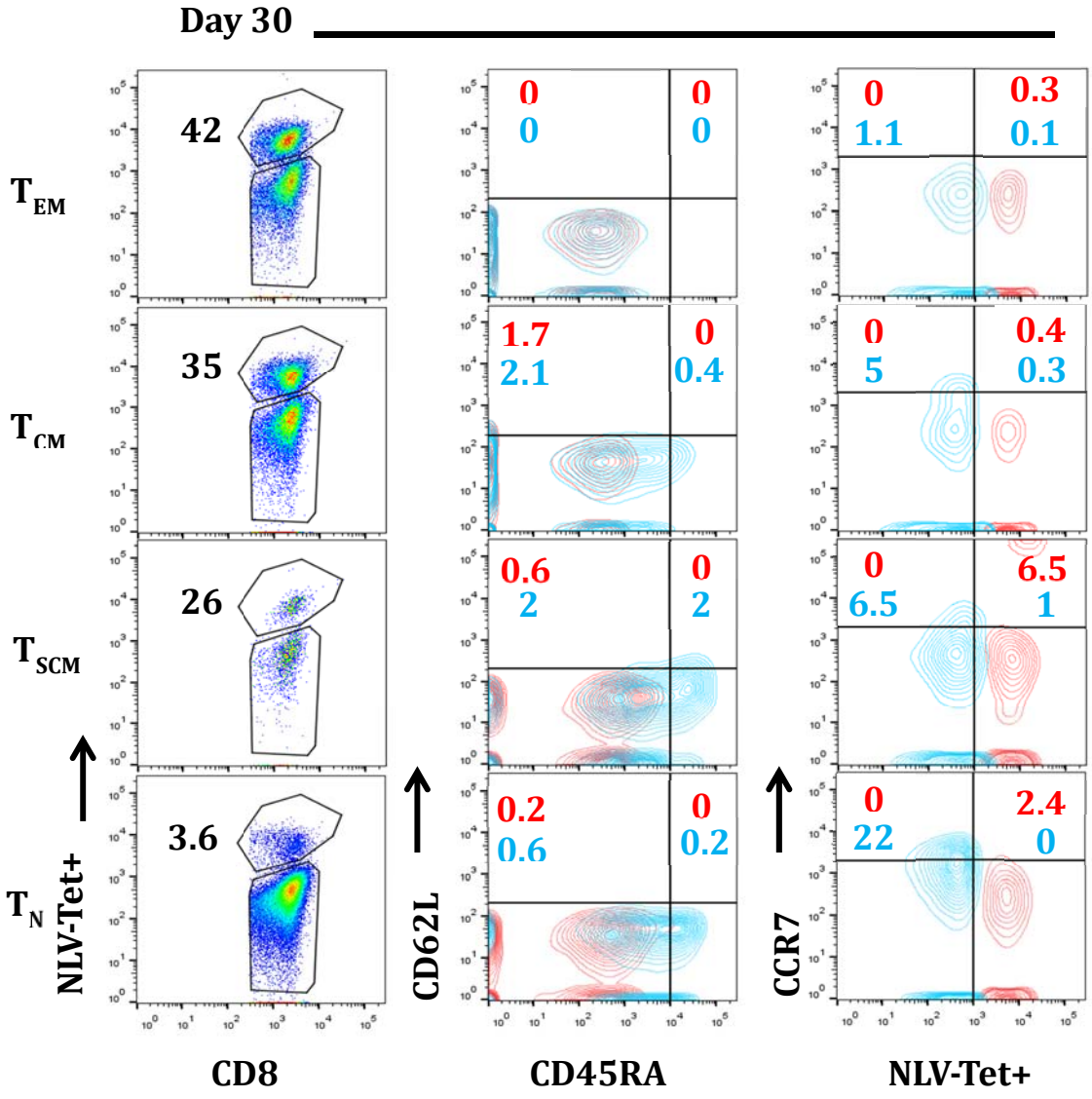

Red: NLV-Tet^{+}

Blue: NLV-Tet^{-}

Figure 3 (Continued)

(D)

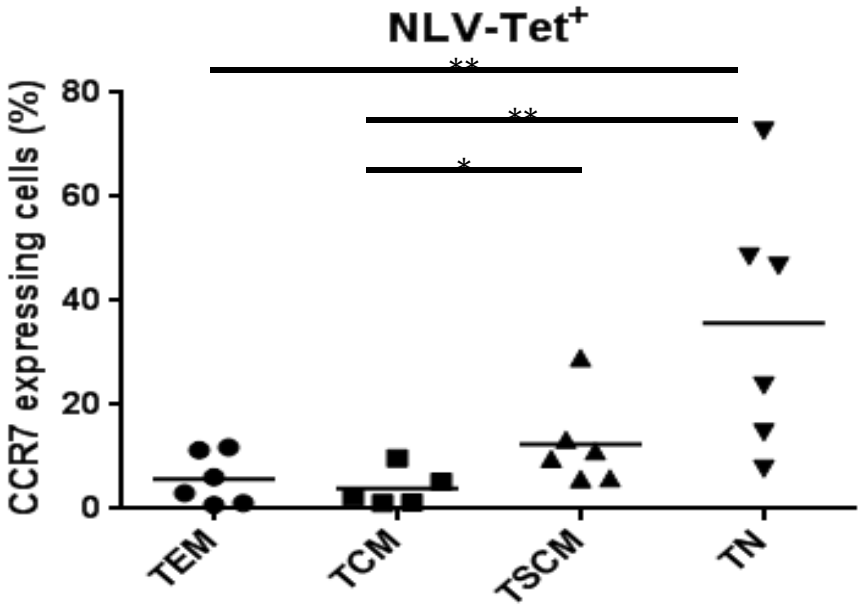

(E)

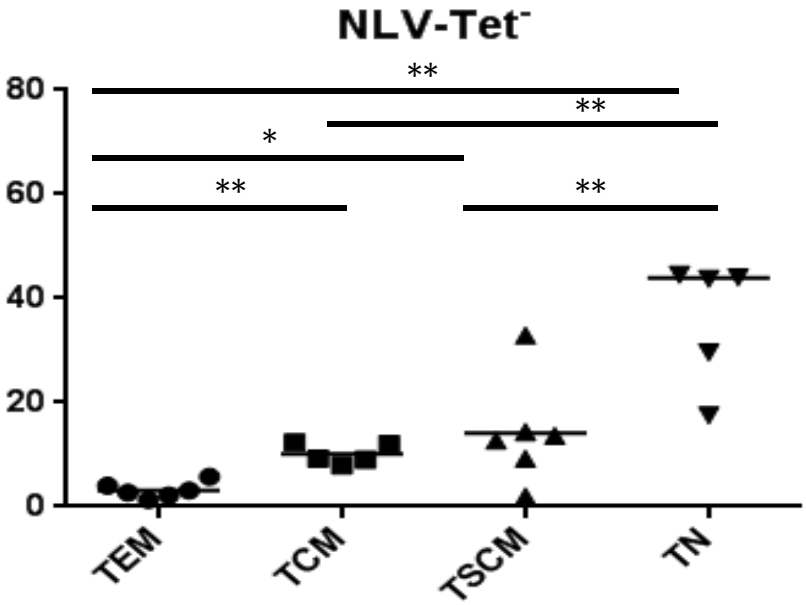

Figure 4.

Distinct expression of co-stimulatory and senescence markers within T_N, T_{SCM}, T_{CM} and T_{EM}

Expression frequencies of CD27, CD57 CD127, CD28, KLRG1, PD1 and CD28 gated on NLV-Tet$^+$ and NLV-Tet$^-$ population after 14 – 18 days of in-vitro stimulation are shown for T-cells expanded from each T-cell subset T_N, T_{SCM}, T_{CM} and T_{EM}. CD27 expression within (A) NLV-Tet$^+$ and (B) NLV-Tet $^-$ CD8$^+$ T cells is shown for 6 donors tested. CD57 expressing (C) NLV-Tet$^+$ and (D) NLV-Tet$^-$ CD8$^+$ T-cells is shown for 8 donors tested. CD 127 expression within (E) NLV-Tet$^+$ and (F) NLV-Tet$^-$ CD8$^+$ T-cells is also shown for 6 donors tested. Within NLV-Tet$^+$ and NLV-Tet$^-$ CD8$^+$ T-cells, the expression levels of KLRG1 (G) and (H), PD-1 (I) and (J) and CD28 (K) and (L) are shown for 9, 11 and 6 donors tested respectively. (*P < 0.05; **P < 0.01 by Mann-Whitney test)

(A)

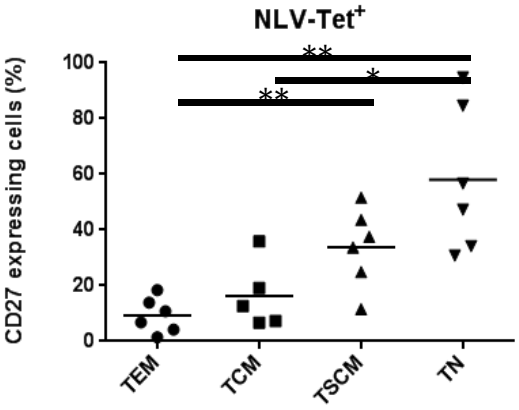
NLV-Tet+
CD27 expressing cells (%)
100
80
60
40
20
0
**
*
**
TEM
TCM
TSCM
TN

(B)

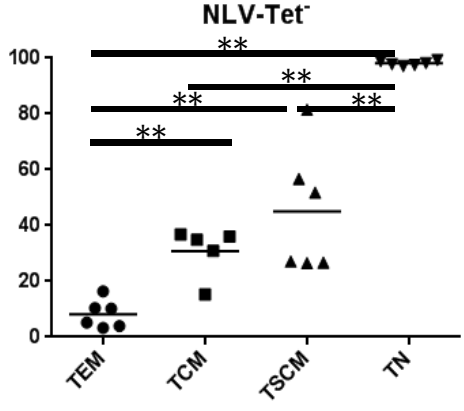
NLV-Tet-
100
80
60
40
20
0
**
**
**
**
**
TEM
TCM
TSCM
TN

(C)

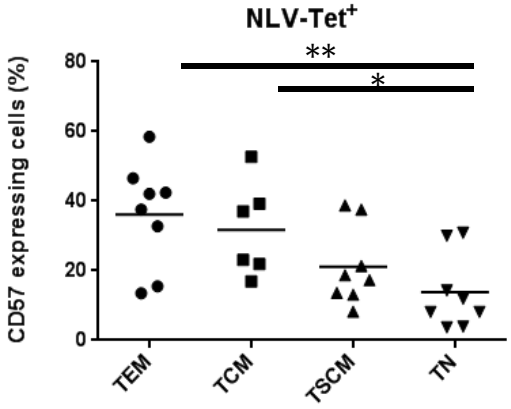
NLV-Tet+
CD57 expressing cells (%)
80
60
40
20
0
**
*
TEM
TCM
TSCM
TN

(D)

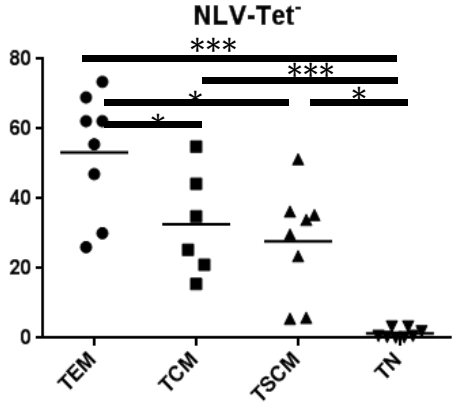
NLV-Tet-
80
60
40
20
0
***
***
*
*
*
TEM
TCM
TSCM
TN

Figure 4 (Continued)

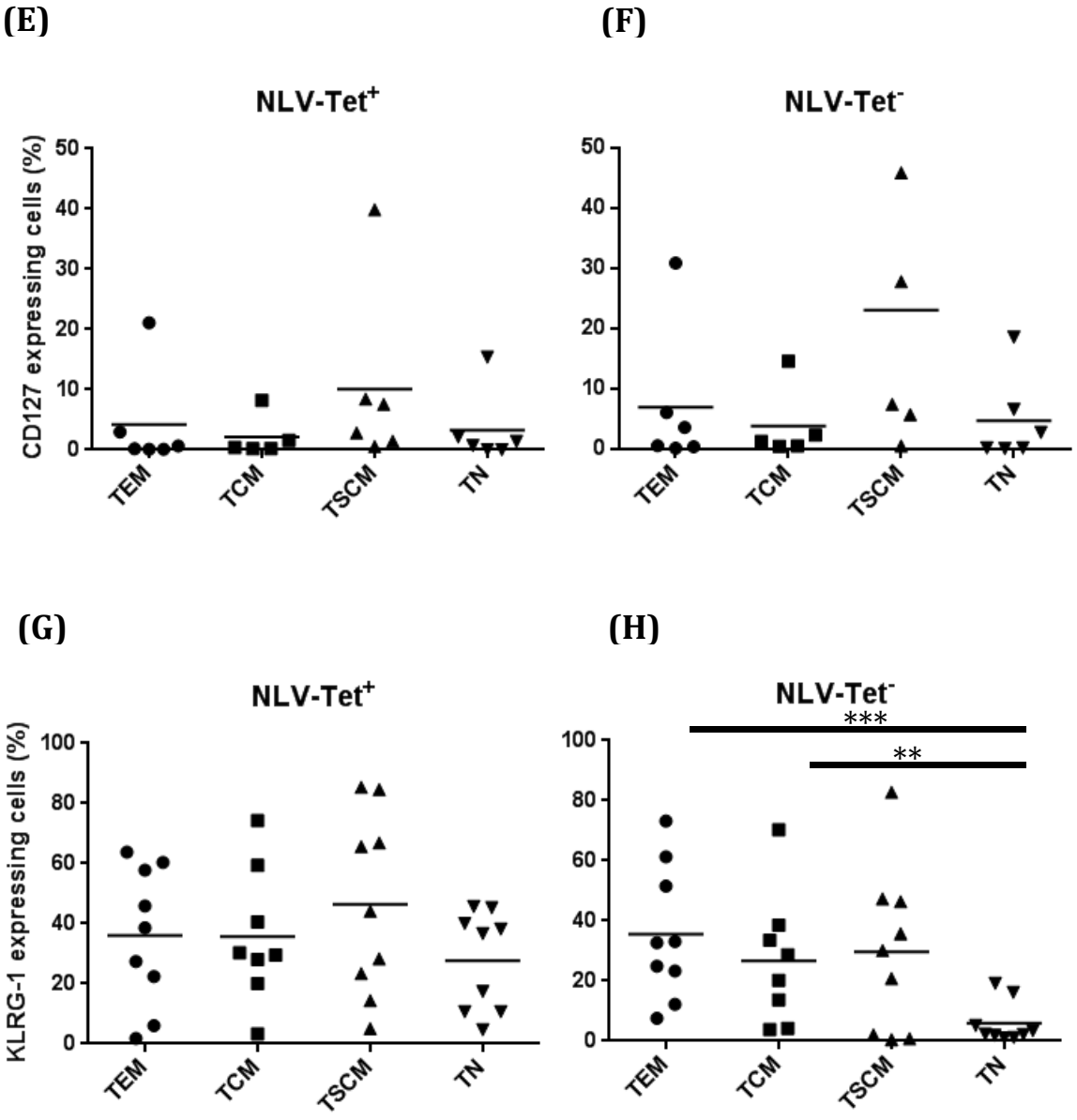

Figure 4 (Continued)

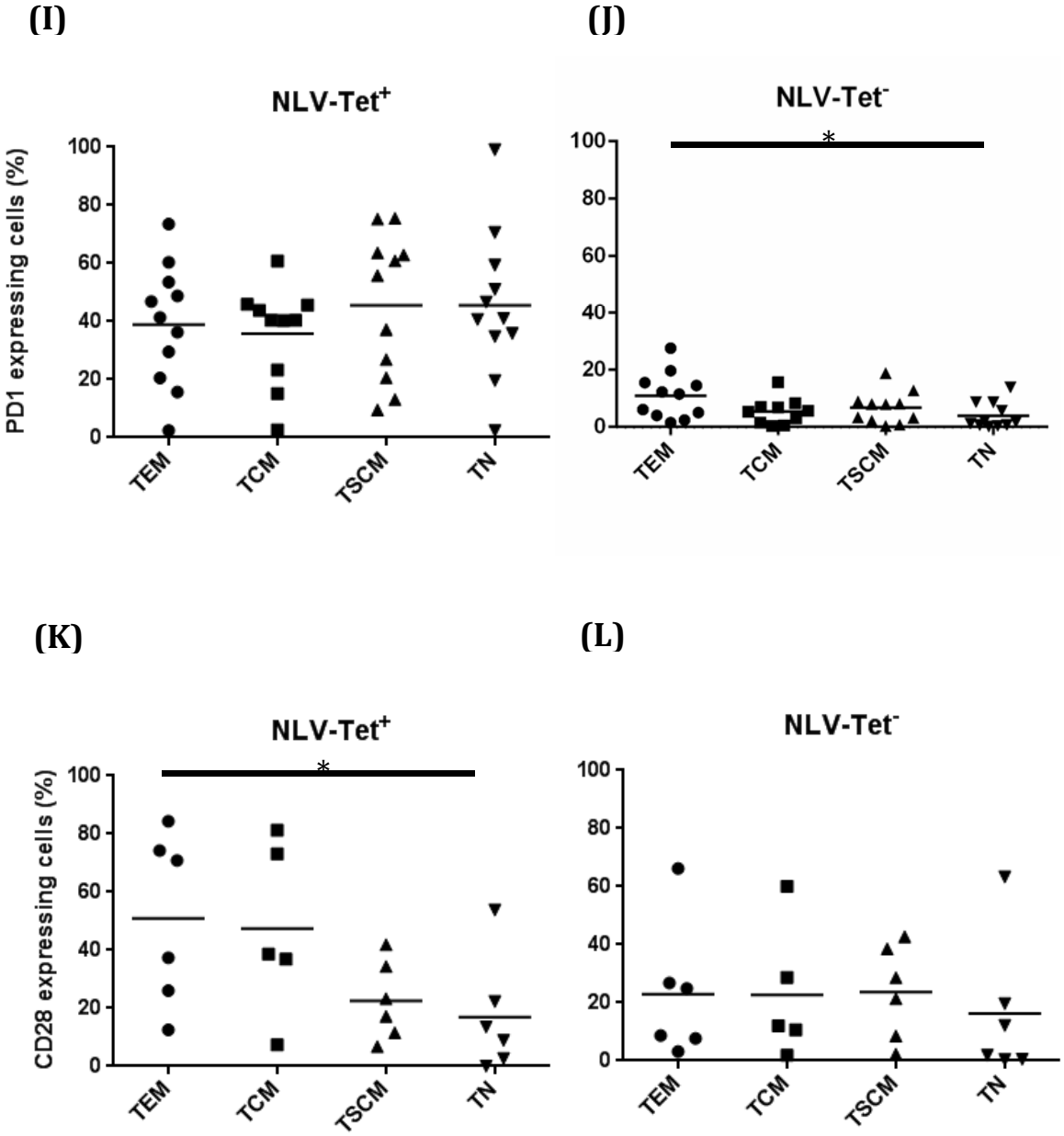

Figure 5.

Enrichment of CMV-specific CD8 T cells results from rapid expansion of early memory T cells

(A) In-vitro proliferation of A2-NLV-Tet $^{+}$ T cells was evaluated after in-vitro sensitization with CMVpp65 antigen by EdU as shown in a representative donor on Day 3, 5 and 7 post- stimulation. $CD3^{+}$ T cells were sensitized with artificial antigen presenting cells (AAPCs) expressing CMVpp65 peptide and HLA-A 0201. The enrichment of NLV-Tet^{+} cell after stimulation was evaluated as shown on the left panel. Percentage of EdU expression gated on single, live $CD8^{+}$ T lymphocytes is shown in the middle panel. Percentage of EdU expression gated on NLV-Tet^{+} $CD8^{+}$ T-cells is shown on the right panel. (B) Phenotypic analysis of NLV-Tet^{+} cells (left panel) in comparison to NLV-Tet^{+} cells with EdU incorporation is shown for a representative donor on the right panel. (Blue: $CD45RO^{+}CD62L^{-}$ T_{EM}; Red: $CD45RO^{+}CD62L^{+}$ T_{CM}; Green: $CD45RO^{-}CD62L^{+}CD95^{+}$ T_{SCM}) $CD45RO^{-}CD62L^{+}CD95^{-}$ T_{N} cells were not detected post antigen stimulation. Fold expansion of A2-NLV-Tet (+) T cells (B) before antigen specific T-cell stimulation and (C) after 14 days of antigen specific T-cell stimulation was evaluated within NLV-Tet^{+} CD8 T cells within the T_{N}, T_{SCM}, T_{CM} and T_{EM} subsets. NLV-Tet^{+} CD8 T cells in TN population was not detected in 4 out of 6 donor tested before exposure to antigen. (n=6) (*P = 0.03; ns, not significant; from Mann-Whitney test).

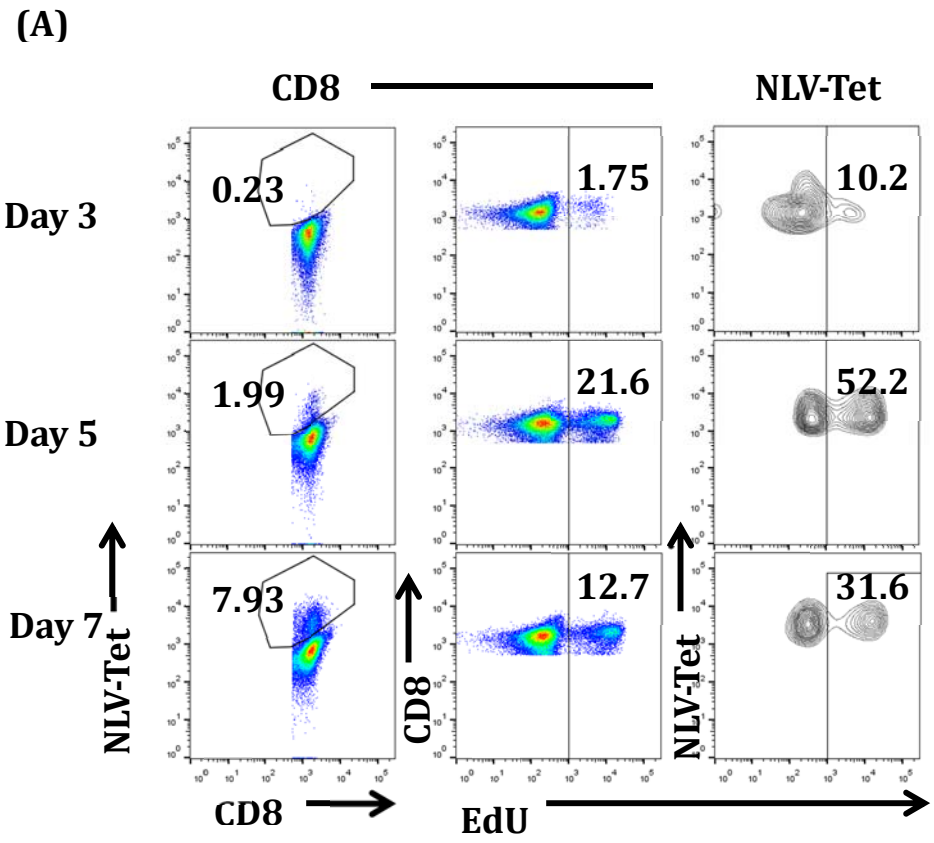
(A)
CD8
NLV-Tet
Day 3
Day 5
Day 7
0.23
1.75
10.2
1.99
21.6
52.2
7.93
12.7
31.6
NLV-Tet
CD8
CD8
EdU
NLV-Tet

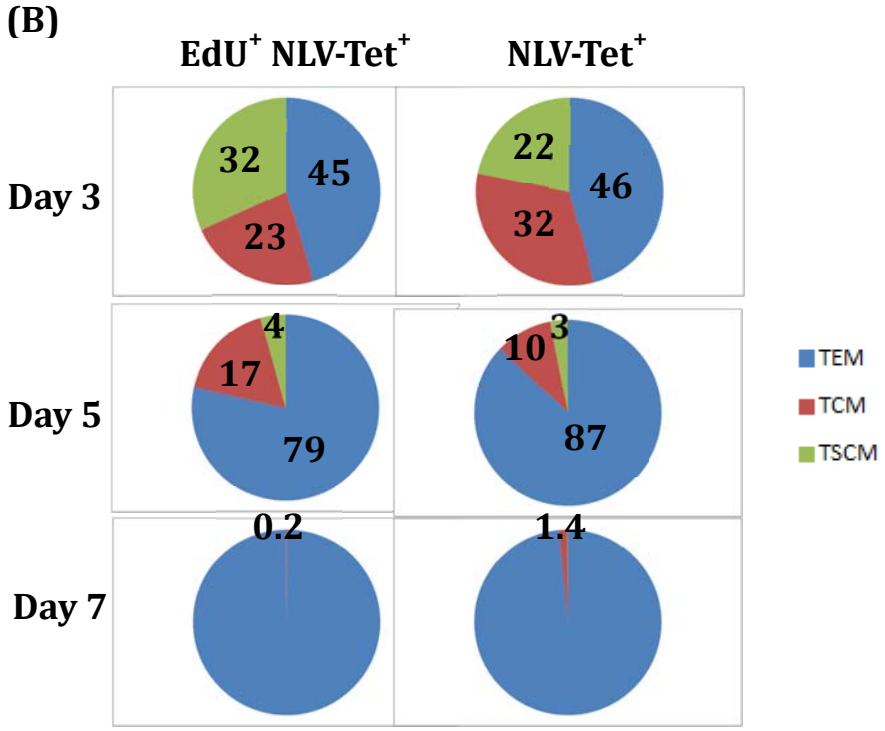
(B)
EdU+ NLV-Tet+
NLV-Tet+
Day 3
Day 5
Day 7
32
45
23
22
46
32
4
17
79
3
10
87
0.2
1.4
TEM
TCM
TSCM

Figure 5 (Continued)

(C)

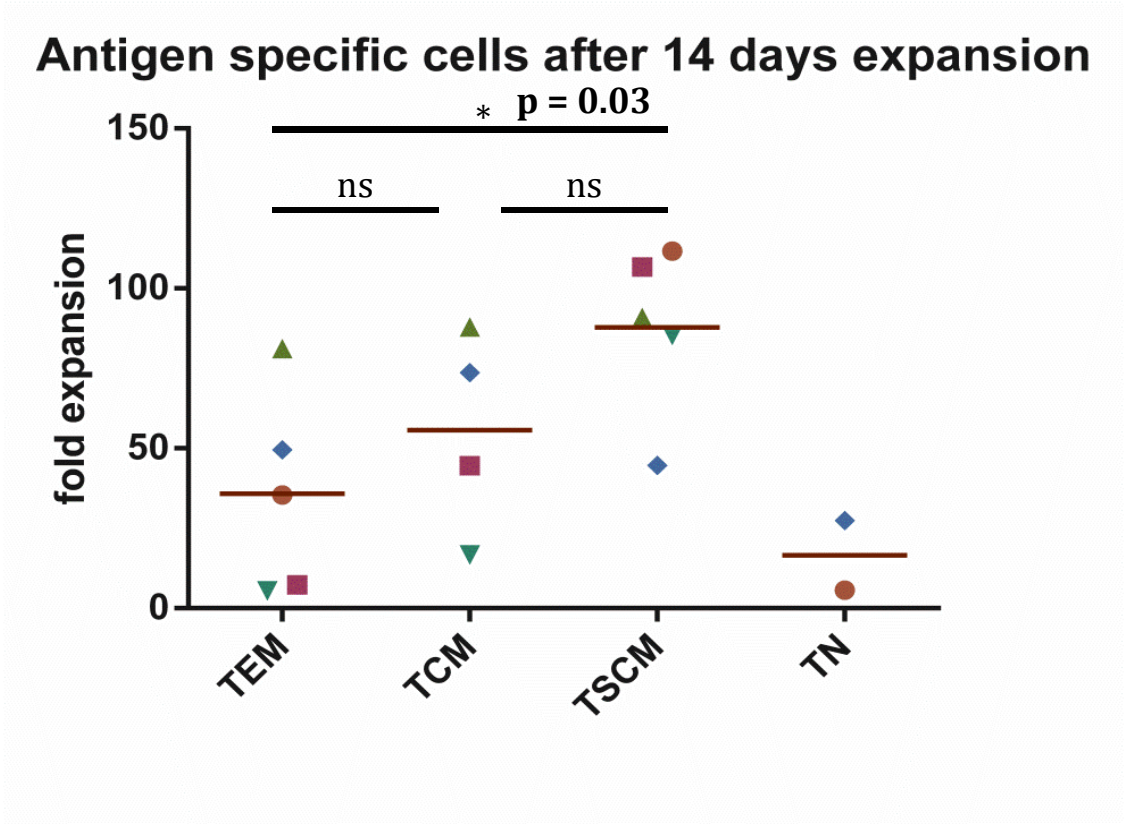

Figure 6.

Functional cytokine profile and cytotoxic activity of in-vitro expanded CMV-specific T cells derived from naïve (T_N) and memory T cells (T_{SCM}, T_{CM} and T_{EM})

(A) Expanded naïve and memory T cell populations were stimulated for 18 hours with NLV peptide loaded autologous BLCLs at a ratio of 5:1. T-cells co-cultures with autologous BLCLs without peptide loading served as controls. $CD8^+$ T-cells secreting IFN-γ and TNF-α were evaluated by intracellular staining within $CD137^+$ T-cells. The percentages of $CD8^+$ T cells co-expressing CD137 are shown on the left 2 panels with or without peptide stimulation. The proportions of $CD137^+$ $CD8^+$ T-cells secreting IFN-γ or TNF-α cytokine are shown in the middle 2 panels. $CD137^+$ $CD8^+$ T cells secreting both IFN-γ and TNF-α cytokine are shown in the right panel. (B) Cytotoxic activity was evaluated by CD107a degranulation. The percentages of $CD8^+$ T cells demonstrating $CD107a^+$ populations with (middle panel) or without (left panel) peptide stimulation are shown. $CD8^+$ T cells expressing both CD137 and CD107a are shown in the right panel. Data are representative of three experiments (n=3).

(A)

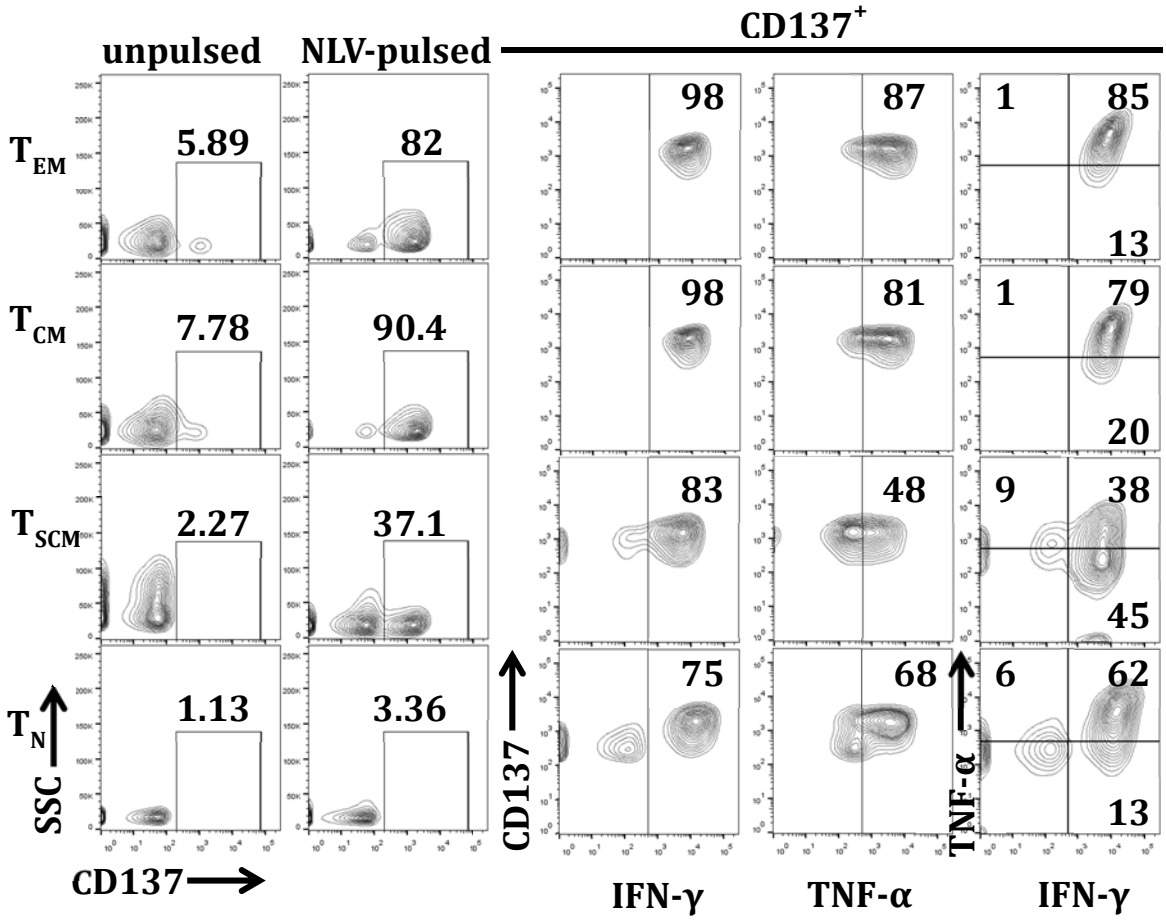
unpulsed
NLV-pulsed
CD137+
T EM
T CM
T SCM
T N
5.89
82
7.78
90.4
2.27
37.1
1.13
3.36
SSC
CD137
98
87
1
85
13
98
81
1
79
20
83
48
9
38
45
75
68
6
62
13
CD137
TNF-α
IFN-γ
TNF-α
IFN-γ

Figure 6 (Continued)

(B)

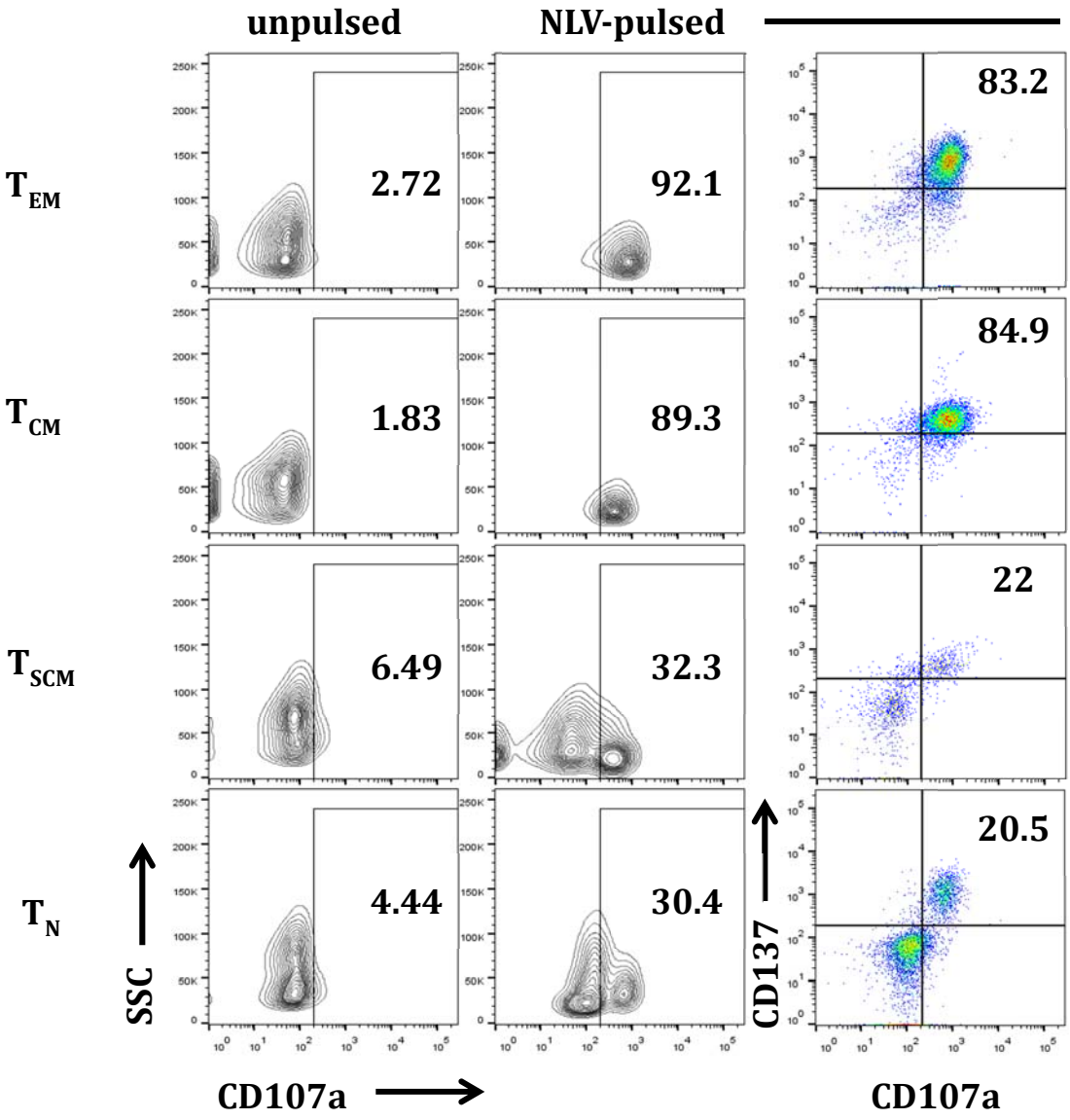

Figure 7.

Clonal diversity and clonotype selection after in vitro expansion in CMV-specific T_N, T_{SCM}, T_{CM} and T_{EM} cells

Next generation sequencing was performed for TCRV_β repertoire analysis. Heat map indicates similarity of sample profiles. The similarity accounts for overlap between unique nucleotide sequences within any two samples. (A) and (B) Naïve (T_N), and memory (T_{SCM}, T_{CM} and T_{EM}) T cell subsets from the same donor after 30 days of in vitro expansion were compared for their TCR sequences within (A) NLV-Tet^+ and (B) NLV-Tet^- T-cells.

Donor CK-200D

NLV-Tet+

(A)

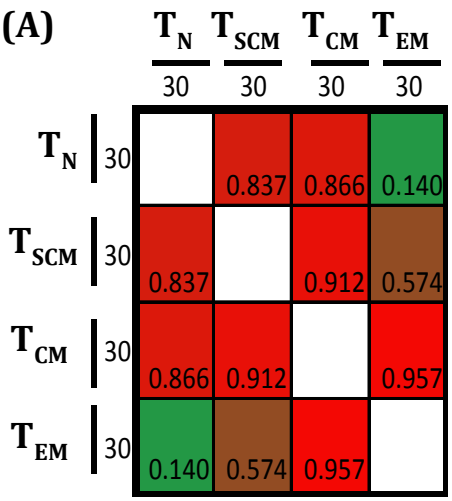

NLV-Tet-

(B)

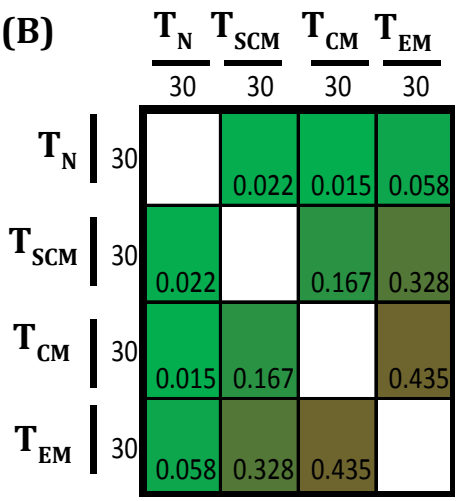

Figure 8.

Tracking of TCR clonotype selection during in vitro expansion

Sorted NLV-Tet$^+$ T-cells within each T_N, T_{SCM}, T_{CM} and T_{EM} subset were subjected to next generation sequencing to evaluate TCRV_β repertoire at day 0 before in vitro stimulation, 15 days, and 30 days after in vitro stimulation. (A) TCR clonality was analyzed using immunoSEQ Analyzer 2.0 for NLV-Tet$^+$ T cells as well as NLV-Tet$^-$ T-cells contained within sorted T_N, $T_{SCM,}$ T_{CM} and T_{EM} T-cell subset populations. The degree of clonal dominance (measured by clonality index) within Tet$^+$ T-cells derived from T_N, $T_{SCM,}$ T_{CM} and T_{EM} T-cell subsets is shown. The heat maps indicate overlap between unique nucleotide sequences within any two samples. This is shown for each time point separately for T cell samples at day 0 (B), 15 days (C) and 30 days (D) after in vitro stimulation. A composite overlap analysis at all time points is shown in (E) for the same donor.

(A)

Donor CK-42202

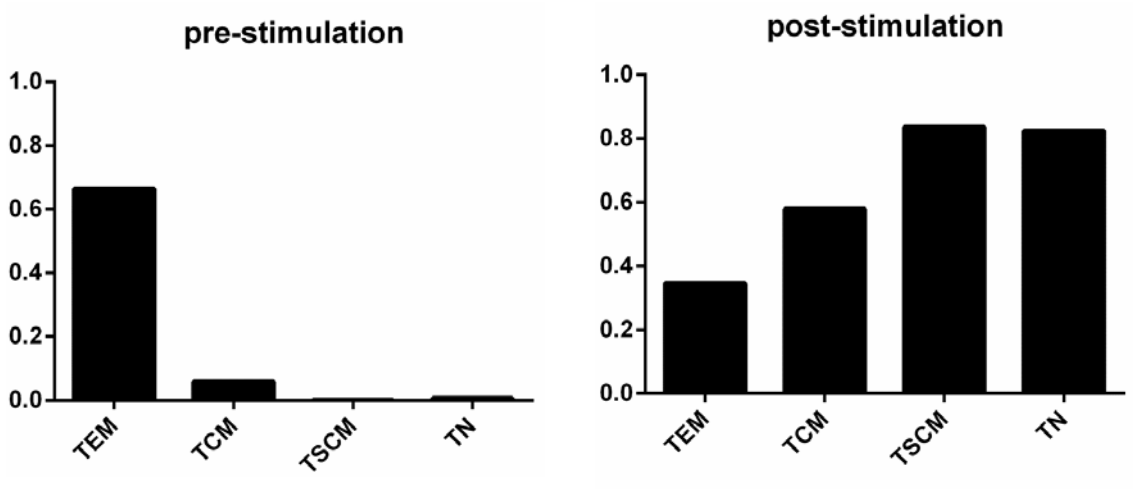

(B) NLV-Tet+

	T_N 0	T_{SCM} 0	T_{CM} 0	T_{EM} 0
T_N 0		0.000	0.000	0.000
T_{SCM} 0	0.000		0.132	0.246
T_{CM} 0	0.000	0.132		0.938
T_{EM} 0	0.000	0.246	0.938	

(C) NLV-Tet+

	T_N 15	T_{SCM} 15	T_{CM} 15	T_{EM} 15
T_N 15		0.656	0.375	0.038
T_{SCM} 15	0.656		0.858	0.948
T_{CM} 15	0.375	0.858		0.971
T_{EM} 15	0.038	0.948	0.971	

(D) NLV-Tet+

	T_N 30	T_{SCM} 30	T_{CM} 30	T_{EM} 30
T_N 30		0.443	0.399	0.040
T_{SCM} 30	0.443		0.876	0.675
T_{CM} 30	0.399	0.876		0.945
T_{EM} 30	0.040	0.675	0.945	

Figure 8 (Continued)

(E) Donor CK-42202

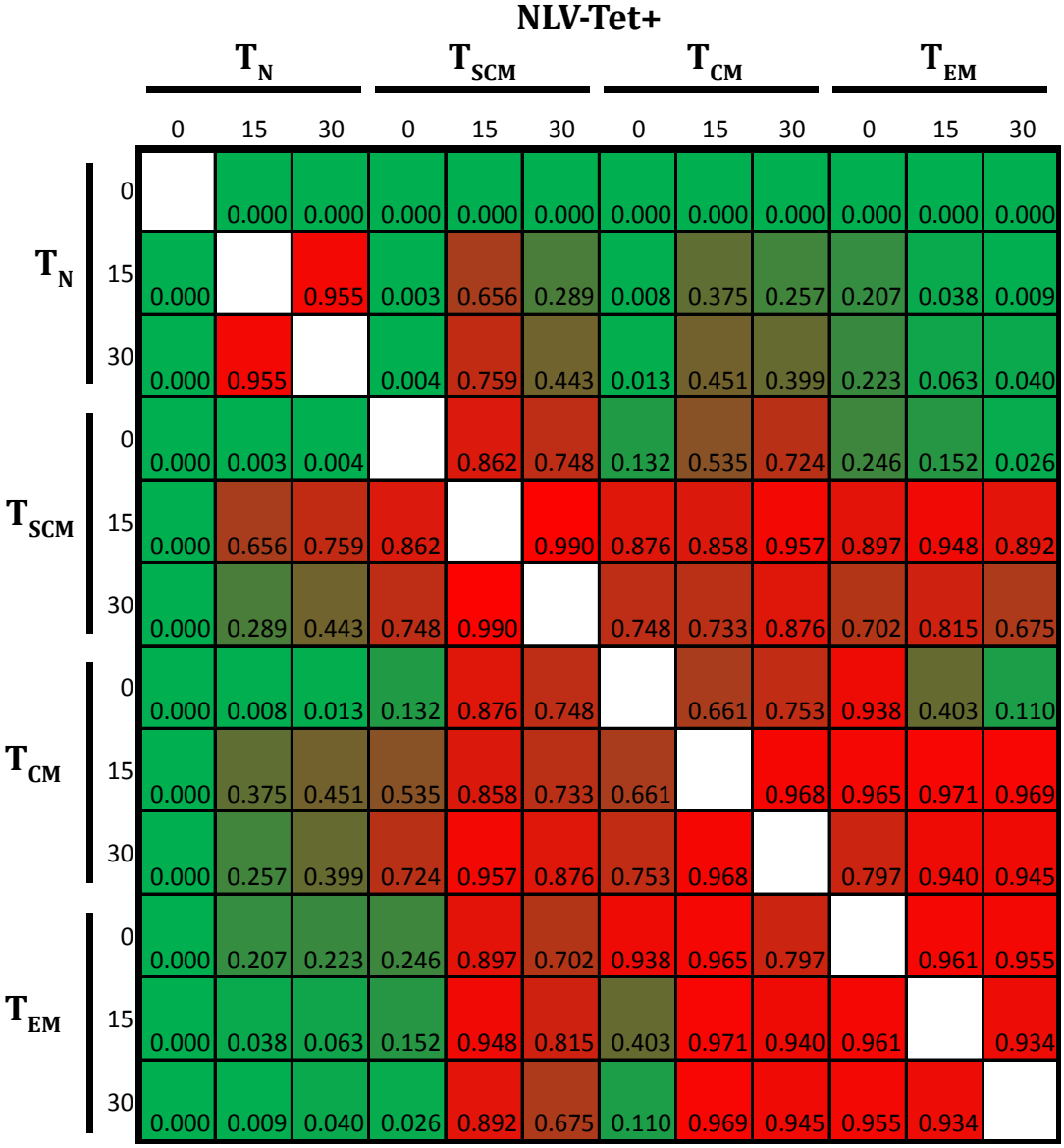

Table 2.

Predominant clonotypes represented within naïve and memory A2-NLV specific CD8 T cells in CMV seropositive donors

				Freq in different days (%)											
				TEM			TCM			TSCM			TN		
Source	aminoAcid	TCRBV	TCRBJ	0	15	30	0	15	30	0	15	30	0	15	30
CK-42202	CASSPQTGASYGYTF	TCRBV06-05	TCRBJ01-02	21.29	10.53	8.13	8.06	46.30	62.72	2.56	83.57	67.66	0.00	0.22	0.11
NLV pos	CASSYVTGTGNYGYTF	TCRBV06-05	TCRBJ01-02	0.00	0.00	0.00	0.00	0.00	0.00	0.00	0.00	0.00	0.00	88.93	87.14
	CSVAGTVNEQFF	TCRBV29-01	TCRBJ02-01	0.81	22.99	18.87	0.00	5.79	2.94	0.00	9.72	14.59	0.00	0.00	0.00
	CAAGGIFGTDTQYF	TCRBV27-01	TCRBJ02-03	0.00	4.29	5.79	0.00	6.57	5.38	0.00	0.00	0.00	0.00	0.00	0.00
	CAWSISDIMNTEAFF	TCRBV30-01	TCRBJ01-01	0.00	1.80	0.83	0.00	12.31	6.95	0.00	0.00	0.00	0.00	0.00	0.00
	CASSLEGYTEAFF	TCRBV27-01	TCRBJ01-01	6.20	4.99	3.31	2.42	2.99	1.47	0.00	0.00	0.00	0.00	0.00	0.00
	CAWSVSDPLNTEAFF	TCRBV30-01	TCRBJ01-01	1.66	1.52	2.20	2.42	1.18	0.29	0.00	0.00	0.00	0.00	0.00	0.00
CK-200D	CASSPKTGAVYGYTF	TCRBV06-05	TCRBJ01-02			10.79			73.07			79.73			46.41
NLV pos	CASSHQTSGNTIYF	TCRBV19-01	TCRBJ01-03			17.04			0.09			0.00			0.00
	CASSLKTGASYGYTF	TCRBV06-05	TCRBJ01-02			1.17			4.64			0.02			1.10
	CASSVLAPTVGSTEAFF	TCRBV10-02	TCRBJ01-01			4.37			3.03			0.00			0.00
	CASSYQTGASYGYTF	TCRBV06-05	TCRBJ01-02			4.22			1.81			0.00			0.00
	CASSEIGATNYGYTF	TCRBV06-01	TCRBJ01-02			2.94			0.16			0.00			0.00

Figure 9.

Immunodominance is not caused by the skewed proliferation of T_{SCM} cells in circulation

(A) T cell population selected from CMV seropositive donor coinheriting HLA A0201 and HLA A2402. CD3 T cells sensitized separately with either AAPC coexpressing HLA A0201 and CMVpp65 or HLA A2402 and CMV pp65. Flow cytometry was performed to evaluate the expression of CD62L and CD45RA within gated Tet^+ population after 4, 5, 7 and 8 days post stimulation (A2: NLV and A24: QYD). The percentages of T_{SCM}, T_{CM} and T_{EM} cells were evaluated within Tet^+ population (T_{SCM}: $CD62L^+CD45RA^+$, T_{CM}: $CD62L^+CD45RA^-$ and T_{EM}: $CD62L^-CD45RA^-$) (B) T cell proliferation and apoptosis within Tet^+ population was evaluated by coexpressing EdU or AnnexinV in comparison to A2 NLV-Tet^+ and A24 QYD-Tet^+ population.

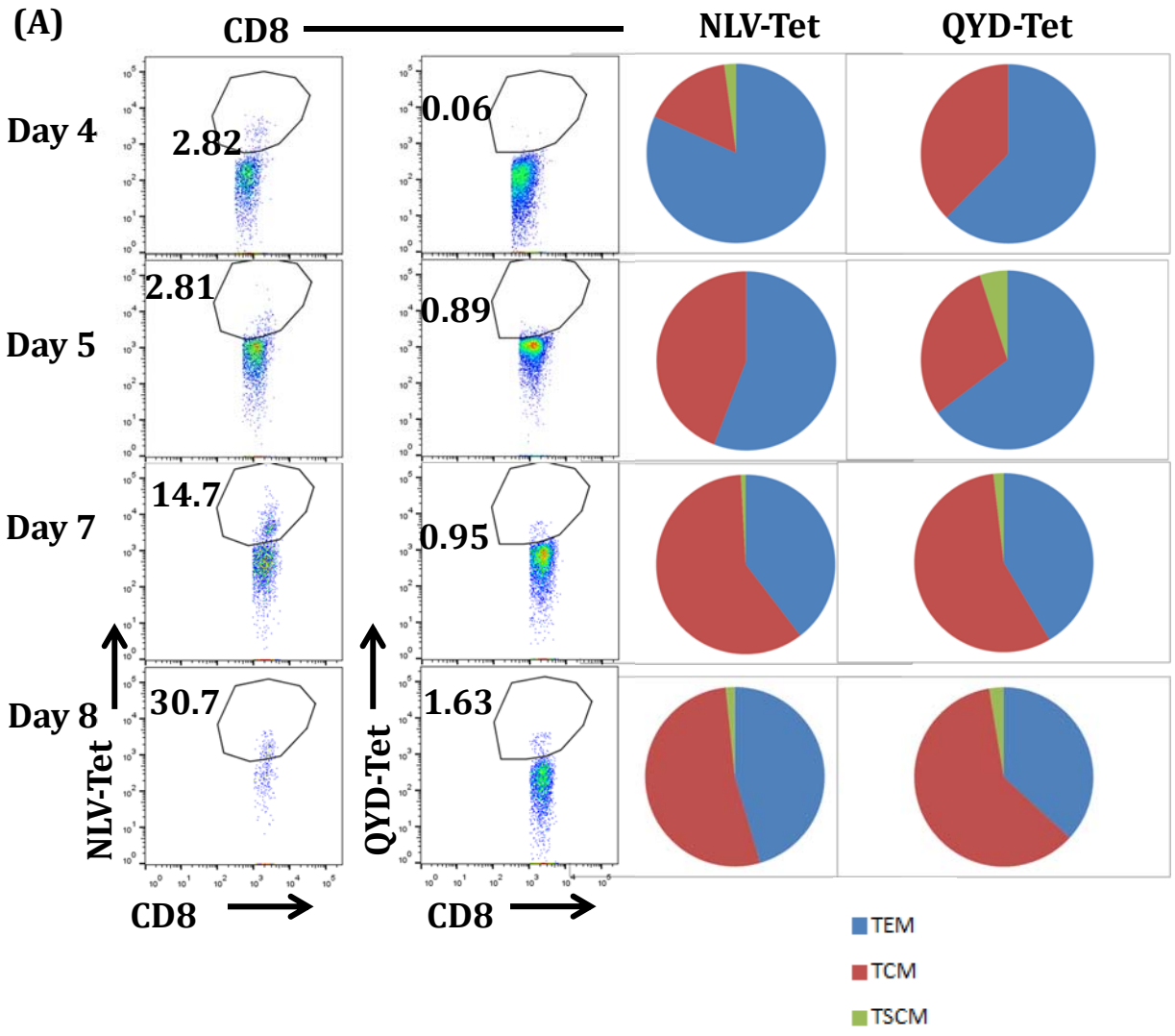
(A)
CD8
NLV-Tet
QYD-Tet
Day 4
Day 5
Day 7
Day 8
2.82
0.06
2.81
0.89
14.7
0.95
30.7
1.63
NLV-Tet
QYD-Tet
CD8
CD8
TEM
TCM
TSCM

Figure 9 (Continued)

(B)

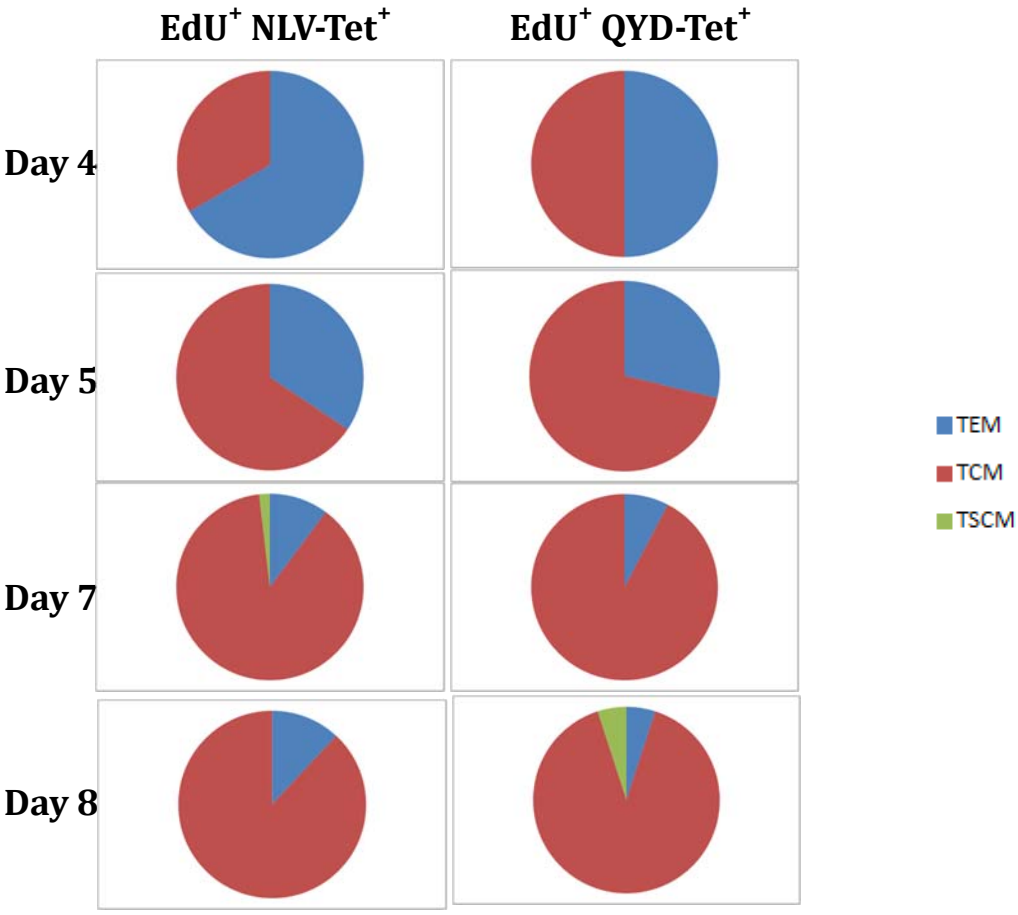

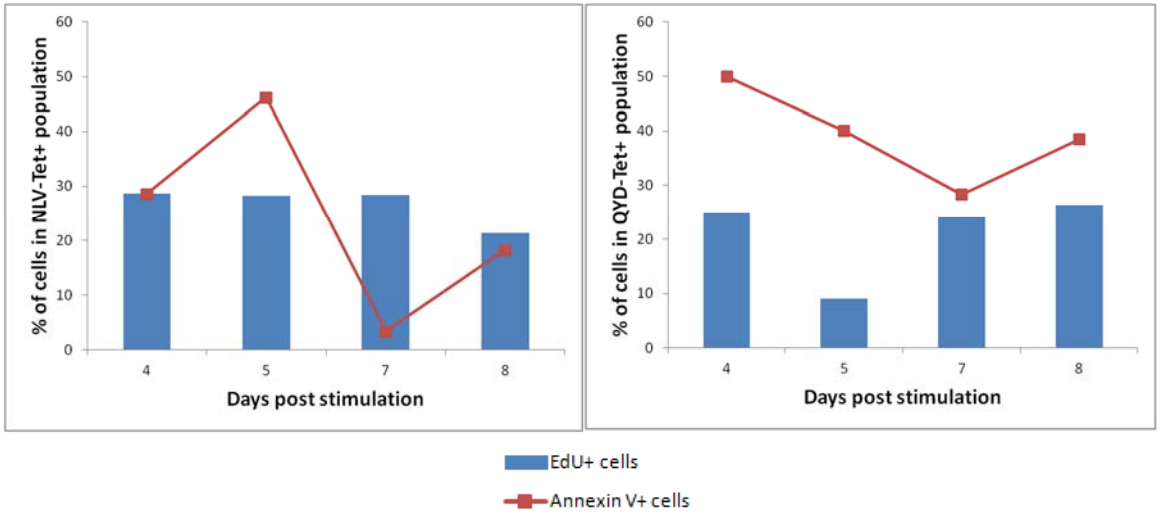

CHAPTER THREE

Affinity maturation of TCR-like antibodies for WT1 peptide greatly enhances therapeutic potential.

1. Introduction

Virus specific T- cells responding to immunodominant epitopes demonstrate the highest functional activity executing effective control of infection. In previous studies, we evaluated the in vitro- expansion and functional activity of T-cells responding to immunodominant and subdominant epitopes. These studies did not reveal a clear role of T_{SCM} cells in establishing epitope-specific immunodominant T-cell populations. The mechanisms of antigen presentation, that affect the repertoire of epitope specific T-cells, including peptide MHC-binding affinity, are very dynamic and primarily focused on the APC. We sought to evaluate the role of T cell receptor affinity on the in vitro expansion and functional activity of epitope specific T-cells.

Antigens expressed on cancer cells are self-antigens. The human immune system has evolved to avoid the generation of high-affinity T cell receptors (TCRs) against self-proteins to preclude autoimmune reactions. In clinical trials, T cells directed against tumor antigens have typically demonstrated weak responses in vivo. Such tumor antigen specific T-cells have also been shown to express TCRs that demonstrate low binding affinity to the target tumor cells. Although soluble TCRs have been successfully developed to target T cell epitope on tumors, their inherent low affinity has limited their potential as therapeutics (*63*). It was therefore thought that increasing the TCR affinity of the endogenous TCRs for tumor antigen specific T-cells would enhance the activity of adoptively transferred T-cells directed against cancer antigens. Attempts to affinity mature

TCRs have been hampered by cross-reactivity (*64, 65*). Affinity enhanced TCR directed to human HLA A01-restricted MAGE A3 antigen, called a3a was identified as the most potent MAGEA3-specific TCR. However, when the a3a-engineered T cells were used in two patients with melanoma, both died through off-target toxicity (*66*). These studies suggest that T cells expressing affinity-enhanced TCRs directed to the tumor antigen have potent tumor activity, as long as improvements in affinity are contained within an appropriate window; above this threshold level, efficacy and specificity would be compromised. In these studies, we utilized a chimeric antigen receptor (CAR) based system expressing a TCR mimic single chain variable fragment (scFv) directed against the RMF epitope of the intracellular protein WT-1 in complex with / presented by HLA A0201. We specifically evaluated the in vitro functional activity of CAR modified T-cells, that expressed antibodies of both high and low binding affinities to determine the differential functional activity between T-cells expressing high and low affinity antibodies as a surrogate for high and low affinity TCRs.

A chimeric antigen receptor (CAR) is a fusion receptor that combines the antigen recognition property of an immunoglobulin with a T cell activation domain. A T cell engineered to express a CAR has the ability to recognize and bind to cell surface antigens via the antibody domain, and then get triggered to be activated through the T-cell signaling and co-stimulatory domains (e.g. CD3 zeta, and 4-1BB), thus emulating interaction with antigen expressing APC. Most CARs typically use an antibody-derived antigen-binding motif to recognize native cell-

surface antigens independently of antigen-processing or major histocompatibility complex (MHC) -restricted presentation. Another strategy for retargeting T cells to specific antigen expressed on cells consists of TCR-mimic CARs expressing a scFv antibody directed against a specific peptide-MHC complex. TCR-like antibodies, with high affinity and controlled specificity, could be ideal therapeutics (*67*). To this end, several TCR-like antibodies targeting peptides derived from viral or tumor antigens in the context of human leukocyte antigen (HLA)-A1 or HLA-A2 have been reported (*68-71*).

The Wilms tumor gene 1 is one of the most studied tumor associated antigens, which encodes a zinc-finger transcription factor (Wilms tumor protein 1; WT1) important in cell growth and differentiation (*72*). WT1 is over expressed in several malignancies such as leukemias, lymphomas and solid tumors including astrocytic tumors, sarcomas, breast, lung and colorectal cancer, and neuroblastoma (*73*), with the characteristics of an oncogene (*74*). Several peptides derived from endogenous WT1 protein are presented in the context of MHC class I molecules and are immunogenic (*75*). The 9-mer WT1-derived peptide 126–134, RMFPNAPYL ($WT1_{126}$), is the most extensively studied (*76*). As a vaccine, the $WT1_{126}$ peptide has induced durable WT1-specific cytotoxic T cell (CTL) responses in patients with acute myeloid leukemia (AML) (*77*).

We developed a novel TCR-like CAR containing the antibody against $WT1_{126}$/HLA-A2. T-cells transduced to express these novel CARs that contain either a low affinity or a high affinity antibody were used as a surrogate system to

evaluate the effect of the binding affinity of the TCR mimic-CAR on the functional activity of such CAR expressing T-cells.

2. Materials and Methods

Human lymphocytes and tumor cell lines

Human peripheral blood mononuclear cells (PBMC) were isolated from whole blood by ficoll Hypaque density gradient separation. T cells were purified by negative magnetic separation using magnetic beads containing antibodies against CD19, CD20, CD14, CD56 (Pan T-cell isolation kit, Miltenyi Biotech). Cells were cultured in RPMI 1640 with 2 mM L-glutamine and 10% fetal bovine serum (FBS).

Retroviral production and transduction

For T-cell or K562 transduction, vector DNA was transfected into H29 packaging cells in the presence of $CaCl_2$. Viral supernatant was collected for two consecutive days to be stored, or to transfect the PG-13 packaging cell line. PG-13 cells expressing the transduced vector DNA were sorted using GFP as the selection marker, cloned and expanded, and culture supernatants collected for T-cell transduction. Purified T-cells were first stimulated with CD3/CD28 beads for 24 hours. PG-13 viral supernatant was added to retronectin coated plates, followed by the suspension of T-cells or K562 cells. The plates were spun down and incubated for 48 h. Cells expressing the transduced vector were detected using GFP and a $WT1_{126}$/HLA-A2-PE-labeled tetramer by FACS.

Cytotoxicity Assay

The cytolytic capacity of T-cells was tested against HLA-A2/$WT1^{+}$ tumor cell lines as well as autologous EBV-BLCL loaded with the $WT1_{126}$ peptide using the standard ^{51}Cr release assay.

3. Results

3.1 Low affinity T-cell receptor-like CAR T cells were not functional

Human scFv-specific HLA-A2/$WT1_{126}$ Clone 45 was isolated and characterized by Dr. Nai-Kong V. Cheung's lab using phage display selection (*78*). WT1 Clone 45 scFv was highly specific for the recombinant HLA-A2-RMFPNAPYL complex. However, The binding affinity of scFv Clone 45 (K_D= 300 nM) was low. We first modified CD3 T cells isolated from the peripheral blood of healthy donors, using retroviral transduction in vitro with the Clone 45- chimeric antigen receptor (CAR) from Dr. Cheung's lab. Transduction efficiency varied between 20% and 40% in both CD4 and CD8 T cells. We FACS sorted for GFP^+ CD3 T cells expressing the Clone 45-CAR in both CD4 and CD8 T cells. We failed to find any HLA-A2-RMF tetramer positive cells in either CD4 or CD8 GFP^+ T cells (figure 1). We then evaluated cytotoxicity activity of T cells expressing Clone 45-CAR by ^{51}Cr release assay. Cytotoxic activity of Clone 45 CAR^+ T cells was examined at an E/T ratio of 25:1 and 10:1 using 3 different target tumor cell lines overexpressing WT1; OVCAR3/pp65 and HTB37/pp65, which coexpress HLA A0201 and SKOV3 which only expresses WT-1. The WT-1 expression level for each of these tumor cell lines was evaluated by western blot, and is shown in figure 2A. We detected minimal lysis of tumor cells expressing NCA A0201 and C high (OVCAR3/pp65) or medium (HTB37/pp65). No lysis was detected against the HLA A0201 negative WT-1 low expressing SKOV-3 (figure 2B) with Clone 45 CAR^+ T-cells. We therefore observed that Clone45-CAR expressing T cells not

only did not bind to the HLA-A2-RMF tetramer, but also failed to kill the WT1 expressing tumor targets.

3.2 Affinity-matured TCR-like CAR T cells greatly enhanced their therapeutic potential

The affinity maturation of Clone 45 was carried out using yeast display by Dr. Nai-Kong V. Cheung's lab (*78*). Q2L, the affinity-matured clone achieved a 100-fold improvement in affinity (K_D = 3 nM). Compared to reported TCR-like antibodies (9.9 to 294 nM) (*68*), it was the highest among all. We first transduced K5G2 cells to express Q2L-CAR so as to validate whether the HLA-A2-RMF tetramer can bind to Q2L-CAR. We achieved a 42% transduction efficiency as assessed by the percentage of GFP^+ cells, and 40% K562 cells demonstrated binding to the HLA A0201-RMF Tetramer representing cells expressing the Q2L-CAR (figure. 3). In GFP expressing cells, almost all of the cells also bound the HLA-A2-RMF tetramer, demonstrating that the high affinity Q2L-CAR expressed in K562 cells was able to bind to RMF complexed with HLAA0201 (figure. 3A). We next isolated $CD3^+$ T cells from the peripheral blood of healthy donors and transduced them *in vitro* to express the Q2L-CAR. HLA-A2-RMF tetramer binding was again demonstrated by the transduced CD4 and CD8 T cells that coexpress GFP (figure. 3B). In assays testing their specific cytotoxicity against WT1-expressing tumor targets, we found that T cells transduced to express Q2L-CAR mediated efficient tumor cell target lysis. Q2L-CAR modified T cells specifically recognized and killed HLA-A2(+)/WT1(+)targets (e.g. BV173, HTB37/pp65 and

OVCAR3/pp65 in a dose-dependent manner, but not HLA-A2(-)/WT1(low) cells (SKOV3), A2(+)/WT1(−) cells (autologous BLCLs) or A2(-)/WT1(+) cells (K562 cells) (figure. 3C). Conventional CARs target cell surface protein and are not restricted by a particular HLA. Our data indicate that CARs can be genetically engineered that are specific for epitopes of processed intracellular proteins that are presented by a defined HLA allele, and that T-cells modified to express such TCR-like CARs, can exert cytotoxic activity against appropriate target cells expressing the CAR targeted HLA-peptide complex.

4. Discussion

In the targeting of class-I peptide-MHC, normal wild-type TCRs with binding affinities in the range of 10–300 μM provide sufficiently sensitive responses. In studies evaluating various TCRs against MHC class-I - peptide, 300 μM appears to be the minimal affinity required for effective CD8 T cell activity, whereas the optimal affinity is about 10 μM (*79*). In our study, we demonstrated that the affinity matured Q2L-CAR modified T cells recognized tumor cells in an HLA restricted WT1-specific fashion. In contrast, minimal target cell lysis was observed using T-cells expressing the low affinity parental Clone 45. Oren et al. (*71*) compared CAR modified T-cells containing either low affinity F2 (400nM Kd) or the moderate affinity F3 (30nM kD) scFvs and found that the higher affinity F3-CAR modified T-cell demonstrated non-specific cross-reactivity, and poor viability. They proposed that this off-target activity and poor viability of the F3-CAR modified T-cells indicates an affinity barrier to developing effective anti-peptide/HLA CAR T cells. Here we show that the affinity matrured Q2L CAR can retain both target specificity and viability despite having high affinity (3nM K_D for the scFv). Overall, both our own and other studies clearly demonstrate higher cytolytic activity with increasing TCR /CAR binding affinity. In order to overcome the undesirable off-target activity, the isolation of appropriate antibody clones and refining the affinity maturation techniques would be critical for further development of these approaches.

Various strategies to improve the affinity of TCRs for adoptive T cell therapy have

been explored. While anti-tumor responses have been observed, there have been serious adverse events with MART-1 TCRs due to on-target/off-tumor activity (*80*), and lethal events with MAGE-3 TCRs due apparently to off-target cross-reactivity with structurally similar epitopes. While there will always remain a risk of unpredicted reactivities in patients receiving adoptive T cell therapies, we believe that the use of TCRs with different affinities and specificities in an expanded set of pre-clinical approaches, will identify some of the possible problems (*81*).

In summary, we describe an experimental comparison of low versus high affinity TCR-like chimeric antigen receptors to evaluate the effect of the binding affinity of the TCR mimic-CAR on the functional activity. Our studies validate the superior specific binding and HLA-restricted WT-1 peptide specific cytoxicity of T-cell expressing the high affinity CAR against HLA A0201^{+}WT-1^{+} human tumor cells. This study highlights the importance of TCR affinity to the T-cell's functional activity. In conclusion, in order to develop a strategy for antigen-specific T-cells to provide long lasting immunity against antigens, the affinity barrier of TCR has to be reached to develop effective function for adoptive T cell transfer.

Figure 1.

Human T cells retrovirally transduced to express an A2-RMF low affinity Clone 45

Human T cells transduced to express low affinity clone 45 was unable to bind A2-RMF Tetramer. Flow cytometry analysis was performed to evaluate the binding of HLA A0201 RMF tetramer in GFP^+ sorted population.

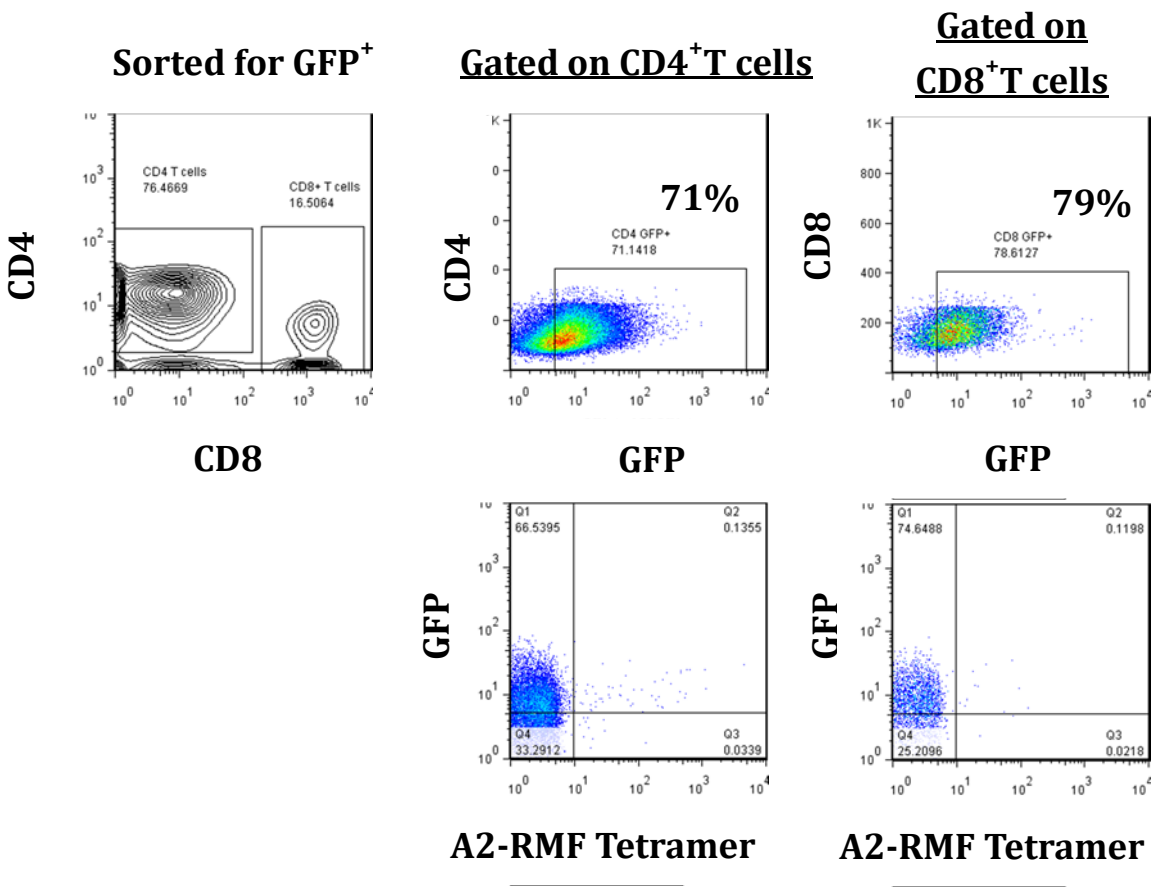
Sorted for GFP+
Gated on CD4+T cells
Gated on CD8+T cells
CD4
CD4 T cells
76.4669
CD8+ T cells
16.5064
CD8
CD4
71%
CD4 GFP+
71.1418
GFP
CD8
79%
CD8 GFP+
78.6127
GFP
GFP
Q1
66.5395
Q2
0.1355
Q4
33.2912
Q3
0.0339
A2-RMF Tetramer
GFP
Q1
74.6488
Q2
0.1198
Q4
25.2096
Q3
0.0218
A2-RMF Tetramer

Figure 2.

A2-RMF low affinity CAR T cells exhibit low cytotoxic activity against WT1 expressing A0201^{+} tumor cells

(A) The level of WT1 expression in different tumor cell line was confirmed by western blot analysis using anti WT-1 antibody. (B) Specific cytotoxicity of Clone 45-CAR T cells against the tumor cell lines by chromium release assay after sorted for GFP^{+} T cells. Samples were prepared in triplicate and values are shown as mean ± SE. Experiment was repeated twice with similar results.

(A)

	WT-1	HLA-A0201
1. K562	+++	–
2. BV173	+++	+
3. OVCAR3	+++	+
4. OVCAR3pp65	++++	+
5. SKOV3	+	–
6. CCl228	+++	–
7. HTB37	++	+
8. BV173 (1:5 dilution)	+++	+
9. OVCAR3pp65 (1:5 dilution)	++++	+

(B)

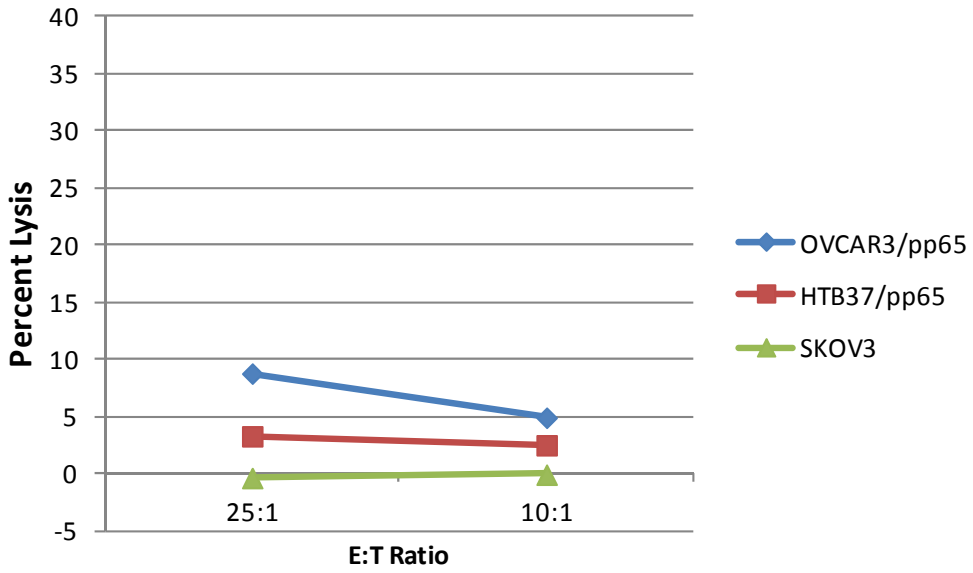

Figure 3.

Phenotypic and functional characterization of high affinity clone Q2L

(A) K562 cells retrovirally transduced to express a high affinity clone Q2L. Flow cytometry analysis was performed to evaluate the binding of HLA A0201 RMF tetramer in GFP^+ population. K562 non-transduced cells served as a control. (B) Human T cells transduced to express high affinity clone Q2L was able to bind A2-RMF Tetramer correlated with GFP^+ transduced population. (C) Specific cytotoxicity of Q2L-CAR T cells against the tumor cell lines by chromium release assay. Samples were prepared in triplicate and values are shown as mean ± SE. Experiment was repeated twice with similar results.

(A)

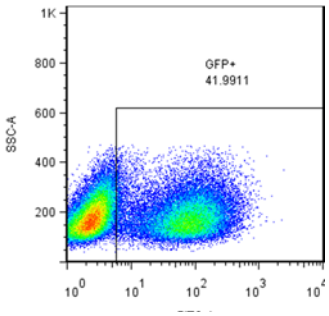

GFP

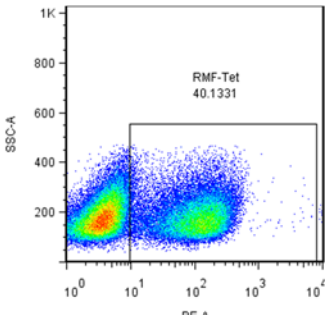

A2-RMF Tetramer

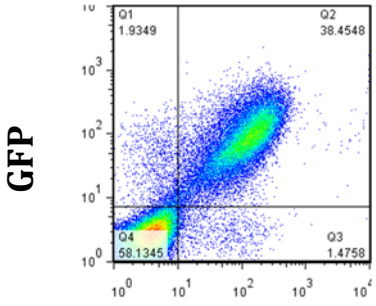

A2-RMF Tetramer

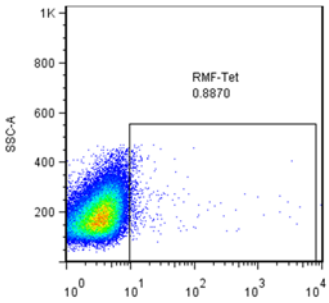

A2-RMF Tetramer

Non-transduced control

Figure 3 (Continued)

(B)

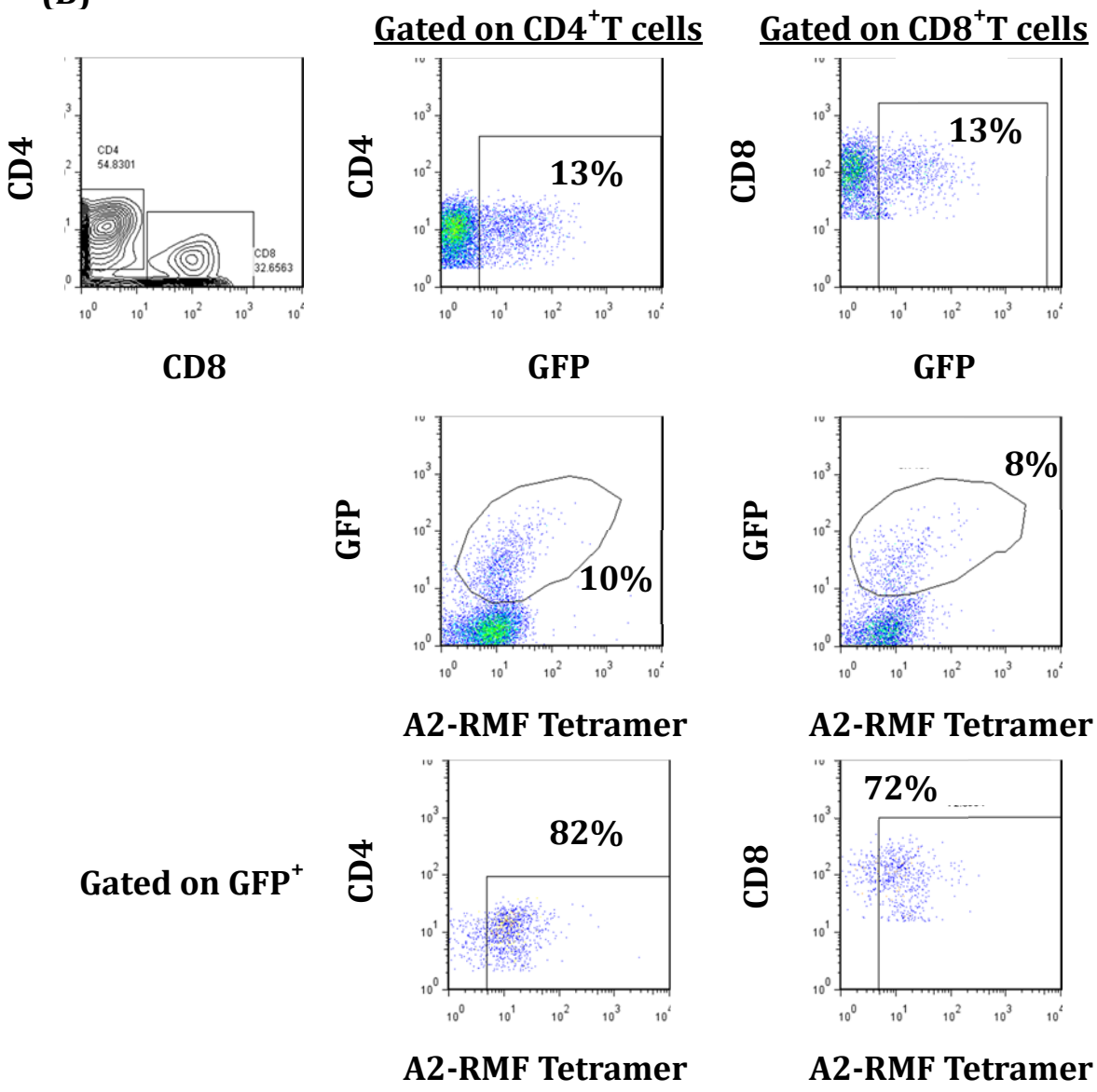

Figure 3 (Continued)

(C)

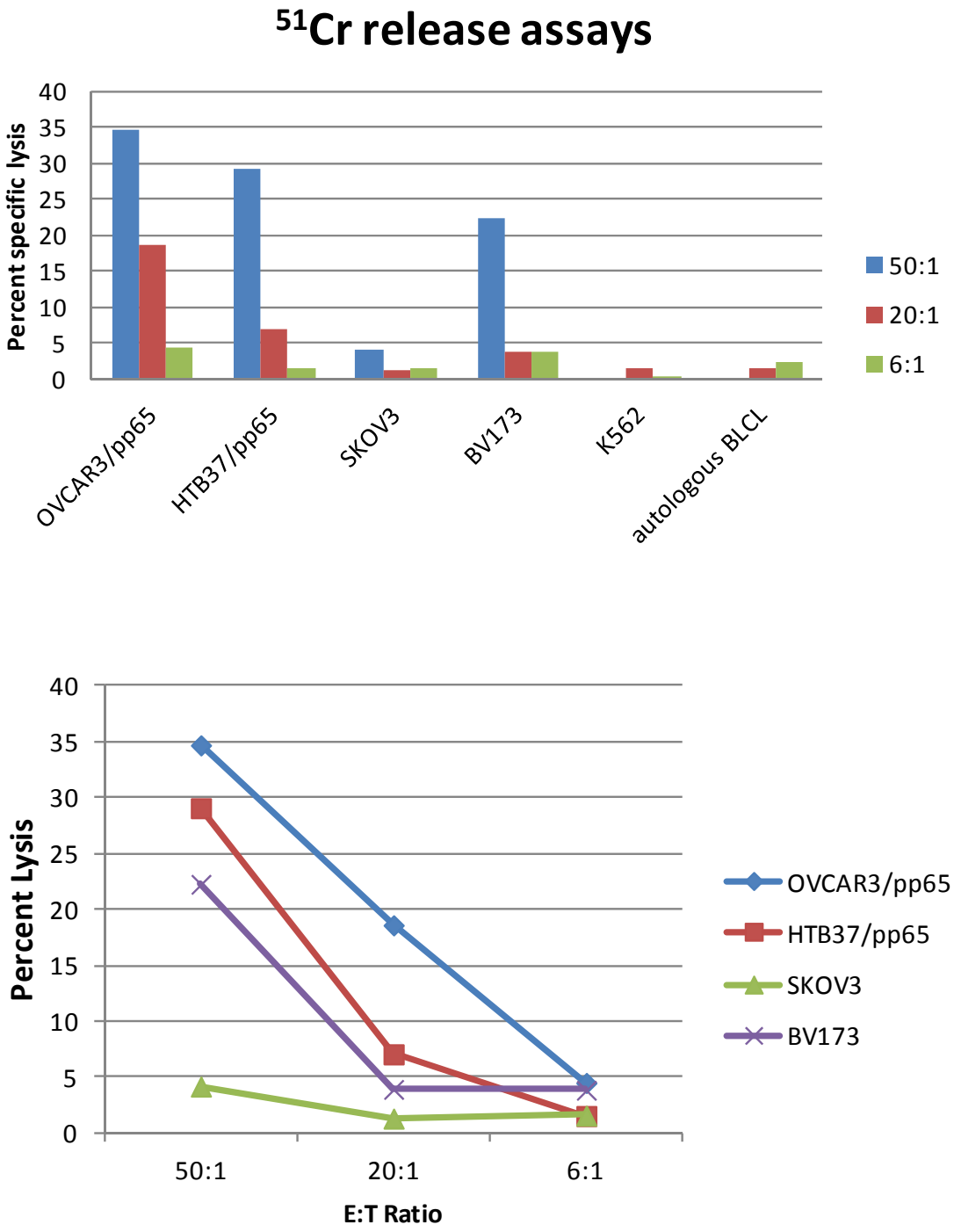

THESIS DISCUSSION

The efficacy of adoptive T-cell therapy, using naturally occurring antigen-specific T cells to treat patients with virus infections or cancers, is often limited by the failure of the T-cells to expand and persist in the patient for periods sufficient to induce eradication or control of the diseased cells and organs. Increasing evidence indicates that several attributes of the T-cells and the environment of the host contribute to or limit the functional longevity of the adoptively transferred T-cells. Among these are: the antigen specificity and avidity of the T-cells transferred, the stage of differentiation of the T-cells, their potential for sustained growth and their susceptibility to apoptosis or growth inhibition by regulatory T-cells or myeloid suppressor cells. The persistence of allogenic T-cells is also determined by the potential of the host environment to provide cytokines and costimulating signals to sustain T-cell growth or, conversely, to generate alloreactive T-cells or antibodies to eliminate the T-cells or to generate inhibiting cells such as myeloid suppressor cells or regulatory T-cells. To develop an approach for enhancing persistence and overall efficacy of adoptive immunotherapy, this thesis has focused on comparatively evaluating the origins, phenotype and functional attributes of different memory T-cell subsets in humans, their proliferation and survival, as well as their in vivo homing and persistence.

Memory T cells can be phenotypically sub classified based on distinct expression patterns of the lymph node–homing molecules CD62L and CCR7, into central

memory T cells (T_{CM}) and effector memory T cells (T_{EM}). The expression of CD95 in naïve phenotype T cells further distinguishes a less differentiated memory T cell subset, termed stem cell memory T cells (T_{SCM}) from the naïve T-cell population. In this thesis, we performed a comparative analysis of different memory T-cell subsets in an antigen-specific T cell population, as well as their antigen non-responsive counterparts. We characterized HLA A0201 restricted T_N, T_{SCM}, T_{CM} and T_{EM} specific for the immunodominant NLV peptide of CMVpp65. Following in vitro sensitization the NLV specific Tet^+ T_N and T_{SCM} derived cells expressed higher levels of CD27 and lower levels of CD57 than T_{CM} or T_{EM}, and expressed similar levels of KLRG-1 and PD-1, which were significantly higher than their Tet^- counterparts (figure). At a functional level, antigen-specific T_N, T_{SCM}, T_{CM} and T_{EM} derived cells all contained cells capable of secreting TNF-α and IFN-γ, and expressed high levels of CD107a. Antigen-specific T_{SCM} were distinguished from T_N, T_{CM} and T_{EM} by a significantly greater level of proliferation and, from T_N, by their rapid and selective expansion of antigen specific T-cells bearing TCR CDR3 sequences identical in sequence to those expressed by dominant, oligoclonal T_{EM} and T_{CM} in the blood. Taken together, our data suggest that antigen-specific T_{SCM} are the principal reservoir for rapid repopulation of immunodominant T-cells in the circulation.

In order for an immune response by cytotoxic T cells against a tumor to be effective, not only must antigen-specific T cells be generated to recognize the tumor, but these T cells must also be able to accumulate at tumor sites, and

thereafter physically contact and kill or otherwise suppress antigen-expressing cancer cell targets. The T-cells must also persist at tumor sites for periods sufficient to induce tumor eradication. A unique finding in our study is the disparity between the transient accumulations of the CMVpp65-specific T_{CM} and T_{EM} in the Cocapp65 tumor in the mice co-treated with IL-15/IL-15Rα and their persistence in the marrow of the same mice for more than 40 days after accumulation of T-cells in the tumors had decreased to levels no longer detectable by bioluminescence or by immunohistology. It is unclear why the CMV-specific T cells were able to persist in the marrow of the xenografted mice but failed to sustain the initial accumulation of the T-cells in the tumor environment to eradicate tumor.

In our study, both T_{CM} and T_{EM} derived CMVpp65 specific T-cells differentially persisted in the bone marrow of NSG mice that received injections of the irradiated BAF-3 cells secreting high levels of IL-15 and IL-15/IL-15Rα complex. Similar to the findings of Wang el al. (*21*) in mice that did not receive IL-15 secreting cell supplementation, neither T_{CM} derived nor T_{EM} derived T-cells were detected in the marrow of mice treated with IL-2. Unlike the findings of Wang et al. (*21*) in mice treated with NSO cells secreting low levels of IL-15 alone, the levels of T_{CM} and T_{EM} derived T-cells that persisted in the marrow of our mice were not significantly different. However, in agreement with their findings, we found that the T-cells in the marrow consisted exclusively of T_{EM} and T_E T-cells. We did not detect any T-cells exhibiting a $CD45RO^+CD62L^+CCR7^+$ T_{CM}

phenotype as has been described in primates infused with autologous CMV-specific T_{EM} and T_E cells generated from T_{CM} precursors in the blood. We did, however, observe that the T_{CM}-derived T_E cells persisting in the marrow differed from T_{EM}-derived T_E cells in that a proportion of these T_E cells expressed IL-15Rα, a finding also reported by Berger et al. (*13*) for T_{CM} derived T-cells that persist long-term in non-human primates. The T_{CM}-derived T_E cells in the marrow were also able to proliferate and to generate IFN-γ in response to CMVpp65 peptide indicating their functional competence.

Since antigen-specific memory $CD8^+$ T-cells have been shown to receive proliferative signals from IL-15 secreting cells in the marrow (*33*), and in human bone marrow, cells expressing IL-15Rα can trans-present IL-15 on their surface (*32*), it could explain why the bone marrow is the site where significant populations of CMVpp65-specific T_{EM} derived T-cells are detected longterm.

The possible reasons why both T_{CM} and T_{EM} derived CMVpp65 specific T-cells persisted in the marrow rather than the Coca pp65 tumor site might also be because of inhibitory signals from the tumor microenvironment and/or the lack of sustaining stimuli required by T cells. The inhibitory signals include PD1/PDL1, MDSCs or regulatory T cells. The high level of Fas (CD95) and PD1 expression that we detected on the CMVpp15-specific T cells might render the T cells in the tumor environment particularly susceptible to inhibition by $PD\text{-}L1^+$ tumor cells, Fas ligand produced by myelomonocytic suppressor cells or other apoptosis-promoting signals such as TNF-related apoptosis inducing ligand (TRAIL). The

inhibitory signal through PD1/PDL1 signaling is being examined by evaluating the level of PD-L1 expression on Coca pp65 tumor cells at different durations of growth in vivo. However, data from separate experiments in our lab have also shown that administration of anti-PD1 to mice treated with CMV-specific T cells enhanced antigen-specific tumor eradication compared to mice without anti-PD1 treatment.

In our NSG mouse model, it is hard to rule out the effect of MDSCs since the mouse myloid cells would cross-react with human CD8 T cells. However, there are no $CD4^+$ T_{reg} cells in our xenograft mouse model since we only transferred human CD8 T cells into the mice.

A deficiency of essential stimuli required for the growth of antigen-specific T cells in the tumor could also explain our findings. For example, the CoCa pp65 tumor cells could downregulate HLA-A2 or critical costimulatory molecules. The T-cells could also lack cytokine support. In our Coca pp65 tumor model, we have evaluated the expression level of HLA-A2, B7.1, LFA-3 and ICAM-1 on our Coca pp65 tumor cell line. Of the costimulatory molecules, the level of B7.1 expression is relatively low (1% positive) compared to BLCLs (92% positive). Therefore, it is possible that the lack of sufficient co-stimulatory signaling through B7.1 could limit the persistence of T cells in the tumor. Down regulation of HLA-A2 in the tumor environment might also occur post transfer in NSG mice. Further experiments are needed to ascertain the level of HLA-A2 and costimulatory molecules in the tumor xenografts over time post transfer. In addition, since we

only transfer CD8 T cells into NSG mice, the lack of CD4 T cells in our model might also result in a lack of essential cytokine support in the tumor environment.

T cells must also locally replicate to further increase their frequency, avoid being killed themselves by hostile elements of tumor microenvironment, and overcome barriers that restrict access to cancer cell targets. In this regard, findings in preclinical models and in patients with melanoma and other malignancies suggest that the tumor microenvironment may be the major site of clonal expansion of cancer-specific T-cells. Furthermore, the $CD8^+$ T cell replicative response at this site is governed by $CD103^+$, Baft3-dependent dendritic cells, which can efficiently cross-present cancer cell antigens (*82, 83*). However, DC function may be adversely affected by hypoxic conditions characteristic of the tumor microenvironments that induce PD-L1 expression on DCs (*84*). These cells in the tumor microenvironment may also directly impair intratumoral T cell proliferation. Indole 2,3-dioxygenase (IDO) which can be expressed by DC, as well as myeloid derived suppressor cells and cancer cells, catabolizes tryptophan and generates hynurenine. Both the deprivation of tryptophan and the generation of its metabolic product inhibit clonal expansion (*85, 86*). Furthermore, both IDO and PD-L1 may not only may impair the intratumoral proliferation of effector T cells but may also induce apoptosis.

Accumulating evidence also implicates other cell elements in the tumor microenvironment, particularly myelomonocytic cells, including several subsets of cells within the general designation of myeloid-derived suppressor cells (MDSCs)

and tumor associated macrophages (TAMs), as cells capable of restricting the sustained accumulation and effector function of T cells at sites of cancer cell growth (*87-89*). In addition, cancer-associated fibroblasts can regulate the spatial distribution of T cells within tumors, and can thus restrict direct contact of T-cells to tumor cell targets by providing a physical exclusion mediated by the extracellular matrix that they produce. Live cell imaging of lung tumor tissue slices from patients has revealed active T cell motility in regions of loose fibronectin and collagen, whereas T cells migrated poorly in dense matrix areas surrounding tumor nests (*90*). The tumor vasculature can also play an active role in restricting T cell entry. For example, the apoptosis inducer Fas ligand (FasL) is expressed in the tumor vasculature of multiple tumor types (*91*). In tumors with high levels of endothelial FasL, antigen-specific CD8 T cells might also be lost due to FasL-mediated killing through Fas (CD95) expressing T cells. Cells in the tumor microenvironment can also release chemokines that preferentially recruit certain immune cell types over others. In addition, posttranslational alterations in chemokines, such as chemokine nitration may prevent T-cell infiltration of the tumors (*92*).

In summary, our studies of the CMVpp65-specific memory T-cell compartments suggest that T_{CM} may accumulate to a greater degree in the antigen-bearing tumor xenografts but that neither T_{CM} nor T_{EM} persist long term in these sites. Our studies also clearly show that co-administration of IL-15/IL-15Rα prolongs the accumulation of T-cells in the CMVpp65^{+} tumor xenografts significantly beyond

that achieved with IL-2, and further, that IL-15/IL-15Rα supplementation fosters the long term persistence of functional CMVpp65-specific T-cells in the marrow. However, a major question that now needs to be addressed is: whether and to what degree the CMVpp65-specific T-cells detected in the marrow long term are capable of migrating to and inhibiting the growth of CMVpp65^{+} tumor xenografts after transfer into a secondary host. Simply put, are the CMVpp65-specific T-cells that persist in the marrow immune and able to provide meaningful resistance on secondary transfer or tolerized in the course of their contact with tumor and its environment. Alternatively, are these T-cells intrinsically different in their capacity to migrate to the CMVpp65^{+} tumor xenografts, (i.e. do they ever migrate to the tumor) or do they just migrate to the tumor and exert effector function, but then move to the marrow where their growth is better supported by the morrow environment. Experiments to address these issues are now being planned.

In this thesis, I also examined whether increasing the TCR affinity of the endogenous TCRs for tumor antigen specific T-cells could enhance the activity of adoptively transferred T-cells directed against cancer antigens. The vast majority of tumor-associated peptide antigens recognized by CD8^{+} T cells originate from autologous proteins and, as such, remain protected by immune tolerance mechanisms configured to prevent autoimmunity (*93*). Indeed, as a consequence of thymic selection, cognate T cell receptor (TCR) binding to these self-derived epitopes occurs at substantially lower affinities compared to pathogen-specific TCRs (*94*). This distinction probably explains why naturally generated T cell

responses against cancer are largely non-protective (*95*). Moreover, the lack of high-affinity tumour-specific TCRs in the periphery may place intrinsic constraints on the efficacy of cancer vaccines designed to elicit T cell immunity.

Antigen-specific TCR gene transfer into T cells is an attractive approach to cancer therapy, with the potential to break self-tolerance. Recent studies have suggested that the use of engineered, affinity-enhanced TCRs may circumvent immune apathy towards tumor-derived antigens. Approximating affinity to mimic optimal pathogen-specific TCRs (KD = 0.1–10 μM) also makes sense from the biological perspective (*96, 97*). Indeed, kinetic models of T cell activation propose that the potency of a T-cell specific for a peptide–major histocompatibility complex (pMHC) ligand is determined primarily by the duration of the TCR–pMHC interaction (*98*). Potent T-cells generally bind with the highest affinities and longest half-lives, although many other parameters also affect T cell activation, antigen sensitivity and the response to TCR triggering (*99, 100*).

Previous reports have described affinity threshold phenomena in other systems. In one study, a single cancer-specific TCR was used with mimotopes to generate a range of affinities up to 4-fold higher than the wild-type interaction (*101*). Although the highest-affinity mimotopes elicited the most vigorous responses in vitro, optimal anti-tumour activity in vivo was observed after vaccination with the intermediate affinity mimotopes. Two studies in the NY-ESO-1 system, spanning a range of TCR affinities up to 1430-fold greater than wild-type, reached similar conclusions (*102, 103*). In particular, target cell lysis was found to increase as a

function of affinity up to a threshold of ~7 μM, beyond which further increments diminished killing activity. These findings were confirmed using a series of seven gp100-specific TCRs (*104*). Excessive affinity enhancement has also been shown to impair T cell function in the 2C system (*105, 106*). In addition, a recent study using APL vaccination in a diabetes/ovalbumin (OVA) mouse model showed that TCR affinity dictates not only the magnitude of T cell activation and target cell conjugation, but also the differentiation status of responding T cells (*107*). Similar observations have been reported for pathogen-specific TCRs (*108*). Thus, each system is constrained by an affinity ceiling, the parameters for which can be highly variable (*109*).

In our study, we demonstrated that the affinity matured Q2L-CAR modified T cells recognized tumor cells in an HLA restricted WT1-specific fashion. In contrast, minimal target cell lysis was observed using T-cells expressing the low affinity parental Clone 45. Here we show that the affinity matured Q2L CAR can retain both target specificity and viability despite having high affinity (3nM K_D for the scFv). Overall, both our own and other studies demonstrate higher cytolytic activity with increasing TCR /CAR binding affinity. T cell activation, signaling and subsequent function are limited to a given TCR-pMHC affinity window. As a result, optimal system-defined affinity windows above the range established for TCR/CAR avidity for specific antigens may allow the enhancement of T cell effector function without off-target effects.

Figure

The role of antigen-experienced memory CD8 T cells

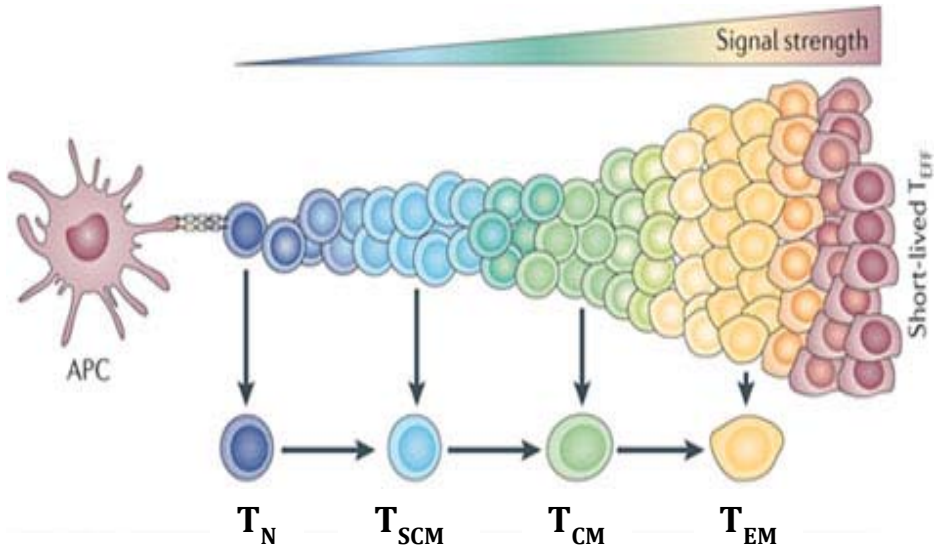

		Antigen-experienced cell				Tet- counterpart			
		T_N	T_{SCM}	T_{CM}	T_{EM}	T_N	T_{SCM}	T_{CM}	T_{EM}
Phenotype	CCR7	+++	++	–	–	+++	+++	++	–
	CD27	+++	++	+	–	+++	+++	++	–
	CD57	–	+	++	+++	–	+	++	+++
	CD127	–	+/–	–	–	–	+	–	–
	CD28	+	+	++	++	+	+	+	+
	KLRG1	+	+	+	+	–	+	+	+
	PD1	++	++	++	++	–	–	–	–
	CD95	+	+	+	+	–	++	+++	+++
Function	IFN-r	+	+	+	+				
	TNF-a	+	+	+	+				
	CD107a	+	+	+	+				
	Proliferation	++	+++	++	+				

1. S. A. Rosenberg *et al.*, Use of tumor-infiltrating lymphocytes and interleukin-2 in the immunotherapy of patients with metastatic melanoma. A preliminary report. *N Engl J Med* **319**, 1676-1680 (1988).
2. N. P. Restifo, M. E. Dudley, S. A. Rosenberg, Adoptive immunotherapy for cancer: harnessing the T cell response. *Nature reviews. Immunology* **12**, 269-281 (2012).
3. C. M. Rooney *et al.*, Infusion of cytotoxic T cells for the prevention and treatment of Epstein-Barr virus-induced lymphoma in allogeneic transplant recipients. *Blood* **92**, 1549-1555 (1998).
4. S. A. Rosenberg, P. Spiess, R. Lafreniere, A new approach to the adoptive immunotherapy of cancer with tumor-infiltrating lymphocytes. *Science* **233**, 1318-1321 (1986).
5. M. E. Dudley *et al.*, Cancer regression and autoimmunity in patients after clonal repopulation with antitumor lymphocytes. *Science* **298**, 850-854 (2002).
6. R. A. Morgan *et al.*, Cancer regression in patients after transfer of genetically engineered lymphocytes. *Science* **314**, 126-129 (2006).
7. J. N. Kochenderfer, Z. Yu, D. Frasheri, N. P. Restifo, S. A. Rosenberg, Adoptive transfer of syngeneic T cells transduced with a chimeric antigen receptor that recognizes murine CD19 can eradicate lymphoma and normal B cells. *Blood* **116**, 3875-3886 (2010).
8. S. R. Riddell *et al.*, Restoration of viral immunity in immunodeficient humans by the adoptive transfer of T cell clones. *Science* **257**, 238-241 (1992).
9. E. B. Papadopoulos *et al.*, Infusions of donor leukocytes to treat Epstein-Barr virus-associated lymphoproliferative disorders after allogeneic bone marrow transplantation. *N Engl J Med* **330**, 1185-1191 (1994).
10. E. A. Walter *et al.*, Reconstitution of cellular immunity against cytomegalovirus in recipients of allogeneic bone marrow by transfer of T-cell clones from the donor. *N Engl J Med* **333**, 1038-1044 (1995).
11. H. E. Heslop *et al.*, Long-term restoration of immunity against Epstein-Barr virus infection by adoptive transfer of gene-modified virus-specific T lymphocytes. *Nature medicine* **2**, 551-555 (1996).
12. C. Yee *et al.*, Adoptive T cell therapy using antigen-specific CD8+ T cell clones for the treatment of patients with metastatic melanoma: in vivo persistence, migration, and antitumor effect of transferred T cells. *Proceedings of the National Academy of Sciences of the United States of America* **99**, 16168-16173 (2002).
13. C. Berger *et al.*, Adoptive transfer of effector CD8+ T cells derived from central memory cells establishes persistent T cell memory in primates. *The Journal of clinical investigation* **118**, 294-305 (2008).
14. D. Masopust, V. Vezys, A. L. Marzo, L. Lefrancois, Preferential localization of effector memory cells in nonlymphoid tissue. *Science* **291**, 2413-2417 (2001).

15. D. L. Farber, N. A. Yudanin, N. P. Restifo, Human memory T cells: generation, compartmentalization and homeostasis. *Nature reviews. Immunology* **14**, 24-35 (2014).
16. L. Gattinoni *et al.*, A human memory T cell subset with stem cell-like properties. *Nature medicine* **17**, 1290-1297 (2011).
17. J. Tang *et al.*, Adenovirus hexon T-cell epitope is recognized by most adults and is restricted by HLA DP4, the most common class II allele. *Gene Ther* **11**, 1408-1415 (2004).
18. M. E. Dudley *et al.*, Adoptive transfer of cloned melanoma-reactive T lymphocytes for the treatment of patients with metastatic melanoma. *J Immunother* **24**, 363-373 (2001).
19. B. Heemskerk *et al.*, Adoptive cell therapy for patients with melanoma, using tumor-infiltrating lymphocytes genetically engineered to secrete interleukin-2. *Human gene therapy* **19**, 496-510 (2008).
20. E. J. Wherry *et al.*, Lineage relationship and protective immunity of memory CD8 T cell subsets. *Nature immunology* **4**, 225-234 (2003).
21. X. Wang *et al.*, Engraftment of human central memory-derived effector CD8+ T cells in immunodeficient mice. *Blood* **117**, 1888-1898 (2011).
22. C. A. Klebanoff *et al.*, Central memory self/tumor-reactive CD8+ T cells confer superior antitumor immunity compared with effector memory T cells. *Proceedings of the National Academy of Sciences of the United States of America* **102**, 9571-9576 (2005).
23. L. Gattinoni, C. A. Klebanoff, N. P. Restifo, Paths to stemness: building the ultimate antitumour T cell. *Nat Rev Cancer* **12**, 671-684 (2012).
24. S. Wei, P. Charmley, M. A. Robinson, P. Concannon, The extent of the human germline T-cell receptor V beta gene segment repertoire. *Immunogenetics* **40**, 27-36 (1994).
25. G. Koehne *et al.*, Quantitation, selection, and functional characterization of Epstein-Barr virus-specific and alloreactive T cells detected by intracellular interferon-gamma production and growth of cytotoxic precursors. *Blood* **99**, 1730-1740 (2002).
26. E. B. Santos *et al.*, Sensitive in vivo imaging of T cells using a membrane-bound Gaussia princeps luciferase. *Nature medicine* **15**, 338-344 (2009).
27. A. N. Hasan *et al.*, Soluble and membrane-bound interleukin (IL)-15 Ralpha/IL-15 complexes mediate proliferation of high-avidity central memory CD8+ T cells for adoptive immunotherapy of cancer and infections. *Clinical and experimental immunology* **186**, 249-265 (2016).
28. T. P. Gade *et al.*, Targeted elimination of prostate cancer by genetically directed human T lymphocytes. *Cancer research* **65**, 9080-9088 (2005).
29. A. A. Jungbluth *et al.*, Immunohistochemical analysis of NY-ESO-1 antigen expression in normal and malignant human tissues. *Int J Cancer* **92**, 856-860 (2001).
30. A. N. Hasan *et al.*, A panel of artificial APCs expressing prevalent HLA alleles permits generation of cytotoxic T cells specific for both dominant and

subdominant viral epitopes for adoptive therapy. *Journal of immunology* **183**, 2837-2850 (2009).
31. G. C. Koo, A. Hasan, R. J. O'Reilly, Use of humanized severe combined immunodeficient mice for human vaccine development. *Expert review of vaccines* **8**, 113-120 (2009).
32. N. Sato, H. J. Patel, T. A. Waldmann, Y. Tagaya, The IL-15/IL-15Ralpha on cell surfaces enables sustained IL-15 activity and contributes to the long survival of CD8 memory T cells. *Proceedings of the National Academy of Sciences of the United States of America* **104**, 588-593 (2007).
33. E. Zhao *et al.*, Bone marrow and the control of immunity. *Cellular & molecular immunology* **9**, 11-19 (2012).
34. N. Cieri *et al.*, IL-7 and IL-15 instruct the generation of human memory stem T cells from naive precursors. *Blood* **121**, 573-584 (2013).
35. L. Xu, Y. Zhang, G. Luo, Y. Li, The roles of stem cell memory T cells in hematological malignancies. *Journal of hematology & oncology* **8**, 113 (2015).
36. L. Biasco *et al.*, In vivo tracking of T cells in humans unveils decade-long survival and activity of genetically modified T memory stem cells. *Science translational medicine* **7**, 273ra213 (2015).
37. A. Roberto *et al.*, Role of naive-derived T memory stem cells in T-cell reconstitution following allogeneic transplantation. *Blood* **125**, 2855-2864 (2015).
38. N. Cieri *et al.*, Generation of human memory stem T cells after haploidentical T-replete hematopoietic stem cell transplantation. *Blood* **125**, 2865-2874 (2015).
39. M. Schmueck-Henneresse *et al.*, Peripheral blood-derived virus-specific memory stem T cells mature to functional effector memory subsets with self-renewal potency. *J Immunol* **194**, 5559-5567 (2015).
40. M. Wolfl, P. D. Greenberg, Antigen-specific activation and cytokine-facilitated expansion of naive, human CD8+ T cells. *Nature protocols* **9**, 950-966 (2014).
41. P. J. Hanley *et al.*, CMV-specific T cells generated from naive T cells recognize atypical epitopes and may be protective in vivo. *Science translational medicine* **7**, 285ra263 (2015).
42. P. Szabolcs, T-lymphocyte recovery and function after cord blood transplantation. *Immunologic research* **49**, 56-69 (2011).
43. R. Q. Hintzen *et al.*, Regulation of CD27 expression on subsets of mature T-lymphocytes. *J Immunol* **151**, 2426-2435 (1993).
44. D. G. Song *et al.*, CD27 costimulation augments the survival and antitumor activity of redirected human T cells in vivo. *Blood* **119**, 696-706 (2012).
45. J. M. Brenchley *et al.*, Expression of CD57 defines replicative senescence and antigen-induced apoptotic death of CD8+ T cells. *Blood* **101**, 2711-2720 (2003).
46. S. M. Kaech *et al.*, Selective expression of the interleukin 7 receptor identifies effector CD8 T cells that give rise to long-lived memory cells. *Nature immunology* **4**, 1191-1198 (2003).

47. N. S. Joshi *et al.*, Inflammation directs memory precursor and short-lived effector CD8(+) T cell fates via the graded expression of T-bet transcription factor. *Immunity* **27**, 281-295 (2007).
48. M. Wolfl *et al.*, Activation-induced expression of CD137 permits detection, isolation, and expansion of the full repertoire of CD8+ T cells responding to antigen without requiring knowledge of epitope specificities. *Blood* **110**, 201-210 (2007).
49. N. Khan *et al.*, Cytomegalovirus seropositivity drives the CD8 T cell repertoire toward greater clonality in healthy elderly individuals. *J Immunol* **169**, 1984-1992 (2002).
50. M. P. Weekes, M. R. Wills, K. Mynard, A. J. Carmichael, J. G. Sissons, The memory cytotoxic T-lymphocyte (CTL) response to human cytomegalovirus infection contains individual peptide-specific CTL clones that have undergone extensive expansion in vivo. *Journal of virology* **73**, 2099-2108 (1999).
51. G. C. Wang, P. Dash, J. A. McCullers, P. C. Doherty, P. G. Thomas, T cell receptor alphabeta diversity inversely correlates with pathogen-specific antibody levels in human cytomegalovirus infection. *Science translational medicine* **4**, 128ra142 (2012).
52. L. Trautmann *et al.*, Selection of T cell clones expressing high-affinity public TCRs within Human cytomegalovirus-specific CD8 T cell responses. *J Immunol* **175**, 6123-6132 (2005).
53. J. Duraiswamy *et al.*, Phenotype, function, and gene expression profiles of programmed death-1(hi) CD8 T cells in healthy human adults. *J Immunol* **186**, 4200-4212 (2011).
54. V. Pulko *et al.*, Human memory T cells with a naive phenotype accumulate with aging and respond to persistent viruses. *Nature immunology* **17**, 966-975 (2016).
55. M. Cornberg *et al.*, Narrowed TCR repertoire and viral escape as a consequence of heterologous immunity. *The Journal of clinical investigation* **116**, 1443-1456 (2006).
56. D. Meyer-Olson *et al.*, Limited T cell receptor diversity of HCV-specific T cell responses is associated with CTL escape. *The Journal of experimental medicine* **200**, 307-319 (2004).
57. H. Li, C. Ye, G. Ji, J. Han, Determinants of public T cell responses. *Cell research* **22**, 33-42 (2012).
58. X. Yang *et al.*, Structural Basis for Clonal Diversity of the Public T Cell Response to a Dominant Human Cytomegalovirus Epitope. *The Journal of biological chemistry* **290**, 29106-29119 (2015).
59. T. H. Nguyen *et al.*, Recognition of distinct cross-reactive virus-specific CD8+ T cells reveals a unique TCR signature in a clinical setting. *J Immunol* **192**, 5039-5049 (2014).

60. N. Khan *et al.*, T cell recognition patterns of immunodominant cytomegalovirus antigens in primary and persistent infection. *J Immunol* **178**, 4455-4465 (2007).
61. D. C. Tscharke, N. P. Croft, P. C. Doherty, N. L. La Gruta, Sizing up the key determinants of the CD8(+) T cell response. *Nature reviews. Immunology* **15**, 705-716 (2015).
62. F. M. Wensveen *et al.*, Apoptosis threshold set by Noxa and Mcl-1 after T cell activation regulates competitive selection of high-affinity clones. *Immunity* **32**, 754-765 (2010).
63. P. Chames, S. E. Hufton, P. G. Coulie, B. Uchanska-Ziegler, H. R. Hoogenboom, Direct selection of a human antibody fragment directed against the tumor T-cell epitope HLA-A1-MAGE-A1 from a nonimmunized phage-Fab library. *Proceedings of the National Academy of Sciences of the United States of America* **97**, 7969-7974 (2000).
64. G. Stewart-Jones *et al.*, Rational development of high-affinity T-cell receptor-like antibodies. *Proceedings of the National Academy of Sciences of the United States of America* **106**, 5784-5788 (2009).
65. P. D. Holler, L. K. Chlewicki, D. M. Kranz, TCRs with high affinity for foreign pMHC show self-reactivity. *Nature immunology* **4**, 55-62 (2003).
66. B. J. Cameron *et al.*, Identification of a Titin-derived HLA-A1-presented peptide as a cross-reactive target for engineered MAGE A3-directed T cells. *Science translational medicine* **5**, 197ra103 (2013).
67. R. Dahan, Y. Reiter, T-cell-receptor-like antibodies - generation, function and applications. *Expert Rev Mol Med* **14**, e6 (2012).
68. A. Sergeeva *et al.*, An anti-PR1/HLA-A2 T-cell receptor-like antibody mediates complement-dependent cytotoxicity against acute myeloid leukemia progenitor cells. *Blood* **117**, 4262-4272 (2011).
69. B. Verma *et al.*, TCR mimic monoclonal antibody targets a specific peptide/HLA class I complex and significantly impedes tumor growth in vivo using breast cancer models. *J Immunol* **184**, 2156-2165 (2010).
70. T. Dao *et al.*, Targeting the intracellular WT1 oncogene product with a therapeutic human antibody. *Science translational medicine* **5**, 176ra133 (2013).
71. R. Oren *et al.*, Functional comparison of engineered T cells carrying a native TCR versus TCR-like antibody-based chimeric antigen receptors indicates affinity/avidity thresholds. *J Immunol* **193**, 5733-5743 (2014).
72. J. Renshaw *et al.*, Disruption of WT1 gene expression and exon 5 splicing following cytotoxic drug treatment: antisense down-regulation of exon 5 alters target gene expression and inhibits cell survival. *Molecular cancer therapeutics* **3**, 1467-1484 (2004).
73. L. Yang, Y. Han, F. Suarez Saiz, M. D. Minden, A tumor suppressor and oncogene: the WT1 story. *Leukemia* **21**, 868-876 (2007).
74. R. J. O'Reilly, T. Dao, G. Koehne, D. Scheinberg, E. Doubrovina, Adoptive transfer of unselected or leukemia-reactive T-cells in the treatment of

relapse following allogeneic hematopoietic cell transplantation. *Semin Immunol* **22**, 162-172 (2010).
75. E. Doubrovina *et al.*, Mapping of novel peptides of WT-1 and presenting HLA alleles that induce epitope-specific HLA-restricted T cells with cytotoxic activity against WT-1(+) leukemias. *Blood* **120**, 1633-1646 (2012).
76. H. E. Kohrt *et al.*, Donor immunization with WT1 peptide augments antileukemic activity after MHC-matched bone marrow transplantation. *Blood* **118**, 5319-5329 (2011).
77. U. Keilholz *et al.*, A clinical and immunologic phase 2 trial of Wilms tumor gene product 1 (WT1) peptide vaccination in patients with AML and MDS. *Blood* **113**, 6541-6548 (2009).
78. Q. Zhao *et al.*, Affinity maturation of T-cell receptor-like antibodies for Wilms tumor 1 peptide greatly enhances therapeutic potential. *Leukemia* **29**, 2238-2247 (2015).
79. J. D. Stone, D. M. Kranz, Role of T cell receptor affinity in the efficacy and specificity of adoptive T cell therapies. *Front Immunol* **4**, 244 (2013).
80. L. A. Johnson *et al.*, Gene therapy with human and mouse T-cell receptors mediates cancer regression and targets normal tissues expressing cognate antigen. *Blood* **114**, 535-546 (2009).
81. G. P. Linette *et al.*, Cardiovascular toxicity and titin cross-reactivity of affinity-enhanced T cells in myeloma and melanoma. *Blood* **122**, 863-871 (2013).
82. M. L. Broz *et al.*, Dissecting the tumor myeloid compartment reveals rare activating antigen-presenting cells critical for T cell immunity. *Cancer Cell* **26**, 638-652 (2014).
83. K. Hildner *et al.*, Batf3 deficiency reveals a critical role for CD8alpha+ dendritic cells in cytotoxic T cell immunity. *Science* **322**, 1097-1100 (2008).
84. M. Z. Noman *et al.*, PD-L1 is a novel direct target of HIF-1alpha, and its blockade under hypoxia enhanced MDSC-mediated T cell activation. *J Exp Med* **211**, 781-790 (2014).
85. D. H. Munn, A. L. Mellor, Indoleamine 2,3 dioxygenase and metabolic control of immune responses. *Trends Immunol* **34**, 137-143 (2013).
86. M. Platten, W. Wick, B. J. Van den Eynde, Tryptophan catabolism in cancer: beyond IDO and tryptophan depletion. *Cancer Res* **72**, 5435-5440 (2012).
87. C. Feig *et al.*, Targeting CXCL12 from FAP-expressing carcinoma-associated fibroblasts synergizes with anti-PD-L1 immunotherapy in pancreatic cancer. *Proc Natl Acad Sci U S A* **110**, 20212-20217 (2013).
88. A. J. Garcia *et al.*, Pten null prostate epithelium promotes localized myeloid-derived suppressor cell expansion and immune suppression during tumor initiation and progression. *Mol Cell Biol* **34**, 2017-2028 (2014).
89. Y. Zhu *et al.*, CSF1/CSF1R blockade reprograms tumor-infiltrating macrophages and improves response to T-cell checkpoint immunotherapy in pancreatic cancer models. *Cancer Res* **74**, 5057-5069 (2014).

90. H. Salmon *et al.*, Matrix architecture defines the preferential localization and migration of T cells into the stroma of human lung tumors. *J Clin Invest* **122**, 899-910 (2012).
91. G. T. Motz *et al.*, Tumor endothelium FasL establishes a selective immune barrier promoting tolerance in tumors. *Nat Med* **20**, 607-615 (2014).
92. B. Molon *et al.*, Chemokine nitration prevents intratumoral infiltration of antigen-specific T cells. *J Exp Med* **208**, 1949-1962 (2011).
93. T. Boon, P. G. Coulie, B. J. Van den Eynde, P. van der Bruggen, Human T cell responses against melanoma. *Annu Rev Immunol* **24**, 175-208 (2006).
94. M. Aleksic *et al.*, Different affinity windows for virus and cancer-specific T-cell receptors: implications for therapeutic strategies. *Eur J Immunol* **42**, 3174-3179 (2012).
95. P. A. Savage, M. M. Davis, A kinetic window constricts the T cell receptor repertoire in the thymus. *Immunity* **14**, 243-252 (2001).
96. D. K. Cole *et al.*, Human TCR-binding affinity is governed by MHC class restriction. *J Immunol* **178**, 5727-5734 (2007).
97. A. Varela-Rohena *et al.*, Control of HIV-1 immune escape by CD8 T cells expressing enhanced T-cell receptor. *Nat Med* **14**, 1390-1395 (2008).
98. T. W. McKeithan, Kinetic proofreading in T-cell receptor signal transduction. *Proc Natl Acad Sci U S A* **92**, 5042-5046 (1995).
99. J. D. Stone, A. S. Chervin, D. M. Kranz, T-cell receptor binding affinities and kinetics: impact on T-cell activity and specificity. *Immunology* **126**, 165-176 (2009).
100. L. Wooldridge *et al.*, Tricks with tetramers: how to get the most from multimeric peptide-MHC. *Immunology* **126**, 147-164 (2009).
101. R. H. McMahan *et al.*, Relating TCR-peptide-MHC affinity to immunogenicity for the design of tumor vaccines. *J Clin Invest* **116**, 2543-2551 (2006).
102. D. A. Schmid *et al.*, Evidence for a TCR affinity threshold delimiting maximal CD8 T cell function. *J Immunol* **184**, 4936-4946 (2010).
103. P. F. Robbins *et al.*, Single and dual amino acid substitutions in TCR CDRs can enhance antigen-specific T cell functions. *J Immunol* **180**, 6116-6131 (2008).
104. S. Zhong *et al.*, T-cell receptor affinity and avidity defines antitumor response and autoimmunity in T-cell immunotherapy. *Proc Natl Acad Sci U S A* **110**, 6973-6978 (2013).
105. A. S. Chervin *et al.*, Design of T-cell receptor libraries with diverse binding properties to examine adoptive T-cell responses. *Gene Ther* **20**, 634-644 (2013).
106. C. M. Soto *et al.*, MHC-class I-restricted CD4 T cells: a nanomolar affinity TCR has improved anti-tumor efficacy in vivo compared to the micromolar wild-type TCR. *Cancer Immunol Immunother* **62**, 359-369 (2013).
107. C. G. King *et al.*, T cell affinity regulates asymmetric division, effector cell differentiation, and tissue pathology. *Immunity* **37**, 709-720 (2012).

108. S. Thomas *et al.*, Human T cells expressing affinity-matured TCR display accelerated responses but fail to recognize low density of MHC-peptide antigen. *Blood* **118**, 319-329 (2011).
109. J. M. Boulter *et al.*, Potent T cell agonism mediated by a very rapid TCR/pMHC interaction. *Eur J Immunol* **37**, 798-806 (2007).